

University of Southern Queensland
Faculty of Engineering and Surveying

**NEAR INFRARED PHOTOGRAMMETRIC
TECHNIQUE ON STRUCTURE BEAM
MONITORING**

A dissertation submitted by
Daniel John Pratt

In fulfilment of the requirements of
Courses ENG4111 and 4112 Research Project

Towards the degree of

Bachelor of Spatial Science

Submitted: October, 2011

Abstract

Current methods used to monitor the strain and stress within structures such as bridges and high-rise buildings are not suitable over a 24-hour or weekly period. Furthermore, these methods are not mobile or compact.

This study aims to determine whether using photogrammetric techniques with both colour and NIR (near-infrared) images are suitable for structural beam deformation monitoring during loading in a low-light environment.

The following are the objectives this study aims to achieve:

1. To determine whether 3D measurements captured from NIR images and colour images are in similar context in different lighting conditions.
2. To evaluate the accuracy of the measurements obtained by Near Infrared and Colour Images.
3. To evaluate the suitability of Near Infrared and Colour photogrammetry for various structural beam materials.

In order to achieve these requirements, research was conducted to determine the best way to use these techniques. There were two experiments conducted. One experiment was conducted in the laboratory on testing strain and stress of structural beams, whilst the other was conducted on a bridge to determine if the structure could be observed.

Photographs were obtained from these simulations and were examined using the photogrammetric program 'Australis'. With this program, photogrammetric bundle adjustments were conducted for experiments which were taken with both colour and NIR imagery. These bundles produced coordinates that were examined to view the beams at various levels of strain as well as the bridge structure to determine if the coordinates were in the same parameters.

To conclude, this study was successful in determining whether colour and NIR imagery were in similar context in monitoring structural beams and a bridge structure. Further work is recommended in relation to considering additional factors, such as rain and foggy weather conditions.

University of Southern Queensland
Faculty of Engineering and Surveying

ENG4111 Research Project Part 1 & ENG4112 Research Project Part 2
--

Limitations of Use

The Council of the University of Southern Queensland, its Faculty of Engineering and Surveying, and the staff of the University of Southern Queensland, do not accept any responsibility for the truth, accuracy or completeness of material contained within or associated with this dissertation.

Persons using all or any part of this material do so at their own risk, and not at the risk of the Council of the University of Southern Queensland, its Faculty of Engineering and Surveying or the staff of the University of Southern Queensland.

This dissertation reports an educational exercise and has no purpose or validity beyond this exercise. The sole purpose of the course pair entitled “Research Project” is to contribute to the overall education within the student's chosen degree program. This document, the associated hardware, software, drawings, and other material set out in the associated appendices should not be used for any other purpose: if they are so used, it is entirely at the risk of the user.



Professor Frank Bullen

Dean

Faculty of Engineering and Surveying

Certification

I certify that the ideas, designs and experimentation work, results, analyses and conclusions set out in this dissertation are entirely my own effort, except where otherwise indicated and acknowledged.

I further certify that the work is original and has not been previously submitted for assessment in any other course or institution, except where specifically stated.

Daniel John Pratt

0050071892

Signature

Date

Acknowledgements

Firstly, this research would not have been successful without the help, assistance, supervision and patience of Doctor Albert Kon-Fook Chong. Without his assistance and expertise, this study would have been ineffective. I would also like to acknowledge my appreciation for the use of equipment Dr Chong provided, as well as his assistance in providing me with suggestions of method options and ideas.

Appreciation is due to Mr Mohan Trada for his assistance, support and time in demonstrating the workings of the testing machine, estimating the level of strain that was applied to each beam and applying stress on the materials during the sessions that were conducted during the evening.

I would like to thank Ms Sandra Cochrane for contributing ideas and assisting me in the direction of research into this study.

In relation to the use of Glass-Polymer-Resin Composite Beam, I would like to thank Wagner, Inc., for their permission to conduct experimentation on this material.

I would like to thank Paul Lenton for the use of the metal C-section guard-rail post and the wooden railway sleeper beams that were included in the experimentation.

In regards to conducting experimentation on the University of Southern Queensland Campus, I would like to thank USQ Security for their permission for the experimentation on the Campus and their assistance in turning off a light that was posing as disruptive in the experimentation.

I would like to acknowledge my appreciation for the use of the facilities at the University of Southern Queensland. I would also like to thank the staff for their time and patience during the past five years in educating and preparing me for a profession involving Spatial Science.

Table of Contents

<u>Contents</u>	<u>Page</u>
<u>Abstract</u>	<u>i</u>
<u>Limitations of Use</u>	<u>ii</u>
<u>Certification</u>	<u>iii</u>
<u>Acknowledgements</u>	<u>iv</u>
<u>List of Figures</u>	<u>viii</u>
<u>List of Tables</u>	<u>xiii</u>
<u>List of Appendices</u>	<u>xv</u>
 <u>Chapter 1 – Introduction</u>	
<u>1.1 Introduction of the study</u>	<u>1</u>
<u>1.2 Statement of Problem</u>	<u>1</u>
<u>1.3 Aim and Objectives</u>	<u>2</u>
<u>1.3.1 Aim</u>	<u>2</u>
<u>1.3.2 Objectives</u>	<u>2</u>
<u>1.4 Conclusion</u>	<u>2</u>
 <u>Chapter 2 – Literature Review</u>	
<u>2.1 Introduction</u>	<u>3</u>
<u>2.2 Background</u>	<u>4</u>
<u>2.3 Structure Standards</u>	<u>4</u>
<u>2.4 Earlier methods of Structural Monitoring</u>	<u>5</u>
<u>2.4.1 Visual Inspection</u>	<u>6</u>

<u>2.4.2 Loading Simulations</u>	<u>6</u>
<u>2.5 Current Methods</u>	<u>7</u>
<u>2.5.1 Strain Gauges</u>	<u>8</u>
<u>2.5.2 Optic Fibres</u>	<u>9</u>
<u>2.5.3 Acoustic Emission</u>	<u>10</u>
<u>2.6 Photogrammetry</u>	<u>11</u>
<u>2.6.1 Advantages</u>	<u>12</u>
<u>2.6.2 Camera Calibration</u>	<u>13</u>
<u>2.6.3 Other Fields</u>	<u>14</u>
<u>2.6.4 Civil Engineering</u>	<u>15</u>
<u>2.6.5 Photogrammetry research on Structural Monitoring</u>	<u>16</u>
<u>2.7 Near Infrared Photogrammetry</u>	<u>17</u>
<u>2.8 Conclusion</u>	<u>19</u>

Chapter 3 – Methodology

<u>3.1 Introduction</u>	<u>20</u>
<u>3.2 Stage 1 Simulation Testing</u>	<u>20</u>
<u>3.3 Stage 2 Laboratory Loading Simulation</u>	<u>22</u>
<u>3.3.1 Equipment</u>	<u>22</u>
<u>3.3.2 Risk Assessment</u>	<u>27</u>
<u>3.3.3 Laboratory Experimentation</u>	<u>28</u>
<u>3.4 Stage 3 Field Study</u>	<u>31</u>
<u>3.4.1 Equipment</u>	<u>32</u>
<u>3.4.2 Experimentation</u>	<u>33</u>
<u>3.5 Stage 4 Camera Calibrations and Camera Control</u>	<u>35</u>
<u>3.5.1 Control and Calibration of cameras in Stage 2</u>	<u>35</u>
<u>3.5.2 Control and Calibration of cameras in Stage 3</u>	<u>37</u>
<u>3.6 Construction of Projects</u>	<u>38</u>
<u>3.7 Bundle Adjustment</u>	<u>39</u>
<u>3.8 Calibration Set-up</u>	<u>39</u>
<u>3.9 Control Set-up</u>	<u>40</u>
<u>3.10 Computation of results</u>	<u>40</u>
<u>3.10.1 3D Distance measurements</u>	<u>41</u>

<u>3.10.2 Diagram comparisons</u>	43
<u>3.10.3 F-Test Distribution</u>	43
<u>3.11 Conclusion</u>	44

Chapter 4 – Analysis of Results

<u>4.1 Introduction</u>	45
<u>4.2 3D Distance measurements</u>	45
<u>4.3 Diagram comparisons</u>	55
<u>4.4 F-Test Distribution</u>	84
<u>4.4.1 Structural Beams</u>	84
<u>4.4.2 Bridge Structure</u>	92
<u>4.5 Conclusion</u>	93

Chapter 5 – Discussion

<u>5.1 Introduction</u>	94
<u>5.2 Experimentation and Analysis of Results</u>	94
<u>5.3 Problems Encountered</u>	95
<u>5.4 Conclusion</u>	96

Chapter 6 – Conclusions

<u>6.1 Introduction</u>	97
<u>6.2 Discoveries of this Study</u>	97
<u>6.3 Further Work</u>	98
<u>6.3.1 Improvements</u>	99
<u>6.3.2 Observations on Top</u>	100
<u>6.3.3 Weather Conditions</u>	100
<u>6.4 Conclusion</u>	100

<u>References</u>	101
--------------------------	------------

List of Figures

<u>Number</u>	<u>Title</u>	<u>Page</u>
2.1	Figure 2.1 An schematic of the setup of the Optical Strain Gauge (Huang et al. 2010, pg. 356).	9
2.2	Principle of acoustic emission (C.S. Cai et al. 2010, pg. 1705).	10
2.3	The use of photogrammetry on motion tracking (A) and craniofacial analysis (B) (Chong 2004, pg. 297; Chong & Mathieu 2006, pg. 17).	15
2.4	An example of where Near Infrared is utilised in the application of surveillance (Chong et al. 2010, pg. 503).	18
3.1	Cracked piece of steel, both photographed in colour (A) and NIR (B).	21
3.2	Deformed piece of concrete, both photographed in colour (A) and NIR (B).	21
3.3	The two cameras, the NIR illuminator (A) and the camera stand (B) that were used.	23
3.4	The universal testing machine. The hydraulic jack and support beam (A) and the controls for operating the machine (B).	26
3.5	The Structural Beam Control Board.	27
3.6	The concrete beam after stress was applied. The circle shows the crack that was created during experimentation.	28
3.7	The Set-up of stage 2 experimentation.	30
3.8	The Plan view of stage 2 experimentation.	30

3.9	The bridge structure showing where the simulation was conducted.	32
3.10	The Bridge Control Board.	33
3.11	A diagram of the camera positions.	34
3.12	The control board, the control plate and target board set-up.	36
3.13	The Camera Calibration Set Up with the Invar bar in the middle (Chong & Mathieu 2006, pg. 18).	37
3.14	The Set-up of both the control and calibration.	38
4.1	Graph of the Imagery Types of Paper-Made targets on the Concrete beam at 0 kN.	56
4.2	Graph of the Imagery Types of Retro-Reflective targets on the Concrete beam at 0 kN.	56
4.3	Graph of the Imagery Types of Paper-Made targets on the Concrete beam at 7 kN.	57
4.4	Graph of the Imagery Types of Retro-Reflective targets on the Concrete beam at 7 kN.	58
4.5	Graph of the Imagery Types of Paper-Made targets on the Concrete beam at 13 kN.	59
4.6	Graph of the Imagery Types of Retro-Reflective targets on the Concrete beam at 13 kN.	59
4.7	Graph of the Imagery Types of Paper-Made targets on the Wood beam at 0 kN.	60

4.8	Graph of the Imagery Types of Retro-Reflective targets on the Wood beam at 0 kN.	61
4.9	Graph of the Imagery Types of Paper-Made targets on the Wood beam at 2.5 kN.	62
4.10	Graph of the Imagery Types of Retro-Reflective targets on the Wood beam at 2.5 kN.	62
4.11	Graph of the Imagery Types of Paper-Made targets on the Wood beam at 4.5 kN.	63
4.12	Graph of the Imagery Types of Retro-Reflective targets on the Wood beam at 4.5 kN.	64
4.13	Graph of the Imagery Types of Paper-Made targets on the Composite beam at 0 kN.	65
4.14	Graph of the Imagery Types of Retro-Reflective targets on the Composite beam at 0 kN.	65
4.15	Graph of the Imagery Types of Paper-Made targets on the Composite beam at 5 kN.	66
4.16	Graph of the Imagery Types of Retro-Reflective targets on the Composite beam at 5 kN.	67
4.17	Graph of the Imagery Types of Paper-Made targets on the Composite beam at 9.5 kN.	68
4.18	Graph of the Imagery Types of Retro-Reflective targets on the Composite beam at 9.5 kN.	68
4.19	Graph of the Imagery Types of Paper-Made targets on the First Steel beam at 0 kN.	69

4.20	Graph of the Imagery Types of Retro-Reflective targets on the First Steel beam at 0 kN.	70
4.21	Graph of the Imagery Types of Paper-Made targets on the First Steel beam at 25 kN.	71
4.22	Graph of the Imagery Types of Retro-Reflective targets on the First Steel beam at 25 kN.	71
4.23	Graph of the Imagery Types of Paper-Made targets on the First Steel beam at 42.5 kN.	72
4.24	Graph of the Imagery Types of Retro-Reflective targets on the First Steel beam at 42.5 kN.	73
4.25	Graph of the Imagery Types of Paper-Made targets on the Second Steel beam at 0 kN.	74
4.26	Graph of the Imagery Types of Retro-Reflective targets on the Second Steel beam at 0 kN.	74
4.27	Graph of the Imagery Types of Paper-Made targets on the Second Steel beam at 25 kN.	75
4.28	Graph of the Imagery Types of Retro-Reflective targets on the Second Steel beam at 25 kN.	76
4.29	Graph of the Imagery Types of Paper-Made targets on the Second Steel beam at 45 kN.	77
4.30	Graph of the Imagery Types of Retro-Reflective targets on the Second Steel beam at 45 kN.	77
4.31	Graph of the Imagery Types of Paper-Made targets on the Timber beam at 0 kN.	78

4.32	Graph of the Imagery Types of Retro-Reflective targets on the Timber beam at 0 kN.	79
4.33	Graph of the Imagery Types of Paper-Made targets on the Timber beam at 25 kN.	80
4.34	Graph of the Imagery Types of Retro-Reflective targets on the Timber beam at 25 kN.	80
4.35	Graph of the Imagery Types of Paper-Made targets on the Timber beam at 45 kN.	81
4.36	Graph of the Imagery Types of Retro-Reflective targets on the Timber beam at 45 kN.	82
4.37	Graph of the Imagery Types of the Bridge Structure.	83

List of Tables

<u>Number</u>	<u>Title</u>	<u>Page</u>
3.1	Specifications of the structural beams utilised in this study and how they were provided.	24
3.2	The Dimensions of each the beams that were used. (Measurements in meters)	25
3.3	The Levels of stress that were applied to each structural beam. (kN = Kilonewtons)	29
4.1	Comparison of Sample Mean 3D distances of the Top Row at Initial Stress. (mm)	46
4.2	Comparison of Sample Mean 3D distances of the Bottom Row at Initial Stress. (mm)	47
4.3	Comparison of Sample Mean 3D distances of both Rows at Initial Stress. (mm)	48
4.4	Comparison of Sample Mean 3D distances of the Top Row at Average Stress. (mm)	49
4.5	Comparison of Sample Mean 3D distances of the Bottom Row at Average Stress. (mm)	50
4.6	Comparison of Sample Mean 3D distances of both Rows at Average Stress. (mm)	51
4.7	Comparison of Sample Mean 3D distances of the Top Row at Maximum Stress. (mm)	52
4.8	Comparison of Sample Mean 3D distances of the Bottom Row at Maximum Stress. (mm)	53

4.9	Comparison of Sample Mean 3D distances of both Rows at Maximum Stress. (mm)	54
4.10	Comparison of Sample Mean 3D distances of the bridge structure. (mm)	55
4.11	The F-Test values that were calculated between the levels of stress and targets of the Concrete beam. (mm)	84
4.12	The F-Test values that were calculated between the levels of stress and targets of the Wood beam. (mm)	86
4.13	The F-Test values that were calculated between the levels of stress and targets of the Composite beam. (mm)	87
4.14	The F-Test values that were calculated between the levels of stress and targets of the First Steel beam. (mm)	88
4.15	The F-Test values that were calculated between the levels of stress and targets of the Second Steel beam. (mm)	90
4.16	The F-Test values that were calculated between the levels of stress and targets of the Timber beam. (mm)	91

List of Appendices

<u>Item</u>	<u>Title</u>	<u>Page</u>
A	Project Specification	105
B	Risk Assessment	109
C	Structural Material Display	120
	C.1 Concrete Material Beam	121
	C.2 Wood Material Beam	121
	C.3 Composite Material Beam	122
	C.4 Steel 01 Material Beam	122
	C.5 Steel 02 Material Beam	123
	C.6 Timber Material Beam	123
D	Camera Calibration Results	124
	D.1 Camera 1 Calibration Parameters (Structural Beams)	125
	D.2 Camera 2 Calibration Parameters (Structural Beams)	126
	D.3 Camera Calibration Parameters (Bridge Structure)	127

Chapter 1

Introduction

1.1 Introduction of the Study

In relation to structures such as bridges and high-rise buildings, there are methods that have been developed to monitor and determine the strain and stress within these formations. This is particularly relevant when there are concerns regarding the health of these structures. Methods determining these factors are crucial. Cracks and deformations may result from both age and environmental conditions. These circumstances can cause structure collapse and have the potential to endanger lives.

Methods have been developed to monitor structures and determine their safety compliance.

1.2 Statement of Problem

However, the techniques that are available have disadvantages that could warrant revision. For example, if a structure such as a bridge is to be monitored, the main concern is that the available methods do not monitor these structures over a 24-hour period on a weekly basis. They are not mobile or compact and pose concerns in relation to health and safety aspects in operation techniques.

Furthermore, the purpose of conducting this study is to determine if using photogrammetry techniques in colour and NIR, can detect the stress of structural beams. It is also anticipated that the study will be able to ascertain whether a 3-D representation of a structure can be computed.

1.3 Aim and Objectives

In reference to any given research or experiment, aims and objectives are to be established in order to identify outcomes.

1.3.1 Aim

The main aim of this study is to determine whether using photogrammetric techniques with both colour and near-infrared images are suitable for structural beam deformation monitoring during loading in a low-light environment.

1.3.2 Objectives

The research sought to achieve positive outcomes in relation to the following three objectives.

1. To determine whether 3D measurements captured from near-infrared images and colour images are in similar context in different lighting conditions.
2. To evaluate the accuracy of the measurements obtained by Near Infrared and Colour Images.
3. To evaluate the suitability of Near Infrared and Colour photogrammetry for various structural beam materials.

1.4 Conclusion

Whilst conducting the research, it is intended to use photogrammetry techniques on materials that are commonly used within the named structures so as to determine if the same accuracy can be achieved with colour photogrammetry. Research on what methods and what details are required to achieve the results will be explained in greater detail in Chapter 2.

Chapter 2

Literature Review

2.1 Introduction

It is important that projects are accompanied by a general history of specific tasks that are involved in their investigation. In relation to this study, an examination was conducted that included a history of monitoring. The study also included the best photogrammetric techniques that would be recommended for a successful outcome.

The examination included the following three areas in its study:

- Structural Deformation Monitoring: Investigating the methods that were utilised before technological advancement, as well as the current methods that determine the strain and stress of bridges and other similar structures.
- Photogrammetry: A spatial science profession, which analyses physical objects using photographs that are processed with greater accuracy that is dependent on a camera.
- Near Infrared Photogrammetry: Analysing physical objects using photographs at a lower light setting.

Through experimentation of these fields and analysis of these results, I aim to be able to determine if using NIR photogrammetry would be a cost-effective, reliable and accurate technique to use.

2.2 Background

As stated previously in Chapter 1, most structures are required to be monitored due to deformations that may form over a length of time due to environmental or other factors.

Using information provided from the American Society for Metals (ASM) Handbooks, a general understanding was gained in relation to how mechanical and civil engineers analyse and handle beam monitoring. A general history of studying the techniques that were utilised before technology was also taken into consideration.

The study of features and details of all deformations and fractures that are within the discussed structures is known as Fractography. These studies may be traced back to the beginning of the Bronze Age. Carl A. Zapffe first developed fractography in 1944. He was able to discover a means of eliminating any difficulty of bringing the lens of a microscope near the surface of a fractured material and determine their details. As a result of this discovery and further development in the advancement of cameras, fractography has played an important role in monitoring structures for fractures or deformities.

2.3 Structure Standards

In relation to this examination of the health of beams and structures, it is of significance to list and determine what standards should be evident with any type of structure. Over the years, there have been experiments, papers and manuals written and produced to determine these standards. The methods and papers have listed possible consequences if the structures were inadequately examined.

One noticeable example in relation to structures would be to view the standards that are in place for bridges. Australian standards require that all bridges are designed and built to the requirements of the 'AS 5100 Bridge Design'. These requirements include an established design philosophy. It is able to assist engineers determine the best way to design bridges and similar structures for long life whilst keeping within safety requirements.

In reference to this philosophy, some of the parameters and performance of these structures must be determined by the following conditions:

- The design life of the structure shall be at least 100 years.
- The limit states whether the structure is unfit according to the criteria.
- Analysis methods of the structure
- Design actions or loads that are applied to the structure.
- The amount of strength that can be applied.

On examination of these conditions, the design and plans of these bridges are based on the basic engineering principles, experimental data that is collected from other areas and general experience of design. Considering these ethics, it is understood that they are in place to ensure the safety and the performance of the structure in question.

With any structure, the standards and plans of the structure are recorded and stored. This is namely for future use such as a possible need to examine a structure, such as a bridge that may require monitoring. If appropriate records are available it is possible for engineers to compare and thus determine if there is any warranted concern for the structure in question.

2.4 Earlier methods of Structural Monitoring

In relation to monitoring the structure and determining the potential risk, there are two methods that were previously used before the technological advancements were available. These are the current procedures and are used today to determine if further work should progress.

- Visual Inspection
- Loading Simulations

2.4.1 Visual Inspection

Before technological advancements became available to the general public, the only suitable way of detecting if a structure was on the verge of collapse due to deformation and cracks was to conduct a visual inspection.

This is still a common method when a beam or any part of the structure is determined to be a risk to life. This technique involves a person with skill and patience to physically inspect the structure and determine whether there are areas in the structure that are of considerable threat to both the structure and people who use it.

However, there are considerable concerns when relying on visual inspection of structures. Even though the surface of an area can be observed, the interior of the deformation cannot be viewed. This may pose a risk by the fact that while the crack may look small on the surface, it may be larger and deeper within the structure itself. There may also be areas where it is difficult to view and the deformations are hidden. These areas could possibly be high above the ground and in the darkened spaces where lighting is not able to reach.

Moreover, new techniques are being developed to assist with inspections. An example of this is by using an automatic robotic system that has been researched and developed by SK. Tso and Tong Feng in 2003. These individuals devised a robotic system to scan the tiles on high-rise buildings in order to make sure that they were not a danger to pedestrians that may have been walking on the pavement below.

2.4.2 Loading Simulations

When conducting any experimentation or research, it may be beneficial to work in an actual field, but it is considered that a controlled environment, such as a laboratory, is a better option. The reason why a controlled environment may be beneficial is that certain parameters can be controlled such as how much strain can be applied to the materials in question.

On examination of the ASME handbook, there is evidence of descriptive analyses when using loading simulations. There is also detailed information regarding the best way to apply the necessary stress to materials when using testing machines and stress gauges. These testing machines are manufactured and there are several types of devices for the measurement of force. Some of these early systems employ a graduated balanced beam in order to hold the material in place.

When using current testing machines a strain-gauge loads cells and pressure transducers in order to apply the strain. These load cells have strain gauges mounted on precision-machine alloy steel elements, which are then sealed within a case with all the necessary electrical outputs. These load cells are then placed on the specimen, either in direct contact, or indirectly through a loaded machine crosshead, table, or columns of the load frame.

2.5 Current Methods

Recent technological developments and techniques show that there are methods that are more suitable to utilise when conducting an inspection of the structure. Most if not all of these methods have been devised from various studies and experiments due to health and safety risks as well as endeavouring to make the process more time-efficient. Consequently, this research has enabled the improved methods to be a more viable option. They are not only more efficient but are non-destructive to the structure itself.

The methods discussed are still used in order to give a general background to engineers. The following methods are those which are most commonly used when dealing with building structures:

- Strain Gauges
- Optic Fibres
- Acoustic Emission

2.5.1 Strain Gauges

The use of Strain Gauges in structural monitoring is a more common method when detecting the strain and stress of structures such as bridges. This method uses a gauge, which is applied, to the area in question. It is then possible to record the stress and strain that is applied to the material under a certain load.

Over the years, there have been many types of strain gauges that have been developed. Some of these are: Electric resistance, Demec mechanical strain and compressometer. (Huang et al. 2010)

In relation to the use of these methods, a number of disadvantages have been revealed:

- Has to be conducted with someone experienced in this field. Unfortunately, it is not only tedious but it consumes a large amount of time.
- Reliability of using a few gauge methods is to be questioned.
- Some gauges are size-fixed which means it is not possible to use samples of other sizes.
- It is difficult to place these gauges in appropriate positions within the structure itself.

There is a recent developed gauge available known as a wire strain gauge. This gauge is widely used in the monitoring of geotechnical works and concrete structures because it can offer significant advantages over other typical gauge types. This includes ease of attachment and accuracy. The strain gauge can also measure the shrinkage of the strains in prestressed concrete bridge segments; monitoring of dam deformations under hydrostatic loads and field testing of concrete breakwater armour units. (Dudescu et al. 2009)

2.5.2 Optic Fibres

In reference to studies that relate to monitoring the strain and stress of bridges, most conventional sensors that are used are based on transmission of electric signals.

Recent developments reveal that optic fibre sensors are usually used for structural monitoring of large civil structures such as dams, bridges, buildings and composite material structures. This is namely due to their unique features. The sensors are attached to the surface of the structures to continually monitor conditions such as damage, strain, stress, crack formation, and temperature. (Gao et al. 2007)

Most of the sensors that are utilised have a variety of advantages. These include small size, light weight, non-conductivity, fast response, resistance to corrosion, immunity to electromagnetic noise and radio frequency interferences thus eliminating the need for costly and bulky shielding and lightning protection accessories (Hong-Nan et al., 2004). These sensors can also sense a variety of physical effects such as pressure, strain, temperature and displacement. In Figure 2.1, a schematic shows how optic fibres are required to be set-up.

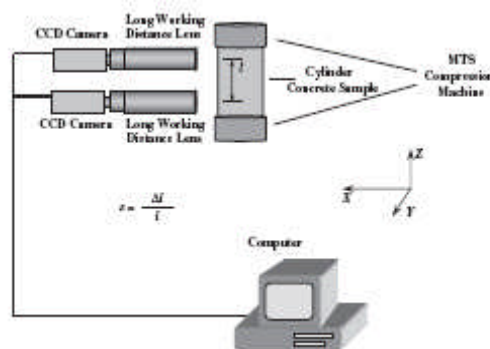


Figure 2.1 An schematic of the setup of the Optical Strain Gauge (Huang et al. 2010, pg. 356).

Furthermore, research has shown that using this method to record the strain and stress, is a more effective approach. (Gao et al. 2007) Advantages are namely:

- High accuracy and superior reliability.
- It can be fully utilised within the field and is non-destructive.
- Data can be extracted more quickly.
- Allows more flexibility due to the inspection of areas that are non-accessible using previous methods.

2.5.3 Acoustic Emission

Acoustic Emission is a common method that has been utilised in civil engineering for several years. With the loading conditions that exist in bridges and the materials that are used, such as concrete and steel, energy is emitted in the form of elastic waves due to various material-relevant damage mechanisms that are caused by environmental and age conditions. Sensors that are attached to the surface of the material pick up these waves. Further evaluation of the collected information gives an analysis in relation to the health of the bridge and helps determine whether there is a need to repair the bridge in order to keep the bridge at the required standard. (C.S. Cai et al. 2010, pg. 1705). Figure 2.2, gives a clear idea of how the principles of Acoustic Emission is conducted.

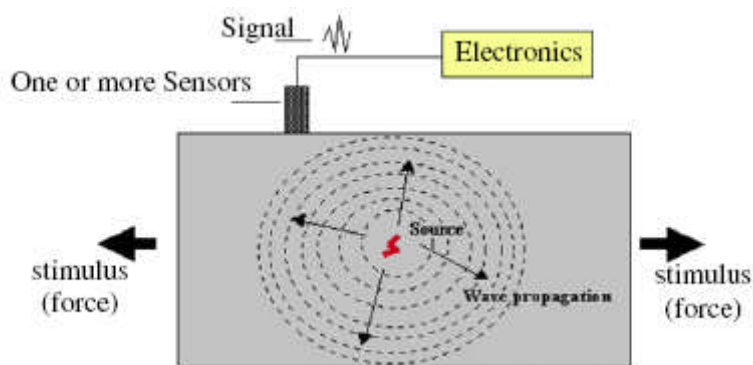


Figure 2.2 Principle of acoustic emission (C.S. Cai et al. 2010, pg. 1705).

With recent developments and research conducted by Archana Nair & C.S. Cai (2010), there are advantages that are useful in monitoring the strain and stress of bridges. The advantages of the AE technique in the context of bridge monitoring may be listed as:

1. Damage growth essentially generates Acoustic Emission and is the outcome of the load history experienced by the structure.
2. Acoustic Emission is applicable for local, global, remote, and continuous monitoring purposes without hindering traffic over the bridge structure.
3. Source detection and location algorithms have been improved to a great extent, assuring reliable analyses.
4. Dynamics of the material are observable in real time due to the technological advancements made in acquisition systems.

However, the research has also revealed various disadvantages. These are as follows:

1. Although the issue of background noise discrimination has been fairly addressed; real-time separation requires several trial monitoring sessions and experienced personnel.
2. Quantitative AE analyses are still difficult for applications to actual bridge structures.
3. Standardized procedures are not available for all types of bridges, as most recommendations cater for bridges under unique conditions of loading, materials, etc.

2.6 Photogrammetry

In a recent study (Jiang et al. 2008), photogrammetry is defined as a method for determining a physical object's location, size and shape by measuring and examining their two-dimensional photographs.

There are two categories that photogrammetry is divided into, these are aerial and terrestrial. Aerial photogrammetry is where photographs are taken from an aircraft. These are more suitable for land use purposes. Terrestrial photogrammetry is photographs that are received at locations that are near or on the surface of the earth. These photographs reveal dimensional information of objects.

Close-Range photogrammetry is where any images that are obtained from the object are photographed very close to the camera. These images are taken from all positions that surround the object and are very close when placed together. Usually, when dealing with multiple images, the points are defined as a 3D co-ordinate system.

2.6.1 Advantages

Development of close-range photogrammetry has revealed several advantages within the field of structural engineering. Miles and Barber (2004) stated that with photogrammetry the advantages are as follows:

- As a result of improved network design, there is better accuracy, precision and reliability.
- Camera self-calibration and the analysing processing techniques allow the use of non-metric cameras and a simplified camera calibration process.
- With the increase in low cost software packages, this results in greater accessibility to the general public.
- With the development of the Internet, photogrammetric techniques can be duplicated and are available on-line with a touch of a button.
- Due to the advances of digital techniques, image digitalisation has been removed and users have an increased digital workflow.
- Modern digital cameras and better analysing tools have been improved and there is greater flexibility.

There is one advantage of photogrammetry that has proven to be the main advantage. With the rapid development of digital camera technology, photogrammetry has become the most influential in relation to fields of acquiring data. Digital cameras have become more freely available and are competitively priced (Chandler et al. 2005). A digital camera ranges in cost from \$500 to \$1000.

As a result of the availability of the cameras in this price range it was feasible to conduct studies and research into examining whether these cameras produced the same accuracy when conducting research. A few examples of research conducted using low-cost cameras included seeing if they could measure a surface at a close range which could construct a Digital Elevation Model (Chandler et al. 2005) and to evaluate the accuracy of utilising this equipment in geotechnical laboratories (Hartwig et al. 2009).

However, it is important to note that when choosing whether or not to use a particular digital camera it is advisable to examine which would be suitable for the particular task. If the task requires precision and accuracy then it is recommended to use the advanced methods such as the laser scanning and fractography methods.

2.6.2 Camera Calibration

When using digital cameras in photogrammetry, calibration of a camera's lens is essential in order to obtain reliable information from the images. With the increased use, various methods have been developed in order to calibrate these cameras (Clarke and Fryer 1998).

The most common method used when calibrating is the 'Self-Calibration Bundle Adjustment', which was developed by Brown in 1956 as a means of simultaneously solving for target co-ordinates, camera locations and lens parameters.

The conditions that Brown discussed for a successful self-calibration are:

1. A single camera must be used to take at least three photographs of a physical object.
2. Both the interior geometry of the camera and the point to be measured on the object must remain secure during the measuring process.
3. The network must be well built and exercise an extreme degree of convergence.
4. One of the images must have a roll angle that is considerably different from the others.
5. A reasonably large number of well-distributed points are to be used.

When the following conditions are met, a camera is regarded as being calibrated: The interior orientation is known, as well as the principle distance, principle offsets, lens distortions and in-plane image distortion principal point of autocollimation (PPA), the principal distance (PD), the radial lens distortion parameters and, in some cases, the dynamic fluctuation (Chong & Mathieu 2006).

2.6.3 Other Fields

In relation to the advantages and accuracy of photogrammetry, there have been studies and research conducted to determine the best approach. After examining the available options and task requirements the decisions rest with the operator. Various examples deal with medical science, security surveillance systems and monitoring as well as the analysis of deformations and cracks within structures.

In regards to medical science, photogrammetry has several benefits. There were two studies that were performed by Albert K. Chong (Chong 2004; Chong & Mathieu 2006). One was focused on acquiring craniofacial data from a patient. The second study involved tracking the patient's movement in order to model prosthetics for the patient. The data acquired could also be used in the treatment of physical therapy. Both of these studies, shown in figure 2.3, were successful in acquiring the data and the data was within the acceptable accuracy.

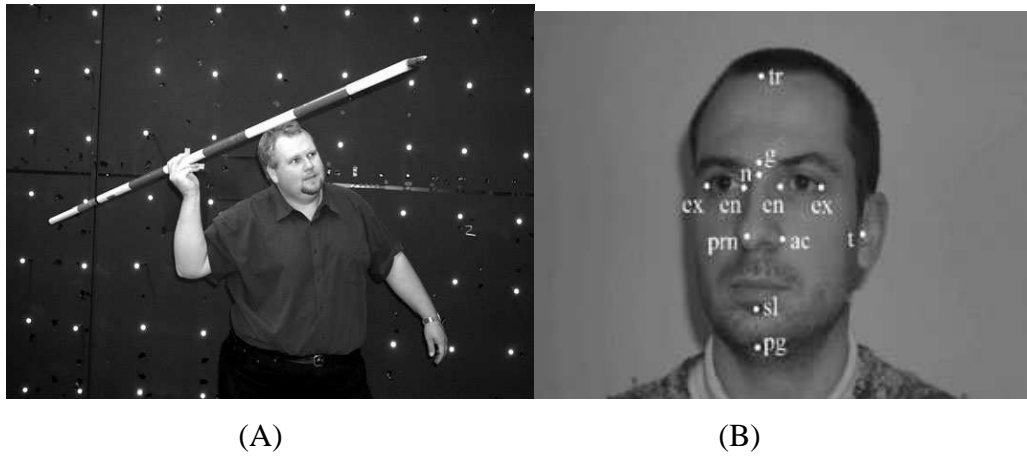


Figure 2.3 The use of photogrammetry on motion tracking (A) and craniofacial analysis (B) (Chong 2004, pg. 297; Chong & Mathieu 2006, pg. 17).

2.6.4 Civil Engineering

In reference to civil engineering, photogrammetry methods are considered to be an excellent choice to use in detecting and monitoring fractures and deformations. Photogrammetry allows simultaneous measurements of deformations at various locations of the structure. When obtaining these measurements, it is usually very quick and the process can be particularly automatic. This is very useful as it allows real-time monitoring at a more accurate rate than the previous methods (Maas et al. 2006). Previous methods would have been more time-consuming and the monitoring inspections would have had to be on a weekly to a monthly basis.

Methods involving photogrammetry have been applied to a wide variety of elements and areas requiring deformation measurements. These range from deformations as small as a hair on concrete probes in load tests (Maas et al. 2006) to monitoring the deformations within bridges and buildings.

Analysis of deformation utilises the precision that photogrammetry addresses, and this is within reliable parameters. In fracture analysis, experiments were conducted where the data was obtained at a continuous rate. It was discovered that when observing a large object, the precision reached the potential of 1:250,000 (Maas et al. 2006).

2.6.5 Photogrammetry research on structural monitoring

Whilst conducting this study, it was discovered that there have been various other papers published that show the use of close-range photogrammetry in measuring and determining the accuracy of the details and stress that is applied to structural materials. There were two case studies that were beneficial in the production of this study. One of these case studies used close-range photogrammetry as well as a variety of other methods to monitor a structural beam in a laboratory. The remaining study was conducted in the field.

Two of these studies were conducted by Petri Rönholm and the Helsinki University of Technology in 2009 where they utilised measurement techniques, such as photogrammetry, as well as laser scanning and total station measurements. This paper revealed that they utilised photogrammetry as it is commonly used for detecting deformations within materials. Analysing these studies proved interesting and was useful for ideas for future research. The following was noted.

- When conducting this photogrammetric method, all data that is required should be based on a control coordinate system with the positions on this board identified.
- To use both paper-made targets, a non-reflective black circle with a white background, and retro-reflective circle with a black background.
- A laboratory simulation is best as the external disturbances can be minimised.
- When taking photographs, the area of monitoring should be in full view so as not to miss any targets.

Another study was conducted by P. Arias, J. Herráez, H. Lorenzo and C. Ordóñez in 2005 where they used close-range photogrammetry to monitor and to determine the areas indicating serious threat to a building. With this study, the following details of research were taken into consideration. The methodology relating to this study will be discussed in the next chapter:

- Each element that is featured must be within three photographs.
- The convergence between the photographs taken from different positions must have most favourable values of 90° so the adjustments are carried out well.
- The photographs have to overlap each other by at least 50%.

2.7 Near Infrared Photogrammetry

The photogrammetry profession has become more successful due to the low costs of digital cameras and their availability. Other features such as near infrared are also available with some of the cameras. In most studies and applications, near infrared's main use is in aerial photogrammetry where all of the details of urban areas, such as cities, are detailed with the population growth as well as the state of the vegetation.

However, with the development of photogrammetry and the availability of video cameras with NIR, there have been many beneficial studies that have been achieved. Two of these studies where NIR has been researched are the areas of medical science. This is in relation to where NIR is used to study the craniofacial features of a person's face (Chong & Mathieu 2006). In contrast, a surveillance security system uses the same process to record people disobeying the law as shown in Figure 2.4 (Chong et al. 2010).

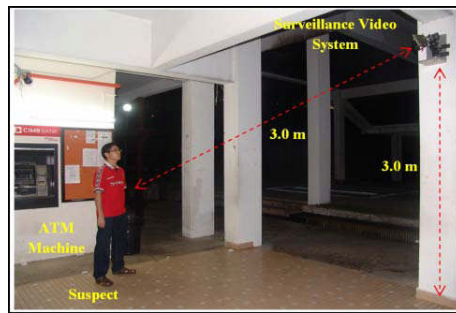


Figure 2.4 An example of where Near Infrared is utilised in the application of surveillance (Chong et al. 2010, pg. 503).

There are many benefits for the spatial science profession when using Near Infrared. Civil and mechanical engineers also benefit by using Near Infrared. In reference to this particular experimentation being conducted, I will be able to determine if using Near Infrared would be acceptable to use with monitoring the strain and stress that is applied to structures, more specifically, bridge structures.

The benefits that I believe NIR will utilise are as follows:

- It is suitable for areas where there is low light. Therefore, when additional lighting is required, such as setting up lamps, it will not be necessary.
- With using NIR, there will be less distraction for the public, such as motorists driving at night as there is no need for extra lighting.
- With photogrammetry, it is established that a 3D analysis of the deformities can be constructed. With the NIR, the monitoring can be accomplished at night as well. This will provide a 24 hour monitoring of the structure and a 4D analysis as well.
- As discussed, with the rapid development of and accessibility to digital cameras, cameras with in-built NIR are now low-cost and available to the general public.
- With this type of technology and monitoring, it is possible for automated cameras to be situated in different positions. It is also possible to photograph the sections on timers. Consequently, there would be no need to physically keep going to the site in question.

2.8 Conclusion

Reviewing the outcomes from this chapter, there is evidence to reveal that there are benefits of utilising photogrammetry to monitor a structure. As discussed, it is also an established fact that photogrammetry has been beneficial to other professions. The chapter also outlines the guidelines that are required for the achievement of determining if Near Infrared is suitable for structural monitoring. Details of how to use Near Infrared to monitor a structural area are explained in greater depth in the Methodology section in Chapter 3.

Chapter 3

Methodology

3.1 Introduction

The research that has been reviewed and discussed in the previous chapter has determined what type of experimentation and equipment would be utilised in this study. The research consisted of four stages that were conducted to complete this project. These stages are:

1. Simulation testing of using NIR photogrammetry on basic materials.
2. Laboratory Simulations using the NIR sensor on structural materials.
3. Field Simulation on a bridge structure using the NIR sensor.
4. Camera Calibration and Camera Control.

3.2 Stage 1 Simulation Testing

In relation to this project, a simulation test was conducted using the NIR illuminator sensor, namely a Sony HVL-HIRL Video light. This was attached to a video camera, a Sony HDR-SR10E where the colour and the night-shot vision were captured. This simulation testing was accomplished in order to compare colour photographs to Near Infrared photographs in normal lighting to lower lighting respectively. This would determine if there would be any significant differences in the spectrum of the camera imagery conditions and also detect any similarities.

There were two materials utilised in this testing. These were a cracked piece of metal and a piece of deformed concrete as shown in figures 3.1 and 3.2.

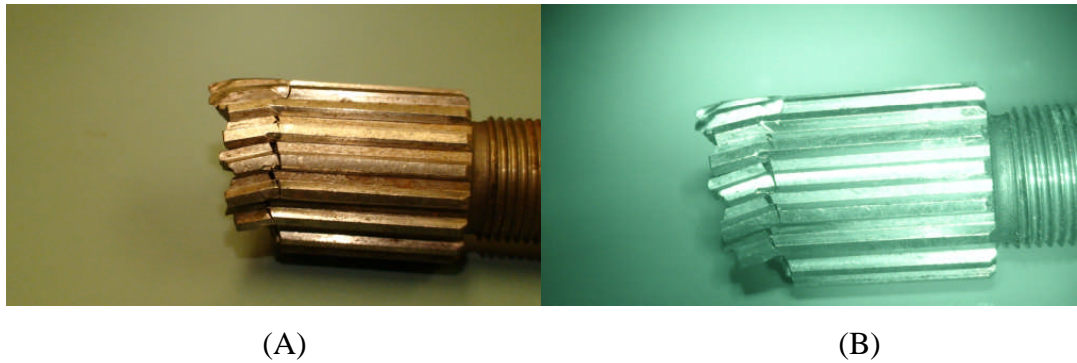


Figure 3.1 Cracked piece of steel, both photographed in colour (A) and NIR (B).

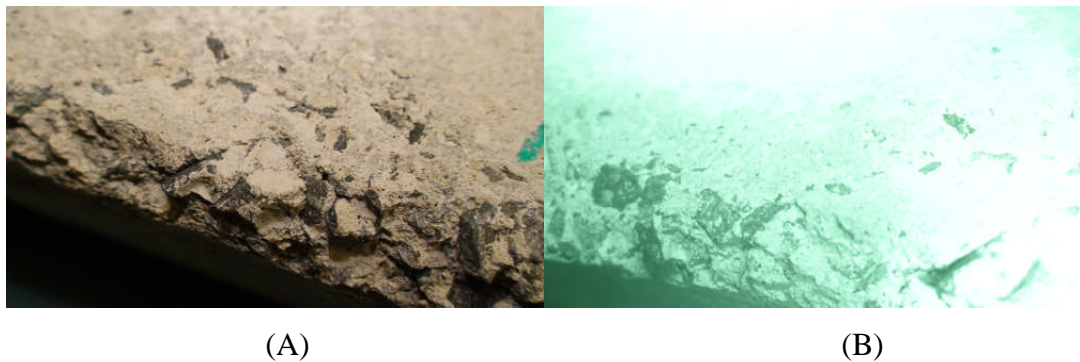


Figure 3.2 Deformed piece of concrete, both photographed in colour (A) and NIR (B).

As demonstrated, the deformities and the material itself can be seen in the steel object. These can be seen clearly with both colour and NIR and both photographs are in similar context. However, when making a comparison of the concrete specimen, the deformities can be seen, but not to the same degree of detail as the steel specimen. When referring to this simulation it is established that experimentation using NIR photogrammetry is within the same context as using colour.

3.3 Stage 2 Laboratory Loading Simulations

In relation to this study, it was determined that it would be best to conduct laboratory-loading simulations. Using this process there would be greater control of environmental factors, such as the lighting. If experimentation was conducted outside, there would be less control and if conducted in the vicinity of the university campus, there would be too much light due to the lamps that surround the campus for students who study late in the evening.

3.3.1 Equipment

Before any experimentation can be carried out, it must be decided, what type of equipment should be used and what structural materials are available for experimentation. All equipment and beams must be fully inspected to determine if they are up to the required standards.

Whilst conducting this study, two cameras were used with thanks to Dr Albert Chong. Both of these cameras were Sony Digital HD video camera recorders; Model No. HDR-SR10E. Similarly, both of these have the full capabilities of utilising colour and NIR photographs. They both have a spatial resolution of 4 megapixels. These cameras also have a range of 300 to 700 nm (nanometre) in the colour spectrum, however the in-built NIR sensors, have a range of 700 to 900 nm in the spectrum range. When conducting the experimentation, a camera stand was used which enabled using both cameras at the same time.

When operating in a low-light setting, and the use of cameras in nightspot, an NIR illuminator was used in order to better illuminate the targets that were placed on the structural beam materials. The NIR illuminator was a Sony HVL-HIRL Video IR Light, which was also provided by Dr Albert Chong. When viewing the photographs taken with the illuminator on, the spectrum range was 700-850 nm. Figure 3.3, displays the two cameras and NIR illuminator that were used, as well as the camera stand.

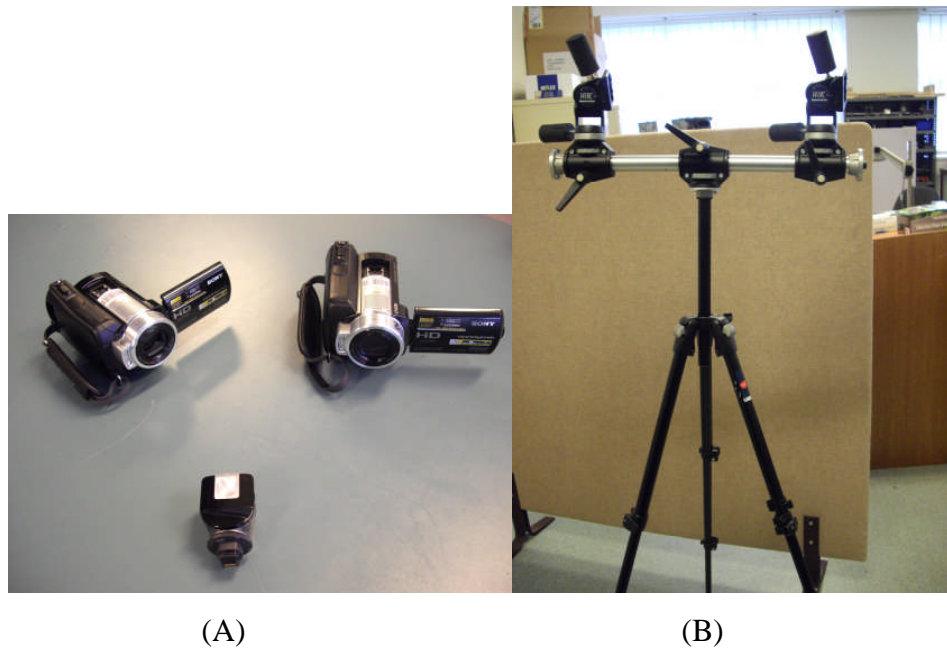


Figure 3.3 The two cameras, the NIR illuminator (A) and the camera stand (B) that were used.

Once the experimentation is completed, it is necessary for the cameras to be calibrated. The calibration of any camera for surveying purposes helps obtain reliable information from the images that are captured and will help adjust any errors that may be encountered. This is discussed in greater detail in Section 3.5.1.

It is necessary for the beams materials, the testing machine and the control board to have a few targets, placed in suitable areas. There must be a few control points for the 3D measurements. With recent studies conducted (Petri Rönholm et al. 2009), the targets that were used were retro-reflective circles approximately 4 mm (millimetres) in diameter and black dot circles approximately 6 mm in diameter. This idea was approached to determine if paper made targets would be a more cost-efficient technique rather than using retro-reflective targets, which are more expensive. The paper targets were glued to the beams, the control board and the testing machine to provide more control for the photographs. The retro-reflective targets were self-adhesive so glue was not necessary.

The targets that were placed on the beams were placed in two rows and there were six retro-reflective targets and seven paper made targets. These targets were deemed necessary as they gave high-precision measurement data when the experimentation was completed and enabled analysis when using the automated digitising technique (Chong 2004).

In reference to the research that was conducted in the Literature Review, there were a total of six structural beams that were used for this experimentation. The materials that were used are mostly found in structures such as bridges for roads and railways. These materials were available immediately from various workshops on the campus. Table 3.1 highlights the details of how the beams were provided and Table 3.2 provides the beams dimensions as well as whether they were hollow or not. In order to illustrate these beams, Appendix C provides a display of each structural beam.

Beam Material	Specifications	Provided By
Concrete	Concrete Reinforced Beam	University of Southern Queensland with appreciation to Atul Sakhiya
Wood	Pine Beam	University of Southern Queensland with appreciation to Adrian Blokland
Composite	Glass-Polymer-Resin Composite Beam	University of Southern Queensland with appreciation to Wayne Crowell and Wagners CFT Manufacturing Pty Ltd.
Steel 01	Steel Post Beam	University of Southern Queensland's metal workshop
Steel 02	Metal C-Section Guard-rail post Beam	Paul Lenton of Main Roads
Timber	Wooden Railway Sleep Beam	Paul Lenton of Main Roads

Table 3.1 Specifications of the structural beams utilised in this study and how they were provided.

Beam Material	Length (metres)	Width (metres)	Height (metres)	Hollow
Concrete	1.397	0.100	0.250	No
Wood	1.557	0.034	0.089	No
Composite	1.111	0.101	0.101	Yes
Steel 01	0.775	0.050	0.075	Yes
Steel 02	2.150	0.110	0.150	Yes
Timber	1.500	0.104	0.209	No

Table 3.2 The Dimensions of each the beams that were used. (Measurements in meters)

When adding the strain onto each beam, the only viable and safe way to apply strain was to use the universal testing machine that is available to students, lecturers and other researchers at the University of Southern Queensland. This machine was manufactured by the Shimazu company and has a range of 0 to 100 Kilonewtons. This machine was also chosen for the purpose of it giving more control, such as changing the strain, rather than using various other means of creating strain. It creates this strain by using a hydraulic jack, which applies the stress on top of the beam and within the centre of the beam. This machine also has a support beam that is approximately a metre long. This is predominately for safety concerns hence the beam material is placed on this support in order for safety standards when people are using this machine. In figure 3.4, both the testing machine and its support beam are displayed to give an idea of what the machine and support beam looked like.

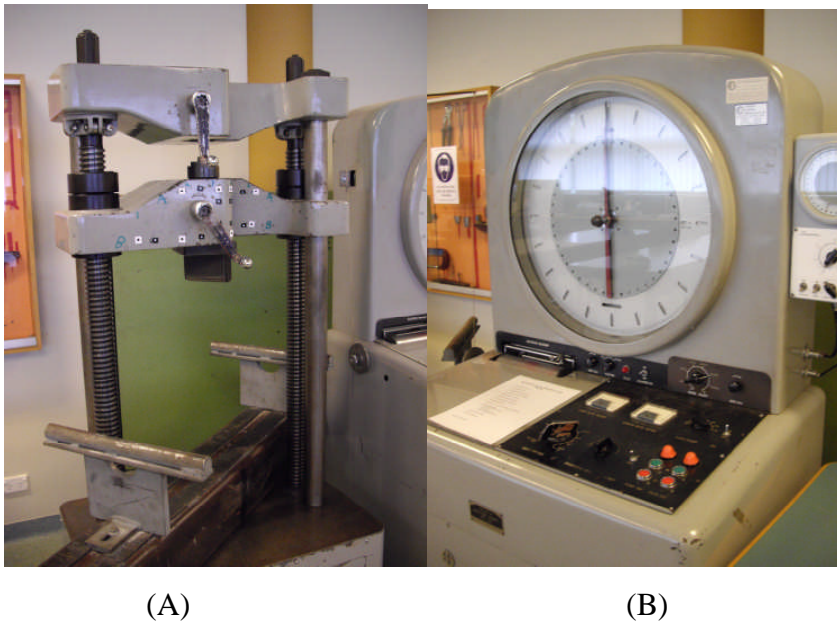


Figure 3.4 The universal testing machine. The hydraulic jack and support beam (A) and the controls for operating the machine (B).

In reference to any experimentation being conducted and in order to provide accurate coordinates of the beams, a control board was built. This served the purpose of having a control coordinate system when analysing the photographs that were taken from the experimentation. This specific board, which is illustrated in Figure 3.5, was built by Adrian Blokland, of the University of Southern Queensland. The board had targets placed evenly, both paper-made and retro-reflective, with a total of six rows and eleven columns. The coordinate system that was established is discussed in further detail in the section 3.5.1.

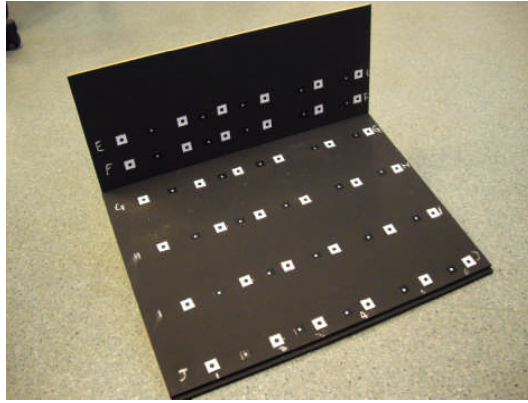


Figure 3.5 The Structural Beam Control Board.

3.3.2 Risk Assessment

It is necessary to determine what risks and safety concerns may be involved when conducting research and study. As a result of examining and reviewing the intended research and methodology, a risk assessment was conducted. This was constructed with the assistance of Mr Mohan Trada and Mr James Farrel. As a consequence it was determined what necessary steps needed be taken.

One such example in relation to the need of a risk assessment was that with using the testing machine, any experimentation that was conducted was always thoroughly inspected by either by myself and by the laboratory technician, Mr Mohan Trada. After this inspection was completed for each beam testing, the machine was operated by either Mohan Trada or myself with supervision from either Mohan Trada, Albert Chong or any laboratory technician that was available. For further information on other risks that were evident and how they were dealt with, please refer to Risk Assessment in Appendix B.

3.3.3 Laboratory Experimentation

After examination of the equipment, the testing of the beams began. In reference to applying stress, each of the beams provided were all placed in the testing machine. The applied stress was placed within the centre of the beams in order to create stress and fractures within the materials.

When performing the loading tests, the beams were tested at various intervals of stress. These intervals were determined by putting significant strain on the beams, whilst adding stress until the beams were about to fail. In order to make sure the beams did not completely break, observations were made when the beams were producing sound and when there was formation of cracks. An example of determining the maximum strain is shown in Figure 3.6 where stress was applied to the concrete beam until a crack was formed.

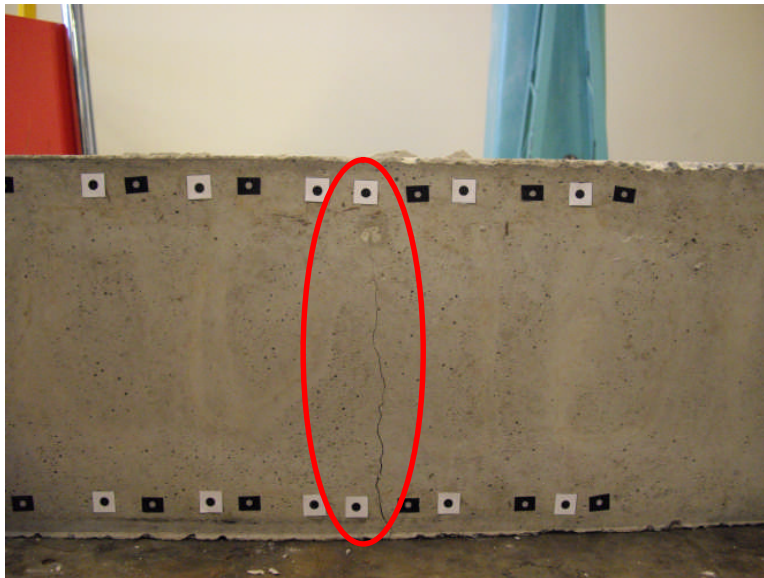


Figure 3.6 The concrete beam after stress was applied. The circle shows the crack that was created during experimentation.

Once each maximum stress level was established, a series of photographs were then taken. The laboratory technician, Mohan Trada, recommended the levels of stress. Mohan was present during the time of experimentation. It is imperative to have suitable supervision in order to avoid serious injury. In table 3.3, the various levels of stress are listed which shows that some of the beams are more fragile than others. For example, the wood beam, was thinner than most and a few deformations were observed before experimentation.

Beam Material	Initial Stress	Average Stress	Maximum Stress
Concrete	0 kN	7 kN	13 kN
Wood	0 kN	2.5 kN	4.5 kN
Composite	0 kN	5 kN	9.5 kN
Steel 01	0 kN	25 kN	42.5 kN
Steel 02	0 kN	25 kN	45 kN
Timber	0 kN	25 kN	45 kN

Table 3.3 The Levels of stress that were applied to each structural beam. (kN = Kilonewtons)

The two cameras were placed on a stand that was capable of holding the two cameras at the same time. The control board that was provided was situated below the beams and placed on a support beam to ensure accurate results were obtained. The cameras were placed in full view of the beams, the control board and the testing machine. They were situated in two positions. On the left of the testing machine, a set of photographs were taken from both cameras, then to the right of the testing machine another set of photographs were taken. Hence, a total of four photographs were taken to ensure accurate results would be achieved when analysing the photographs. Figure 3.7 displays how the experiment was designed and Figure 3.8 shows the plan view of where the cameras were positioned when documentation took place.

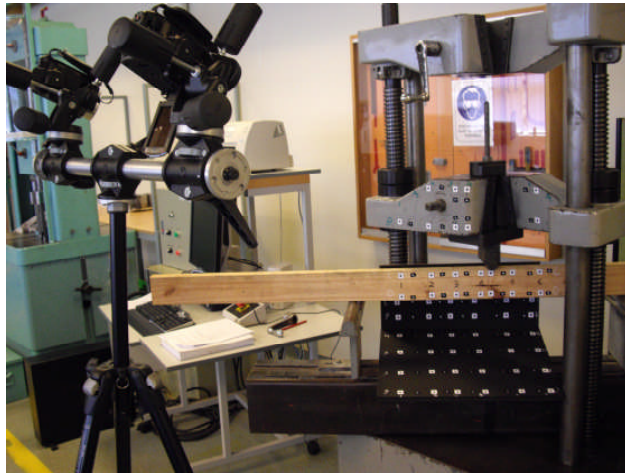


Figure 3.7 The Set-up of stage 2 experimentation.

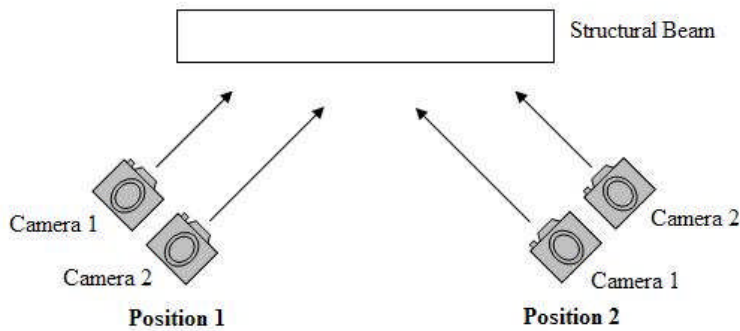


Figure 3.8 The Plan view of stage 2 experimentation.

When taking the photographs, they were initially taken using the colour imagery of the cameras in the first position. Following this, the cameras were moved to the second position and another set of photographs were taken with the laboratory lights turned on. This was performed during the day. After completion of the initial stress, a moderate level of strain was applied and the same procedure as previously discussed, was applied again. Finally, the estimated maximum stress was applied and the same procedure was conducted.

On completion of this procedure with the colour imagery of the cameras, another set of photographs were taken, however, instead of the colour, the NIR imagery of the cameras was utilised and the lights in the laboratory turned off. This was also performed during the day. The same procedure was conducted as previously discussed.

Finally, another set of photographs was taken during a night session with the laboratory lights switched off. When conducting this session, the photographs were taken using the NIR imagery of both cameras. This was performed using the same procedure by documenting the beams and experimenting with the other two steps that were explained earlier. The one difference with this procedure was when taking the photographs in the first position the NIR illuminator was situated on the cameras. After viewing the photographs, it was best to put the illuminator on the minimal setting. Initially, the illuminator was on the first camera and a photograph was taken. This was followed by taking the NIR illuminator off the first camera and placing it on the second camera and subsequently taking another photograph.

3.4 Stage 3 Field Study

On completion of the laboratory simulation, it was interesting to determine whether or not a field study would produce similar results of accuracy what was discovered with the laboratory simulations. The structure that was ideal to record was a bridge structure that was in the vicinity of the University of Southern Queensland, between Z-Block and the Water Engineering/Thermofluids Laboratory. Figure 3.9 shows where the experimentation took place.



Figure. 3.9 The bridge structure showing where the simulation was conducted.

3.4.1 Equipment

The equipment that was used in this stage was similar to the equipment that was used in the laboratory simulations.

Whilst conducting this stage, only one camera was used. This camera was used in the previous stage. This section of the experimentation was conducted in a night session. The NIR illuminator was also used in order to better illuminate the targets that were placed on the bridge structure. Similarly, Dr Albert Chong provided this camera and NIR illuminator. When documenting the photographs in this simulation, the illuminator was set to the higher setting. To ensure that the camera was in a steady position, a stand was used which Dr Albert Chong again provided.

In relation to the night session and considering the observations from the previous simulation, it was best to use retro-reflective circle targets that were approximately 10 mm in diameter. When analysing the photographs from the previous stage, the paper-made targets were difficult to view. These targets were placed in two rows with a total of fourteen columns. It was discovered that by using the colour imagery of the camera, it was difficult to view the targets. In order to view the targets properly, a spot lamp was used to illuminate the targets.

Finally, and similarly to the laboratory simulation, another control board was built in order to have a control coordinate system when analysing the photographs that were taken during the experimentation. Adrian Blokland of the University of Southern Queensland again built this board. This board, in figure 3.10, had retro-reflective targets placed with three rows and columns with a total of nine points. It should be noted that a few of these control points were elevated in order to have these points change in their z-value coordinates. The coordinate system that was established is discussed in further detail in section 3.5.2.

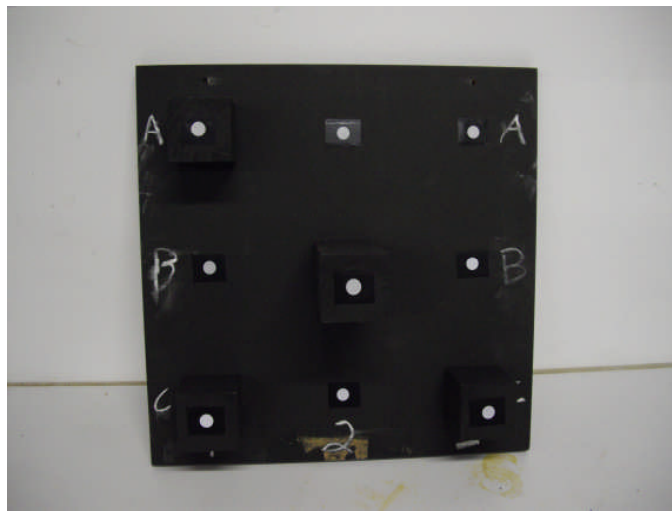


Figure 3.10 The Bridge Control Board.

3.4.2 Experimentation

This stage was conducted in the same manner as the laboratory simulations on structural beams. However, knowledge gained from those simulations indicated that it was best to conduct this field simulation during a night session. In relation to the control board, it was placed on the pillar that was in the centre of the bridge structure and duct tape was used to make sure it was secure.

Upon examining the bridge area with all of the targets in place, it was determined that there should be at least three positions. These were namely to the left of the structure, to the centre of the structure and finally to the right of the structure. This was to ensure that each of the targets were in full view of both the bridge structure and the control board. From these positions, there were a total of five photographs taken from this session. These consisted of two from the left position, one from a central position and two from the right position. Figure 3.11 illustrates a set-up of the testing as well as showing the positions of the camera.

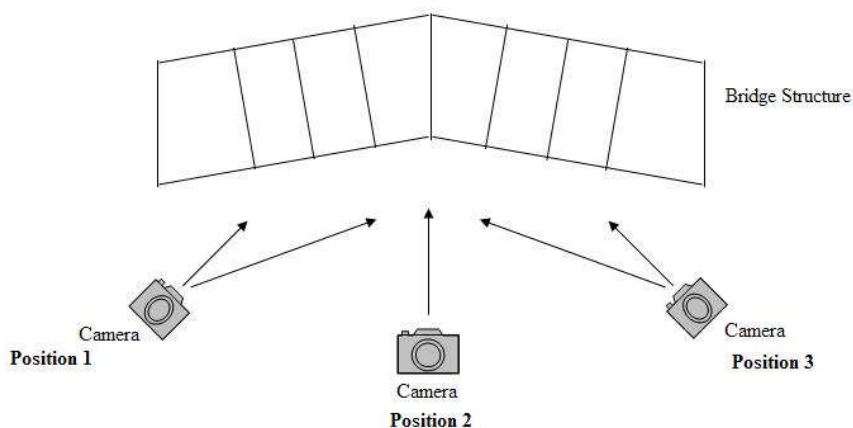


Figure 3.11 A diagram of the camera positions.

Whilst conducting this simulation, the first of a series of five photographs were taken with the colour imagery of the camera. However, as stated previously, in order to view the targets in greater detail with the colour imagery, a spot lamp is required so as to illuminate the targets. The first two photographs were taken in the first position, which viewed the left of the structure and the right. At this point, the camera was moved to the centre of the structure where another photograph was taken. Finally, the last two photographs were taken in the third position. This position captured the left of the structure and the right.

With the completion of this step, another set of photographs was taken by using the NIR imagery of the camera. The procedure was the same as previous and used the colour imagery. The differences during this procedure with the NIR imagery were that the spot lamp and other lights were turned off, the entrance to the Z-block door was covered to ensure that the lights did not interfere with the process and finally the NIR illuminator was attached to the camera.

3.5 Stage 4 Camera Calibrations and Camera Control

As discussed in section 2.6.2, it is necessary for the cameras being used whilst conducting research to be calibrated. In order for the experimentation to be completed in both stages, a calibration device was utilised for both cameras.

3.5.1 Control and calibration of cameras in Stage 2

In reference to the second stage and in order to establish a control system and hence begin the experimentation, the control board that was built needed to be photographed and digitised with a control system that was recognised. This was done by using a control orientation device known as an 'Anhui Dissection control plate', which was provided by Dr Albert Chong. Dr Albert Chong also provided the control coordinates of each position on the plate. In Figure 3.12 shows how the control system was set-up.

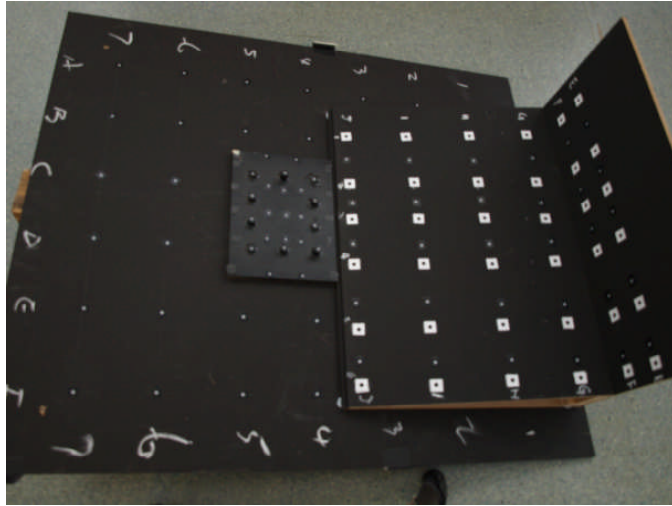


Figure 3.12 The control board, the control plate and target board set-up.

This set-up was conducted using a different camera, the Olympus Digital Camera Model No. E-420, which has a spatial resolution of ten megapixels. Both the control board and the control plate were placed on the board with retro-reflective targets. This ensured the control board had accurate coordinates. Subsequently, a series of photographs were taken. Four were taken on all sides, four were taken with the camera rotated at 90 degrees on each side and finally another four were taken on the corners of the boards. The photographs were digitised and correctly labelled. The resulting bundle file was used in conjunction with the photographs of each documented structural beam.

Following the completion of the control set-up and laboratory simulations, the two cameras that were used were then calibrated using the target board that is displayed in Figure 3.13 and was developed by Albert K. Chong (Chong & Mathieu 2006). This particular target board has a high precision Invar bar that is placed in the middle of the board in order to establish accurate results. The target board was rotated to produce four photos on the sides, another four on the corners to achieve eight photos and finally another four with the camera rotated 90 degrees. Upon completion, a maximum of twelve photographs were obtained in order to converge with each other for self-calibration.

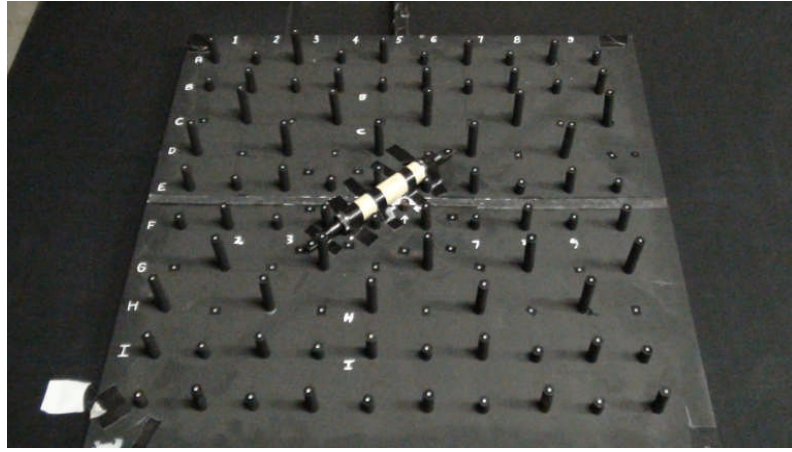


Figure 3.13 The Camera Calibration Set Up with the Invar bar in the middle (Chong & Mathieu 2006, pg. 18).

The first set of photographs was taken in colour and after these were obtained another set of photographs was taken using the NIR imagery. These photographs were then digitised and the parameters of the imagery type, such as the correct focal length, then became available. After obtaining this information, it was applied to bundles that were created for each of the beams that were documented.

3.5.2 Control and calibration of cameras in Stage 3

In reference to the third stage, the procedure was similar to that which was conducted in the second stage. Whilst conducting this stage however, the control set-up and the calibration were done at the same time.

The control board that was built for the bridge structure was placed next to the ‘Small-Orientation Device’. Dr Albert Chong also provided this device, together with the control coordinates. The set-up of these tests are illustrated in figure 3.14.

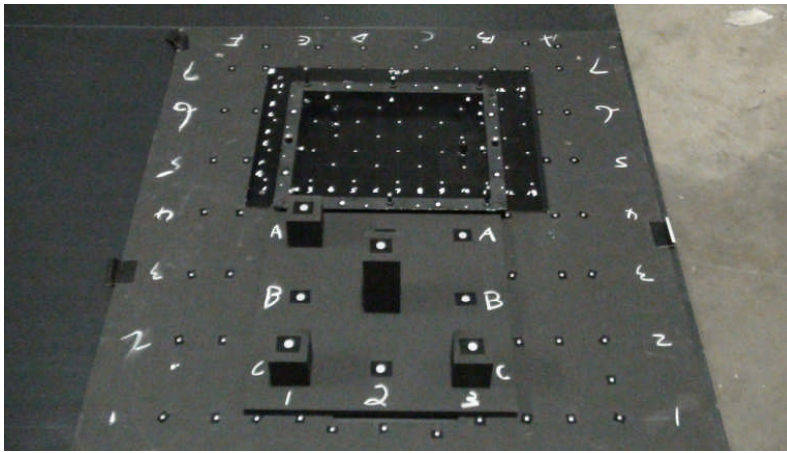


Figure 3.14 The Set-up of both the control and calibration.

The procedure was the same as previous. The only exception was that the camera that was used in stage three was used in the control set-up and calibration. The control and calibration of this stage consisted of four photographs on the side of the board, four photographs taken with the camera rotated to 90 degrees and finally four photographs taken on the corners of the board. Hence, this resulted in a total of twelve photographs. These photographs were taken in both colour and NIR imagery of the camera. They were then digitised, which in turn again provided the correct parameters of the camera, whilst also establishing a control coordinate system on the control board that was used. Analysis of the results was now able to proceed after obtaining these details.

3.6 Construction of Projects

The colour and NIR photographs that were taken during the calibration, control set-up and simulations, were then analysed using the photogrammetric program 'Australis' (Version 6.0, 2002). As discussed in sections 3.3.3 and 3.4.2, the photographs were taken in various conditions. These photographs were then placed into the projects correlating with the specific conditions that they were conducted in, as well as creating projects that examine only the specific target. An example of this was observing the Retro-Reflective targets on the beam at maximum stress while utilising the NIR imagery of the camera in the dark.

Once these photographs were in their correct projects, each photograph was viewed and the targets that were in full view were correctly labelled. Whilst labelling each target, care was needed to ensure that each label was within the centre point of the target. If this were not the case, there would be significant errors in obtaining the correct co-ordinates. In order to ensure this position, each target was zoomed in and it was able to be determined that the label was within the centre of the target.

3.7 Bundle Adjustment

After correctly labelling the targets for each trial, the next stage was the computation of the coordinates of the targets using the main features of 'Australis'. This is known as Bundle Adjustments. This is not the only major feature, however, it is commonly utilised in the photogrammetry profession, as it is a technique that uses these targets and the project's coordinate system to combine into a global model. This model may then be examined in a three dimensional model. Consequently, the results from these adjustments are estimated 3D coordinates of each target that was inserted with the coordinate system that was provided. (Luhmann et al. 2006)

3.8 Calibration Set-up

Before conducting any bundle adjustments of the structural beams and the bridge area, the calibration photographs that were placed in their own projects must be examined first. Without the proper camera parameters of each camera, the coordinates would have been inaccurate. After the completion of labelling each target, a control file of the coordinate system was inputted within the project, which by then, the program completes as a bundle adjustment.

After the completion of all the bundle adjustments with each calibration, the parameters of the cameras have been established. These parameters are inserted within each of the camera properties within their corresponding project. This is done in order to ensure that there are no errors when making comparisons with each imagery condition, level of stress and structural material.

All these parameters are listed in Appendix D in order to illustrate what parameters were applied to each project.

3.9 Control Set-up

On completion of the calibration results that were inserted into all of the camera properties in each project, the control coordinate system now needed to be setup. With a control coordinate system, accurate coordinates can be obtained from each correctly labelled target.

Setting up of the control files for the beams and bridge was conducted by a similar procedure, which was done when calibrating the cameras. After the targets were labelled and the control devices were in place, the control files of the devices were incorporated. Bundle adjustments were made of these control projects, which resulted in control bundle files. Following this, these were then incorporated into every corresponding project in order to produce the 3D coordinates.

This experimentation included a total of two control bundle files, which were based on the control board that was used in the laboratory simulations and the control board that was used in the field-testing.

3.10 Computation of results

After establishing the calibration parameters, making the control bundle files and labelling the targets, a number of bundle adjustments were made of each beam in the various conditions. These included stress levels and imagery conditions. The bridge structure was also under two imagery conditions.

Various bundle adjustments had to be recreated again. This was as a result of some of the targets not being placed in the correct positions as well as a few targets being mislabelled. After these errors were corrected, the coordinates that were obtained were then analysed to determine their accuracy.

In order to determine the accuracy of these coordinates, three measurement techniques were used:

- 3D Distance measurements: Using the coordinates to measure 3d distances between a random set of targets.
- Diagram Comparisons: In reference to the coordinates, a series of graphs were created illustrating the comparisons between the different camera filters at the various levels of stress, as well as which targets were used.
- F-Test Distribution: Finally, a series of F-Test Distributions were conducted on each structural beam and bridge to determine whether there were random errors when comparing colour to NIR.

3.10.1 3D Distance measurements

On examination of the coordinates that were obtained from the bundle adjustments from the structural beam and bridge bundle's, comparisons were made showing the different conditions that were conducted in sections 3.3.3 and 3.4.2. This was shown by calculating the distance from one target to another target. Equation 3.1 shows how this process is calculated.

$$3D \text{ Distances} = \sqrt{(X_2 - X_1)^2 + (Y_2 - Y_1)^2 + (Z_2 - Z_1)^2} \quad (3.1)$$

Where

- X_1 is the 'X-value' of the first target;
- X_2 is the 'X-value' of the second target;
- Y_1 is the 'Y-value' of the first target;
- Y_2 is the 'Y-value' of the second target;
- Z_1 is the 'Z-value' of the first target; and
- Z_2 is the 'Z-value' of the second target.

In relation to this equation, a random set of distances was calculated of the targets that were on the beams and bridge. There were a total of fifteen distances that were calculated in relation to the materials, level of stress and to what type of target this was calculated on. With these fifteen distances, there were five sets on the top row and five sets of the bottom row. Finally, there were another five, which consisted of a combination of both the top and bottom rows. In reference to the bridge structure, a total of fifteen distances were obtained from using the same sets as previously discussed with the structural beams.

After these distances were calculated, they were compared by subtracting the first imagery type to the second imagery type, after which the sample mean of each set was calculated. The sample mean is calculated in equation 3.2.

$$\bar{x} = \frac{x_1 + x_2 + \dots + x_n}{n} = \sum_{i=1}^n \frac{x_i}{n} \quad (3.2)$$

Where x_i is the total sum of observations; and
 n is the number of observations.

When examining these sample means, the next step was to determine how much difference there was in context between these imagery conditions. This is to make sure that these distances are within accurate parameters. This is done by utilising equation 3.3.

$$\begin{aligned} \text{Colour} - \text{NIR} &= \bar{x}_{\text{Colour}} - \bar{x}_{\text{NIR}} \\ \text{Colour} - \text{Total NIR} &= \bar{x}_{\text{Colour}} - \bar{x}_{\text{Total NIR}} \\ \text{NIR} - \text{Total NIR} &= \bar{x}_{\text{NIR}} - \bar{x}_{\text{Total NIR}} \end{aligned} \quad (3.3)$$

On examination of these differences, it is determined that with each colour imagery type to be in similar context with each other, a maximum difference of ± 1 mm (millimetre) is required to be achieved. These calculated distances can be viewed in section 4.2 in the next chapter.

3.10.2 Diagram comparisons

After the completion of the 3D distance calculations, it was decided that it would be best to construct a representation of each target that was placed on the structure with the level of stress being applied as well as the bridge structure that was conducted in the field-testing. This was done in order to see if the imagery conditions of the targets on the materials were in similar context to each other or if there was a considerable difference between the targets. These graphs also illustrate what level of stress was applied for the structural beam materials as well as displaying where the stress was positioned. They were all created with the program 'Microsoft EXCEL' by using the coordinates that were provided by the bundles. Closer examinations of these graphs are discussed in section 4.3 in the next chapter.

3.10.3 F-Test Distribution

In reference to this study, the main hypothesis that was established was to determine whether observations that were taken in both colour and NIR imagery would be in a similar context. In order to prove this hypothesis, a series of F-Test Distributions were conducted. In relation to the F-Test Distributions, comparisons were made through the image types and types of targets that were used. The distributions were conducted and comparisons made between the Colour against the individual NIR sessions and Colour against the Total NIR session.

In order to calculate these F-Test values, the Total Sigma Estimates that were obtained from the bundles were examined and then placed within the following equation. This was performed in order to calculate the standard deviation of the targets in question:

$$e = \sqrt{(sX^2 + sY^2 + sZ^2)} \quad (3.4)$$

Where sX is the Total Sigma Estimates of the 'x-value' of the observations;
 sY is the Total Sigma Estimates of the 'y-value' of the observations;
 sZ is the Total Sigma Estimates of the 'z-value' of the observations; and
 e is the standard deviation of the observations.

After the standard deviations were calculated for each target, the F-Tests values were calculated from the program 'Microsoft EXCEL' which then produced the F-Test Values between Colour to NIR and Colour to Total NIR. Following these calculations, the 90% and 99% confidence limits were obtained. This was made possible by examining the F-Distribution table, hence determining the degrees of freedom for both image types. These were determined by the number of observations that were conducted with Colour and the NIR sessions minus one.

Once the F-Test values and the confidence limits were obtained the following was concluded. If the F-Test values are lower than the confidence limit, the hypothesis that was stated above is accepted as a null hypothesis (H_0), which is a correct assumption. However, if the F-Test values are above the confidence limit, then the null hypothesis is rejected and this is known as an alternative hypothesis (H_A).

The F-Test Distribution's of each target are discussed in further detail in section 4.4 in the next chapter.

3.11 Conclusion

Each beam and bridge structure was documented in both camera imagery types whilst conducting the experimentation of the laboratory simulations and field-testing. A night session was conducted as well as the day session.

Whilst analysing the photographs in 'Australis', it seemed that the retro-reflective targets are best suited for NIR imagery. The paper-made targets proved difficult to view. Each of the measurement techniques discussed in this chapter are calculated and the results that were generated from each beam and bridge are discussed in greater detail in Chapter 4.

Chapter 4

Analysis of Results

4.1 Introduction

In relation to the experimentation that was discussed in Chapter 3, all of the photographs that were obtained were successfully analysed by using the ‘Australis’ software. On examination of the three measurements techniques discussed in section 3.10, it can be determined whether or not using NIR photogrammetry will be in similar context with colour imagery.

4.2 3D Distance measurements

In reference to the differences and calculations that were discussed in section 3.10.1 from the previous chapter, the following tables were created. These tables illustrate each row, as well as the level of stress that was applied for the structural beam materials. In relation to the bridge structure, a table was constructed with the mean top and bottom rows as well as a combination of both.

Beam Material	Target	Image type Comparisons		
		Colour – NIR	Colour – Total NIR	NIR – Total NIR
Concrete	Paper	0.293	-0.085	-0.378
	Retro	-0.260	0.189	0.449
Wood	Paper	0.087	0.170	0.083
	Retro	-0.089	-0.145	-0.056
Composite	Paper	0.061	-0.130	-0.192
	Retro	-0.023	-0.214	-0.191
Steel 01	Paper	0.158	0.095	-0.064
	Retro	-0.236	0.228	0.465
Steel 02	Paper	0.048	-0.110	-0.158
	Retro	-0.243	0.170	0.413
Timber	Paper	-0.303	0.173	0.476
	Retro	0.159	0.316	0.157

Table 4.1 Comparison of Sample Mean 3D distances of the Top Row at Initial Stress. (mm)

Table 4.1, displays the sample means of each of the 3D distances of the Top Row of each structural beam while no stress was being applied to the beam in question. After examining these results, it can be seen that these distances are within acceptable parameters, as they have not exceeded ± 1 mm.

Upon further examination, there are a few of these distances that are in similar context to each image type. These distances illustrate that the following corresponding comparisons are within close resemblance to each other:

Colour – NIR: Retro-Reflective targets of the Composite Beam

Colour – Total NIR: Paper-Made targets of the Concrete Beam

NIR – Total NIR: Retro-Reflective targets of the Wood Beam

The next set of results that are shown are the sample means of each of the 3D distances of the Bottom Row of each structural beam while no stress was being applied to the beam in question.

Beam Material	Target	Image type Comparisons		
		Colour – NIR	Colour – Total NIR	NIR – Total NIR
Concrete	Paper	0.127	0.083	-0.044
	Retro	-0.033	0.156	0.189
Wood	Paper	0.008	-0.127	-0.136
	Retro	0.156	-0.015	-0.171
Composite	Paper	0.047	-0.056	-0.103
	Retro	0.054	-0.114	-0.167
Steel 01	Paper	0.009	-0.160	-0.169
	Retro	-0.054	-0.144	-0.089
Steel 02	Paper	0.059	-0.265	-0.323
	Retro	-0.188	0.087	0.275
Timber	Paper	-0.045	0.153	0.198
	Retro	-0.010	0.140	0.150

Table 4.2 Comparison of Sample Mean 3D distances of the Bottom Row at Initial Stress. (mm)

In Table 4.2, it can be seen that these distances are within acceptable parameters as they have not exceeded ± 1 mm. Upon further examination, there are a few of these distances that are in similar context to each image type. These distances show that the following corresponding comparisons are within close resemblance to each other:

Colour – NIR: Paper-Made targets of the Wood Beam

Colour – Total NIR: Retro-Reflective targets of the Wood Beam

NIR – Total NIR: Paper-Made targets of the Concrete Beam

The next set of results that are shown are the sample means of each of the 3D distances of combinations of the two rows of each structural beam while no stress was being applied to the beam in question.

Beam Material	Target	Image type Comparisons		
		Colour – NIR	Colour – Total NIR	NIR – Total NIR
Concrete	Paper	0.404	0.155	-0.249
	Retro	-0.288	0.350	0.638
Wood	Paper	-0.015	-0.121	-0.106
	Retro	-0.058	0.027	0.085
Composite	Paper	0.046	-0.136	-0.182
	Retro	-0.083	-0.133	-0.050
Steel 01	Paper	0.100	-0.055	-0.154
	Retro	-0.119	0.007	0.126
Steel 02	Paper	-0.077	-0.074	0.002
	Retro	-0.448	0.236	0.684
Timber	Paper	-0.399	0.260	0.659
	Retro	-0.224	0.414	0.638

Table 4.3 Comparison of Sample Mean 3D distances of both Rows at Initial Stress. (mm)

In Table 4.3, it can be seen that these distances are within acceptable parameters as they have not exceeded ± 1 mm. Upon further examination, there are a few of these distances that are in similar context to each image type. Looking at these distances, it is evident that the following corresponding comparisons are within close resemblance to each other:

Colour – NIR: Paper-Made targets of the Wood Beam

Colour – Total NIR: Retro-Reflective targets of the first Steel Beam

NIR – Total NIR: Paper-Made targets of the second Steel Beam

The next set of results that are shown are the sample means of each of the 3D distances of the Top Row of each structural beam while moderate stress was being applied to the beam in question.

Beam Material	Target	Image type Comparisons		
		Colour – NIR	Colour – Total NIR	NIR – Total NIR
Concrete	Paper	0.375	-0.163	-0.538
	Retro	-0.265	0.454	0.719
Wood	Paper	0.107	0.022	-0.085
	Retro	0.017	-0.078	-0.094
Composite	Paper	0.166	-0.104	-0.270
	Retro	-0.191	0.024	0.215
Steel 01	Paper	0.066	-0.127	-0.193
	Retro	-0.111	-0.079	0.101
Steel 02	Paper	-0.115	0.027	0.143
	Retro	-0.082	0.038	0.120
Timber	Paper	-0.284	0.182	0.466
	Retro	0.181	0.047	-0.134

Table 4.4 Comparison of Sample Mean 3D distances of the Top Row at Average Stress. (mm)

In Table 4.4, it can be seen that these distances are within acceptable parameters as they have not exceeded ± 1 mm. Upon further examination, there are a few of these distances that are in similar context to each image type. These distances illustrate that the following corresponding comparisons are within close resemblance to each other:

Colour – NIR: Paper-Made targets of the Wood Beam

Colour – Total NIR: Retro-Reflective targets of the first Steel Beam

NIR – Total NIR: Paper-Made targets of the second Steel Beam

The next set of results that are shown are the sample means of each of the 3D distances of the Bottom Row of each structural beam while moderate stress was being applied to the beam in question.

Beam Material	Target	Image type Comparisons		
		Colour – NIR	Colour – Total NIR	NIR – Total NIR
Concrete	Paper	0.219	-0.004	-0.223
	Retro	-0.208	0.199	0.408
Wood	Paper	0.029	-0.126	-0.154
	Retro	0.181	0.001	-0.180
Composite	Paper	0.096	-0.084	-0.181
	Retro	-0.013	-0.123	-0.110
Steel 01	Paper	0.096	-0.027	-0.122
	Retro	-0.079	-0.011	0.068
Steel 02	Paper	-0.137	-0.067	0.070
	Retro	-0.069	-0.024	0.045
Timber	Paper	-0.086	0.063	0.149
	Retro	-0.062	0.036	0.098

Table 4.5 Comparison of Sample Mean 3D distances of the Bottom Row at Average Stress.
(mm)

In Table 4.5, it can be seen that these distances are within acceptable parameters as they have not exceeded ± 1 mm. Upon further examination, there are a few of these distances that are in similar context to each image type. On examination of these distances, it can be shown that the following corresponding comparisons are within close resemblance to each other:

- Colour – NIR: Retro-Reflective targets of the Composite Beam
- Colour – Total NIR: Retro-Reflective targets of the Wood Beam
- NIR – Total NIR: Retro-Reflective targets of the second Steel Beam

The next set of results that are shown are the sample means of each of the combinations of the two rows of each structural beam while moderate stress was being applied to the beam in question.

Beam Material	Target	Image type Comparisons		
		Colour – NIR	Colour – Total NIR	NIR – Total NIR
Concrete	Paper	0.428	-0.178	-0.605
	Retro	-0.533	0.491	1.024
Wood	Paper	0.124	-0.152	-0.276
	Retro	0.033	0.011	-0.023
Composite	Paper	0.181	-0.100	-0.281
	Retro	-0.173	-0.022	0.152
Steel 01	Paper	0.110	-0.117	-0.228
	Retro	-0.267	-0.023	0.170
Steel 02	Paper	-0.125	0.047	0.172
	Retro	-0.156	0.212	0.368
Timber	Paper	-0.204	0.588	0.791
	Retro	-0.337	0.327	0.664

Table 4.6 Comparison of Sample Mean 3D distances of both Rows at Average Stress. (mm)

In Table 4.6, it can be seen that all but one of these distances are within acceptable parameters, as they have not exceeded ± 1 mm. The Retro-Reflective targets of the Concrete beam that was compared between the NIR and Total NIR sessions showed that it surpasses the intended limit of accuracy. This could be due to errors in labelling the targets in the projects, and or the quality of the photograph when it was digitised.

Upon further examination, there are a few distances that are in similar context to each image type. In reference to these distances, the retro-reflective targets on the wood beam for all comparisons showed that they were in close resemblance to each other in each imagery type.

The next set of results that are shown are the sample means of each of the 3D distances of the Top Row of each structural beam while the estimated maximum stress was being applied to the beam in question.

Beam Material	Target	Image type Comparisons		
		Colour – NIR	Colour – Total NIR	NIR – Total NIR
Concrete	Paper	0.157	-0.168	-0.325
	Retro	-0.449	-0.021	0.428
Wood	Paper	0.297	0.076	-0.220
	Retro	0.364	0.011	-0.352
Composite	Paper	0.037	-0.244	-0.281
	Retro	-0.125	-0.051	0.074
Steel 01	Paper	-0.132	-0.253	-0.121
	Retro	0.246	0.169	-0.127
Steel 02	Paper	-0.048	0.046	0.093
	Retro	-0.331	0.173	0.503
Timber	Paper	-0.208	0.038	0.246
	Retro	-0.359	-0.069	0.291

Table 4.7 Comparison of Sample Mean 3D distances of the Top Row at Maximum Stress. (mm)

In Table 4.7, it can be seen that these distances are within acceptable parameters as they have not exceeded ± 1 mm. Upon further examination, there are a few of these distances that are in similar context to each image type. In reference to these distances, it can be determined that the following corresponding comparisons are within close resemblance to each other:

Colour – NIR: Paper-Made targets of the Composite Beam

Colour – Total NIR: Retro-Reflective targets of the Wood Beam

NIR – Total NIR: Retro-Reflective targets of the Composite Beam

The next set of results that are shown are the sample means of each of the 3D distances of the Bottom Row of each structural beam while the estimated maximum stress was being applied to the beam in question.

Beam Material	Target	Image type Comparisons		
		Colour – NIR	Colour – Total NIR	NIR – Total NIR
Concrete	Paper	-0.063	-0.231	-0.168
	Retro	-0.100	0.067	0.168
Wood	Paper	0.173	0.189	0.016
	Retro	0.310	-0.007	-0.317
Composite	Paper	0.031	-0.190	-0.221
	Retro	-0.008	-0.002	0.006
Steel 01	Paper	-0.064	-0.062	0.002
	Retro	0.109	0.017	-0.092
Steel 02	Paper	-0.012	-0.090	-0.078
	Retro	-0.098	0.055	0.153
Timber	Paper	-0.114	-0.166	-0.052
	Retro	-0.258	-0.053	0.206

Table 4.8 Comparison of Sample Mean 3D distances of the Bottom Row at Maximum Stress. (mm)

In Table 4.8, it can be seen that these distances are within acceptable parameters as they have not exceeded ± 1 mm. Upon further examination, there are a few of these distances that are in similar context to each image type. Results of these distances show that the following corresponding comparisons are within close resemblance to each other:

- Colour – NIR: Retro-Reflective targets of the Composite Beam
- Colour – Total NIR: Retro-Reflective targets of the Composite Beam
- NIR – Total NIR: Paper-Made targets of the first Steel Beam

The next set of results that are shown are the sample means of each of the combinations of the two rows of each structural beam while the estimated maximum stress was being applied to the beam in question.

Beam Material	Target	Image type Comparisons		
		Colour – NIR	Colour – Total NIR	NIR – Total NIR
Concrete	Paper	-0.236	-0.025	0.211
	Retro	-0.626	0.202	0.829
Wood	Paper	0.141	0.053	-0.087
	Retro	0.223	0.051	-0.172
Composite	Paper	0.106	-0.228	-0.334
	Retro	-0.122	-0.032	0.090
Steel 01	Paper	-0.138	-0.149	-0.011
	Retro	0.220	0.107	-0.148
Steel 02	Paper	0.034	0.128	0.094
	Retro	-0.331	0.261	0.592
Timber	Paper	-0.072	0.124	0.196
	Retro	-0.608	0.078	0.687

Table 4.9 Comparison of Sample Mean 3D distances of both Rows at Maximum Stress. (mm)

In Table 4.9, it can be seen that these distances are within acceptable parameters as they have not exceeded ± 1 mm. Upon further examination, there are a few of these distances that are in similar context to each image type. On examination of these distances, it is evident that the following corresponding comparisons are within a close resemblance to each other:

Colour – NIR: Paper-Made targets of the second Steel Beam

Colour – Total NIR: Paper-Made targets of the Concrete Beam

NIR – Total NIR: Paper-Made targets of the first Steel Beam

The next set of results that are shown are the sample means of each row and a combination of both rows of the bridge structure that was conducted in the field-testing.

Set of Rows	Colour – NIR
Top Row	-0.057
Bottom Row	0.144
Both Rows	-0.198

Table 4.10 Comparison of Sample Mean 3D distances of the bridge structure. (mm)

The examination of these results in Table 4.10, reveals that these distances are within acceptable parameters as they have not exceeded ± 1 mm.

After completing the calculations of these distances, they achieved an accuracy that did not surpass ± 1 mm. This illustrates that the targets were labelled in precise order and when comparing colour to NIR, they are in similar context.

4.2 Diagram comparisons

In reference to section 3.10.2, the following graphs depict the figures that were created in relation to each material. Below are two figures that are representations of the Concrete Beam at 0 kN. The first figure displays the Paper-Made targets and the second figure displays the Retro-Reflective targets.

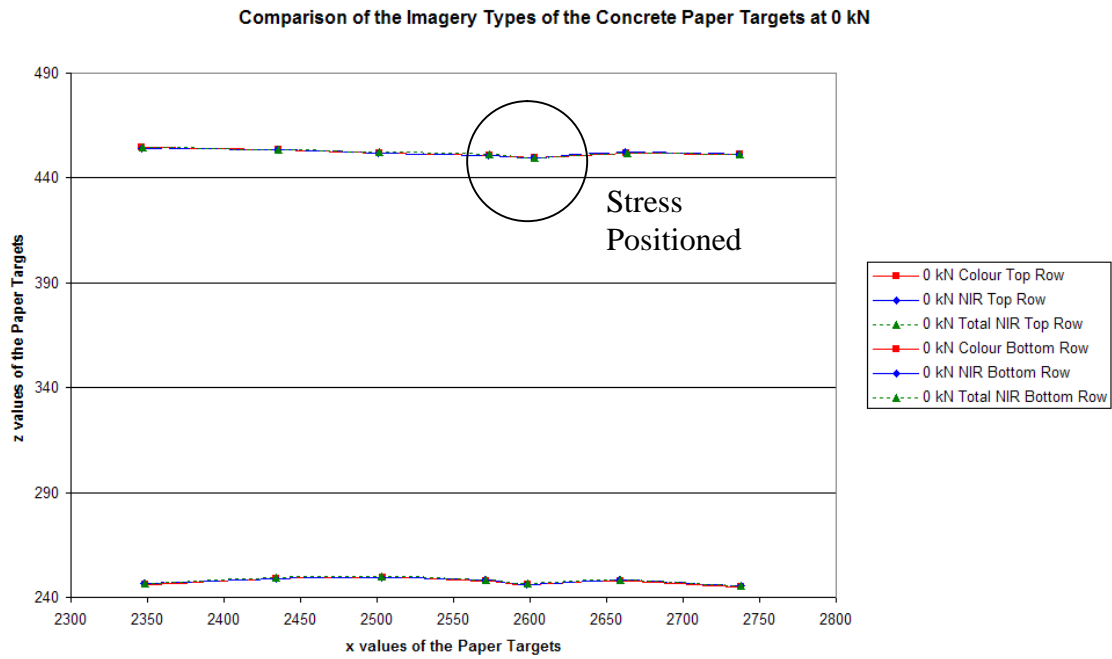


Figure 4.1 Graph of the Imagery Types of Paper-Made targets on the Concrete beam at 0 kN.

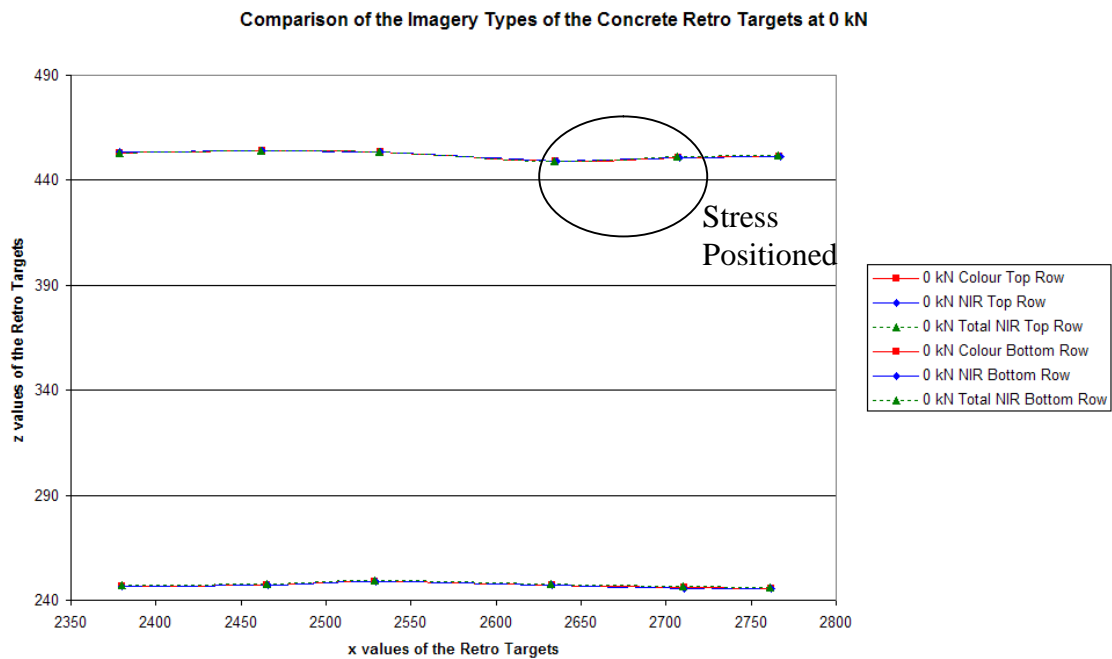


Figure 4.2 Graph of the Imagery Types of Retro-Reflective targets on the Concrete beam at 0 kN.

Whilst viewing Figures 4.1 and 4.2, it can be seen that the imagery types are within similar context to each other regardless of which target is being documented at the time. The next set of figures are of the concrete beam where stress is being applied at 7 kN. The first figure shows the Paper-Made targets, while the second shows the Retro-Reflective targets.

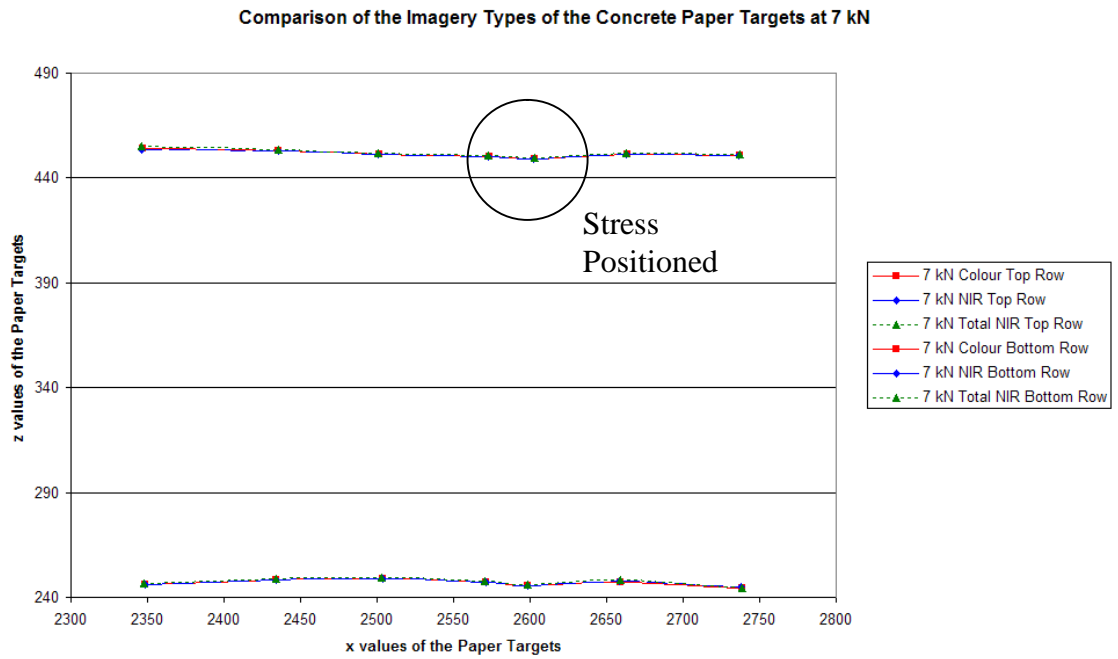


Figure 4.3 Graph of the Imagery Types of Paper-Made targets on the Concrete beam at 7 kN.

Comparison of the Imagery Types of the Concrete Retro Targets at 7 kN

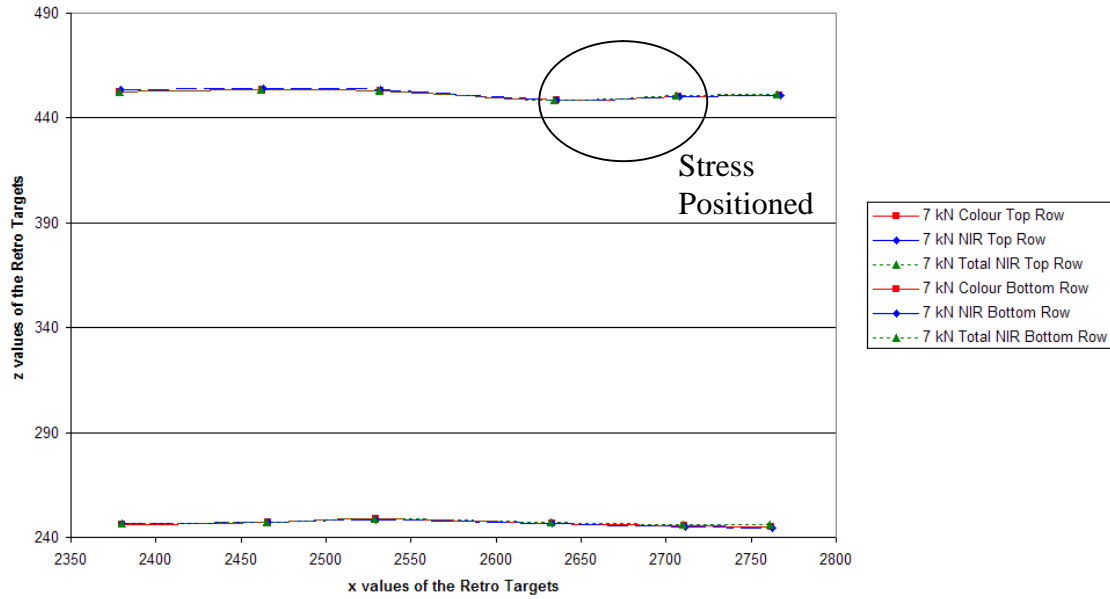


Figure 4.4 Graph of the Imagery Types of Retro-Reflective targets on the Concrete beam at 7 kN.

Whilst viewing Figures 4.3 and 4.4, it can be seen that the imagery types are within a similar context to each other regardless of which target is being documented at the time. The next set of figures are of the concrete beam where stress is being applied at 13 kN. The first figure shows the Paper-Made targets, while the second shows the Retro-Reflective targets.

Comparison of the Imagery Types of the Concrete Paper Targets at 13 kN

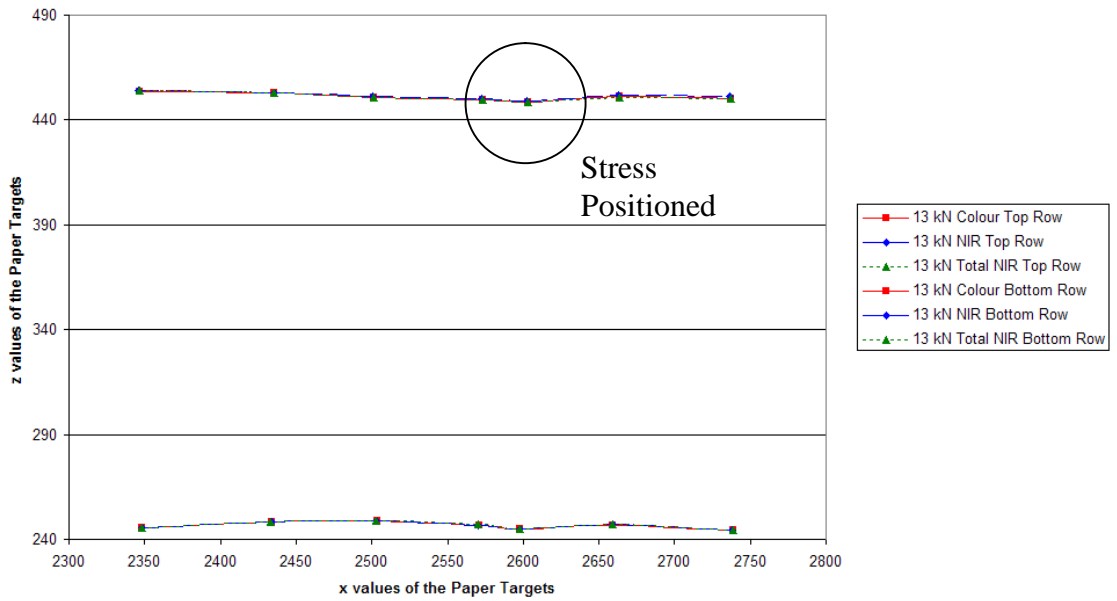


Figure 4.5 Graph of the Imagery Types of Paper-Made targets on the Concrete beam at 13 kN.

Comparison of the Imagery Types of the Concrete Retro Targets at 13 kN

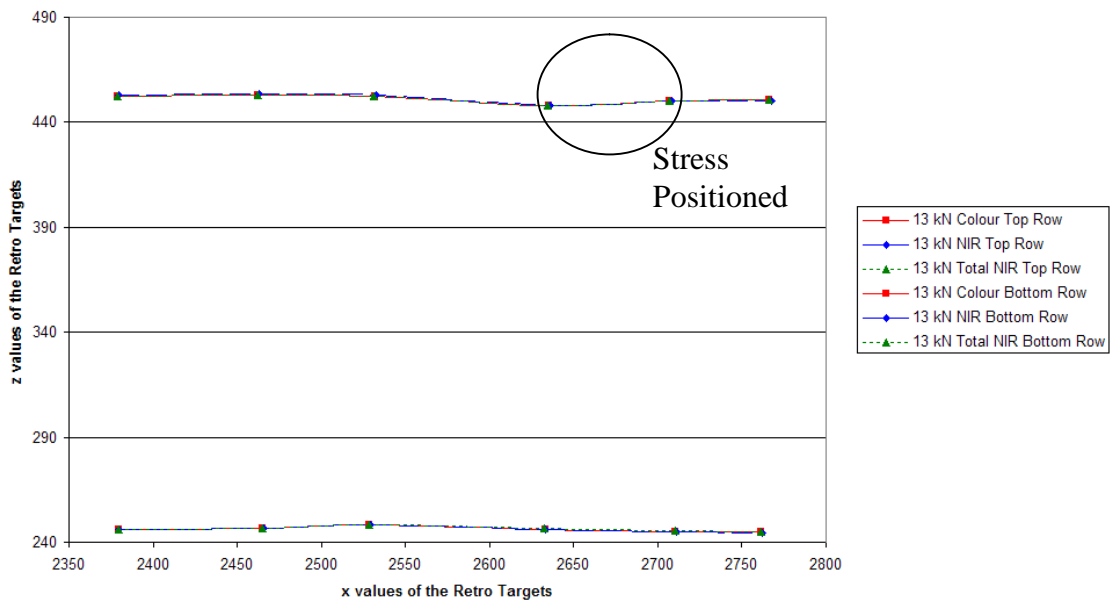


Figure 4.6 Graph of the Imagery Types of Retro-Reflective targets on the Concrete beam at 13 kN.

Whilst viewing Figures 4.5 and 4.6, it can be seen that the imagery types are within a similar context to each other regardless of which target is being documented at the time. The next set of figures are of the wood beam where there is no stress being applied. The first figure shows the Paper-Made targets, while the second shows the Retro-Reflective targets.

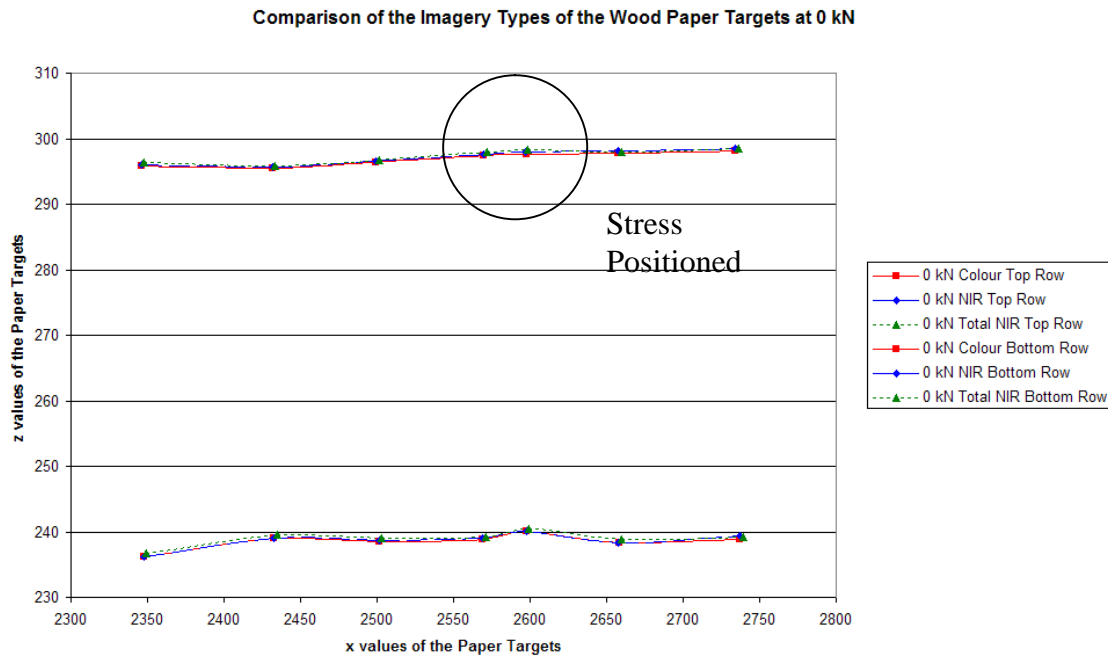


Figure 4.7 Graph of the Imagery Types of Paper-Made targets on the Wood beam at 0 kN.

Comparison of the Imagery Types of the Wood Retro Targets at 0 kN

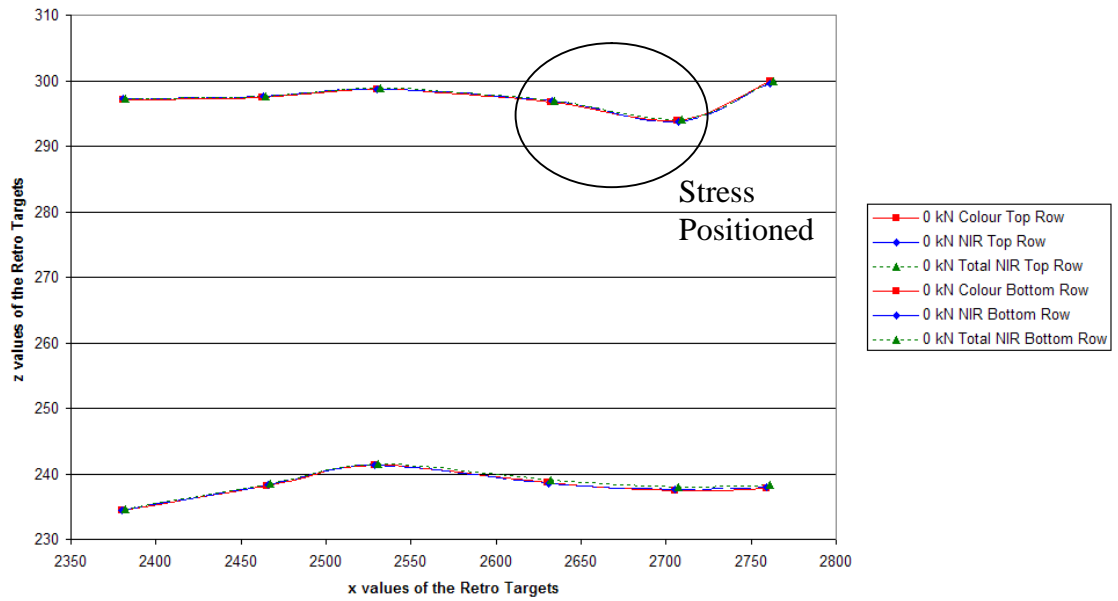


Figure 4.8 Graph of the Imagery Types of Retro-Reflective targets on the Wood beam at 0 kN.

Whilst viewing Figures 4.7 and 4.8, it can be seen that the imagery types are within a similar context to each other regardless of which target is being documented at the time. The next set of figures is of the wood beam where stress is being applied at 2.5 kN. The first figure shows the Paper-Made targets, while the second shows the Retro-Reflective targets.

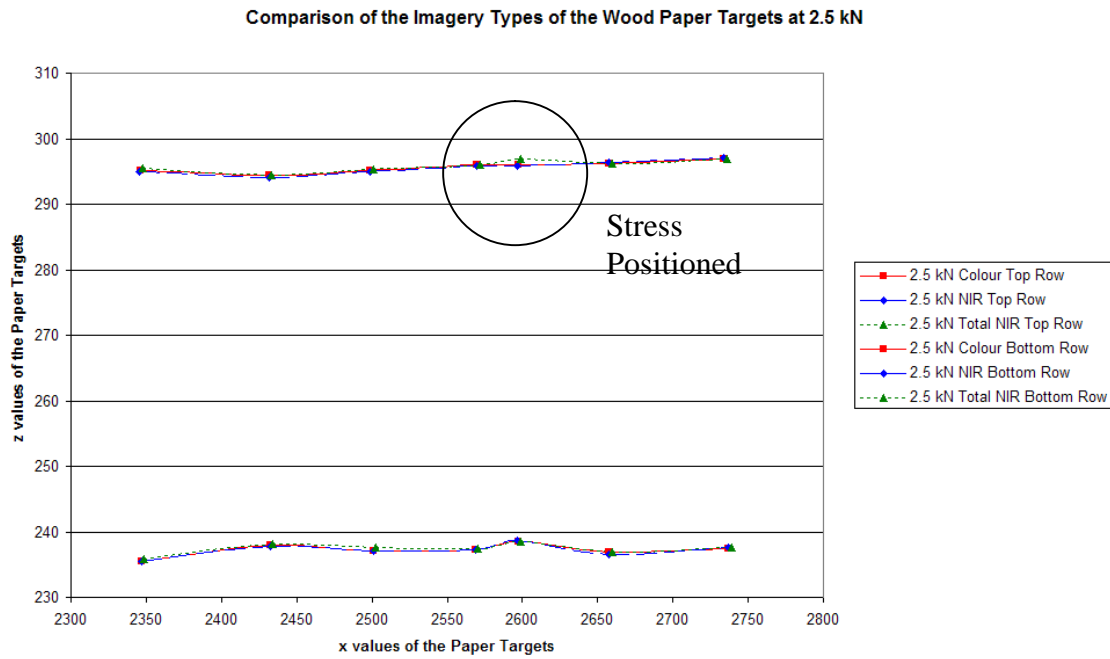


Figure 4.9 Graph of the Imagery Types of Paper-Made targets on the Wood beam at 2.5 kN.

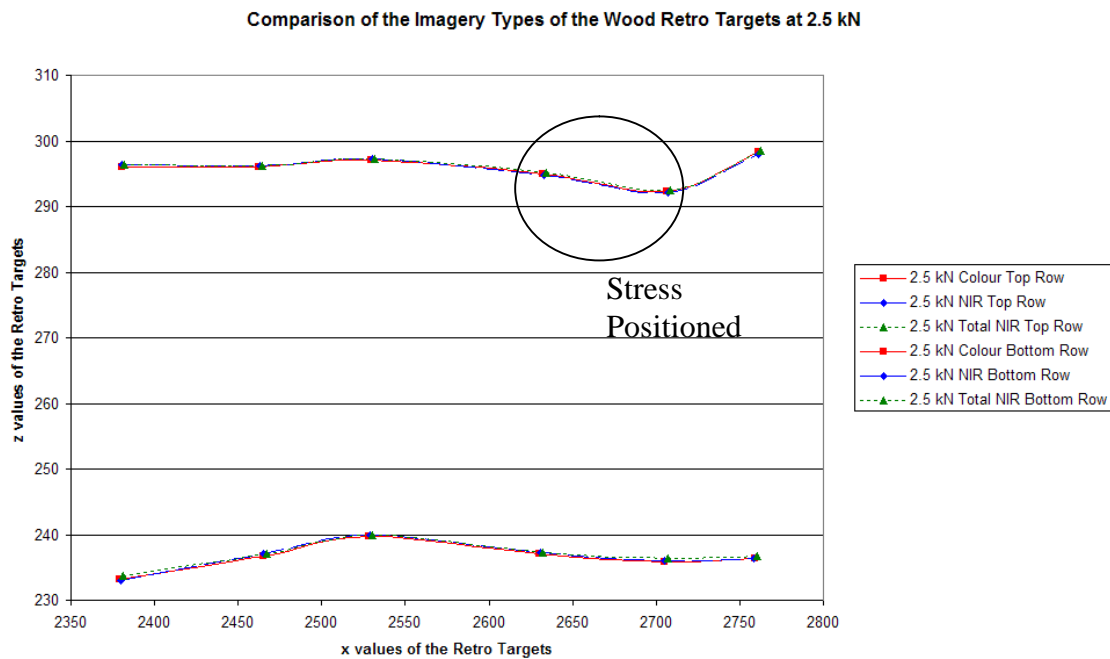


Figure 4.10 Graph of the Imagery Types of Retro-Reflective targets on the Wood beam at 2.5 kN.

Whilst viewing Figures 4.9 and 4.10, it can be seen that the imagery types are within a similar context to each other regardless of which target is being documented at the time. The next set of figures is of the wood beam where stress is being applied at 4.5 kN. The first figure shows Paper-Made targets, while the second shows Retro-Reflective targets.

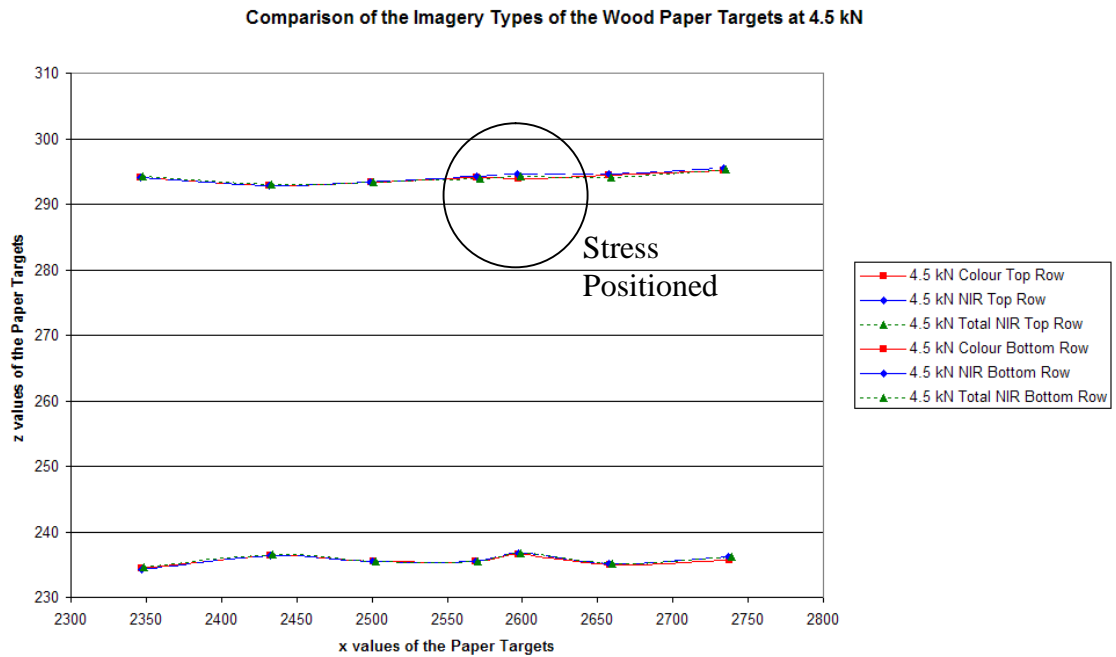


Figure 4.11 Graph of the Imagery Types of Paper-Made targets on the Wood beam at 4.5 kN.

Comparison of the Imagery Types of the Wood Retro Targets at 4.5 kN

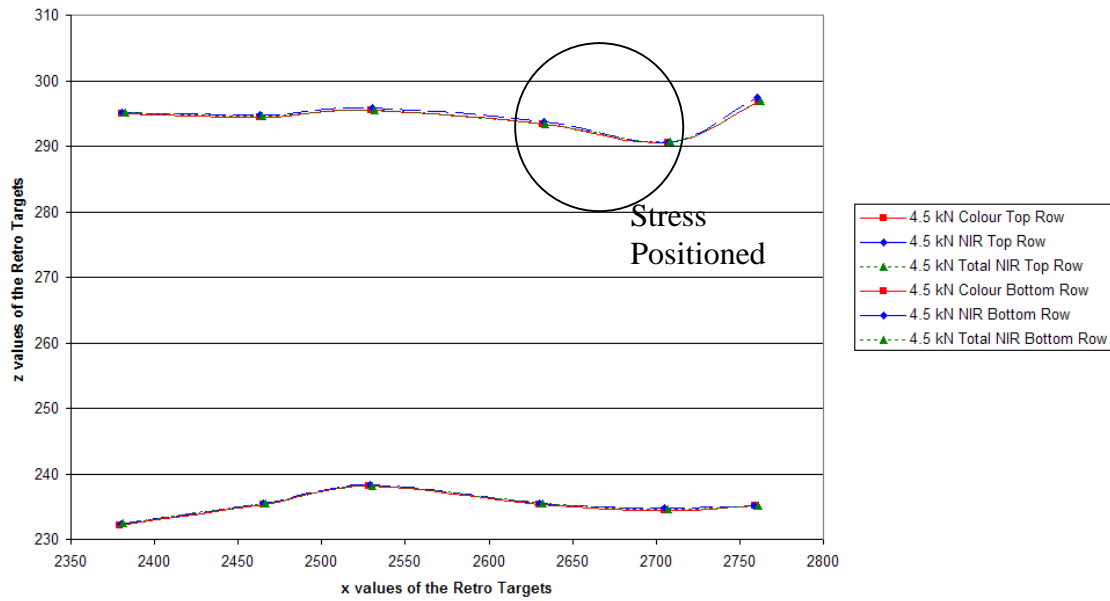


Figure 4.12 Graph of the Imagery Types of Retro-Reflective targets on the Wood beam at 4.5 kN.

Whilst viewing Figures 4.11 and 4.12, it can be seen that the imagery types are within a similar context to each other regardless of which target is being documented at the time. The next set of figures is of the composite beam where there is no stress being applied. The first figure shows the Paper-Made targets and the second shows the Retro-Reflective targets.

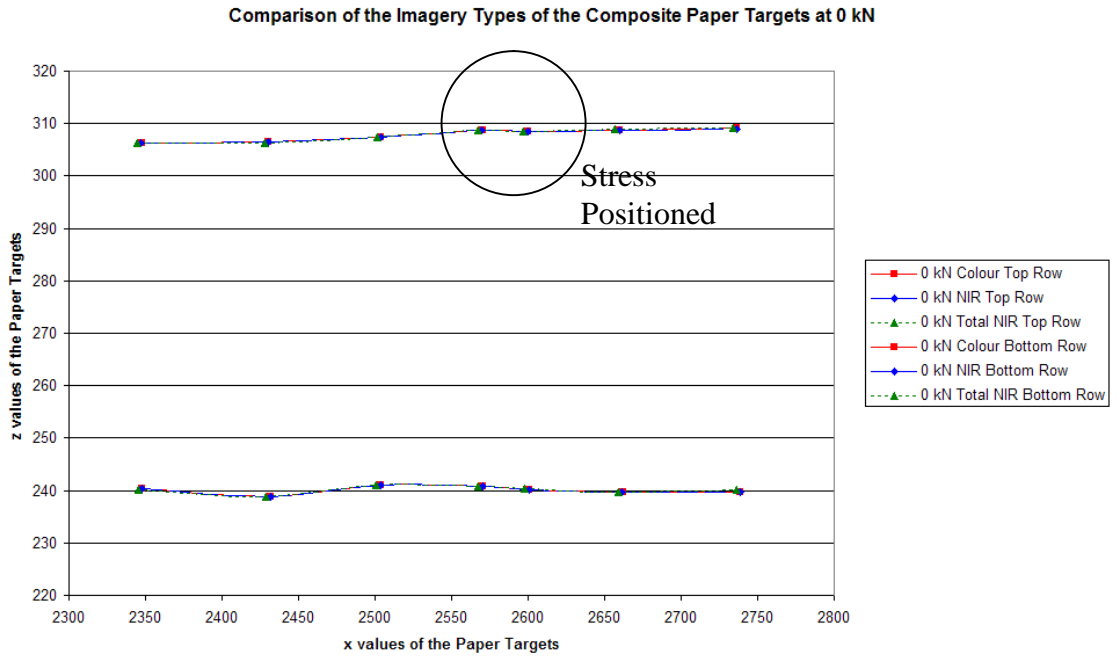


Figure 4.13 Graph of the Imagery Types of Paper-Made targets on the Composite beam at 0 kN.

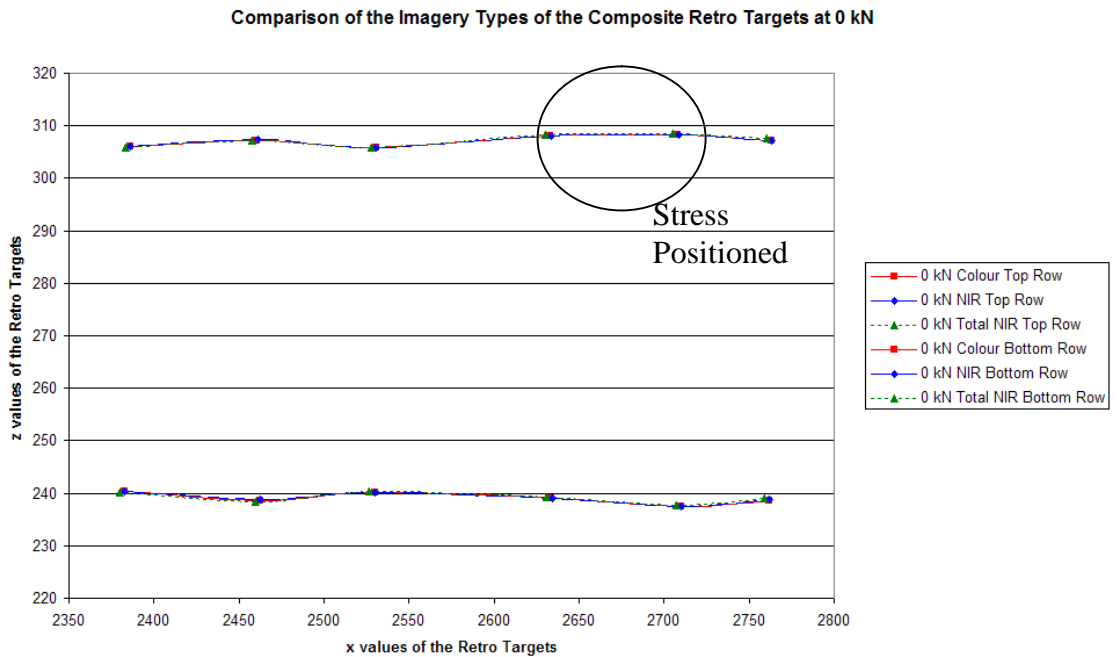


Figure 4.14 Graph of the Imagery Types of Retro-Reflective targets on the Composite beam at 0 kN.

Whilst viewing Figures 4.13 and 4.14, it can be seen that the imagery types are within a similar context to each other regardless of which target is being documented at the time. The next set of figures is of the composite beam where stress is being applied at 5 kN. The first figure shows the Paper-Made targets and the second shows the Retro-Reflective targets.

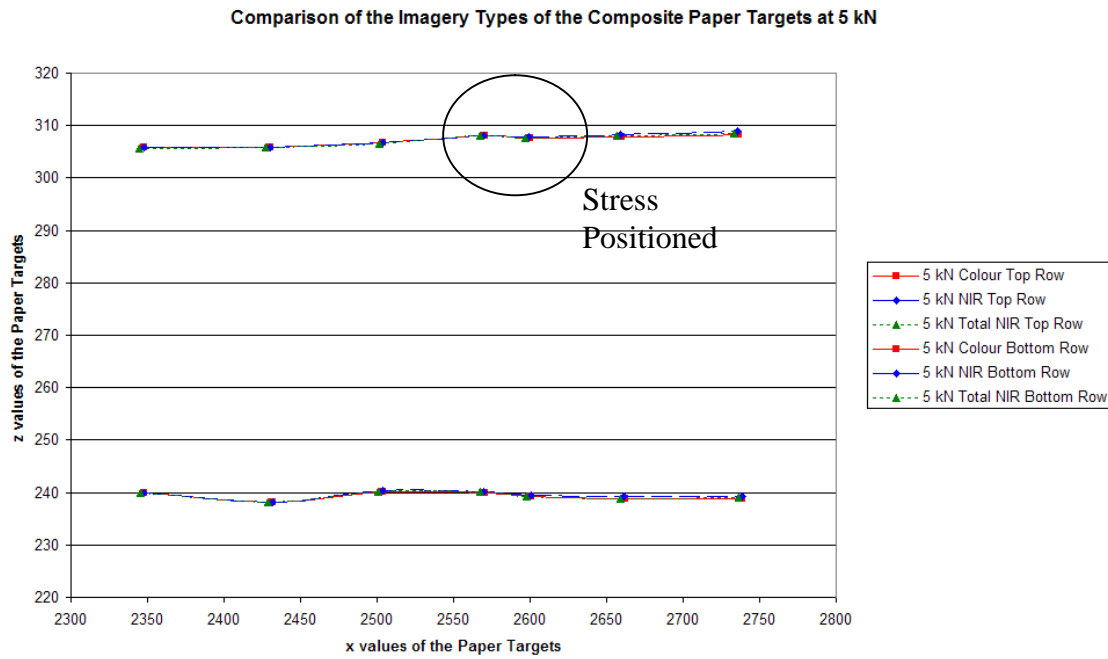


Figure 4.15 Graph of the Imagery Types of Paper-Made targets on the Composite beam at 5 kN.

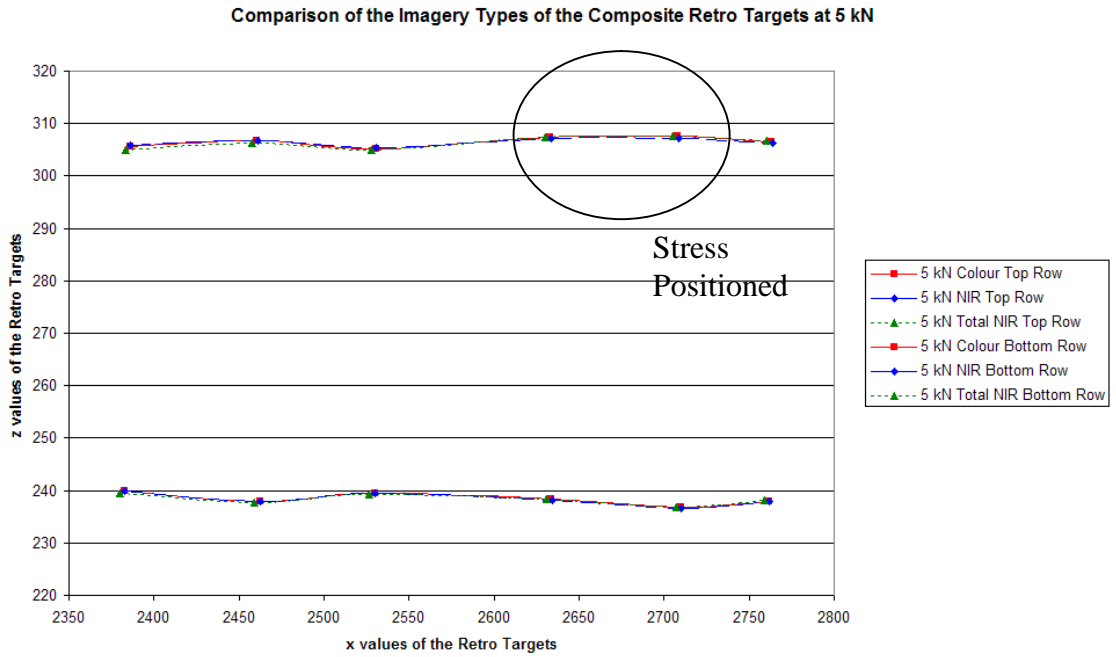


Figure 4.16 Graph of the Imagery Types of Retro-Reflective targets on the Composite beam at 5 kN.

Whilst viewing Figures 4.15 and 4.16, it can be seen that the imagery types are within a similar context to each other regardless of which target is being documented at the time. The next set of figures is of the composite beam where stress is being applied at 9.5 kN. The first figure shows the Paper-Made targets and the second shows the Retro-Reflective targets.

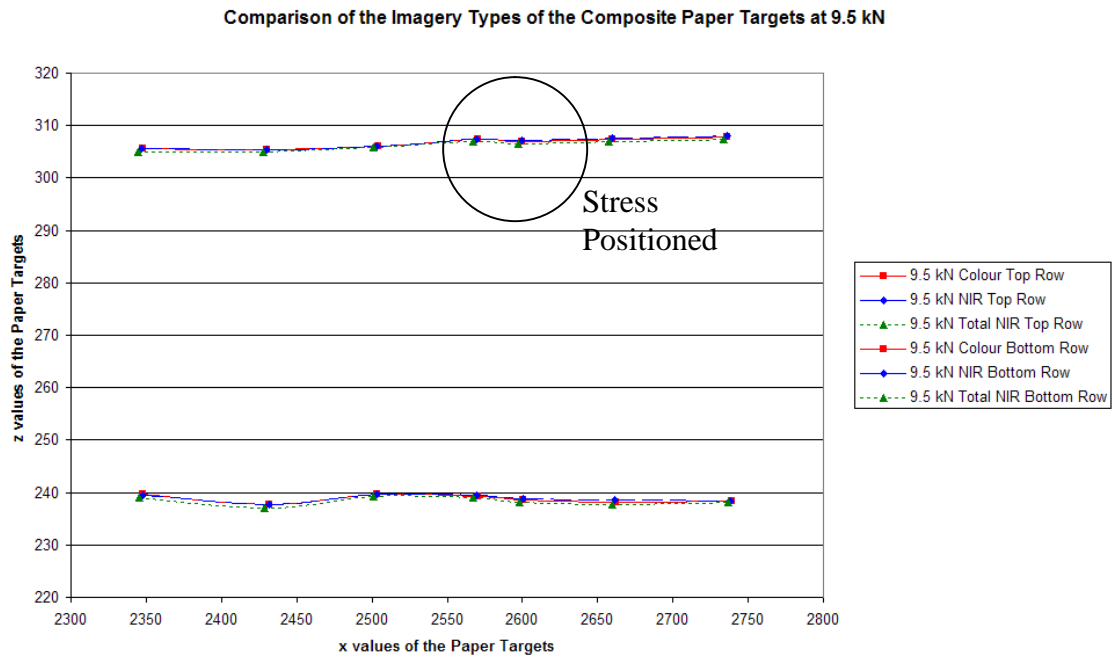


Figure 4.17 Graph of the Imagery Types of Paper-Made targets on the Composite beam at 9.5 kN.

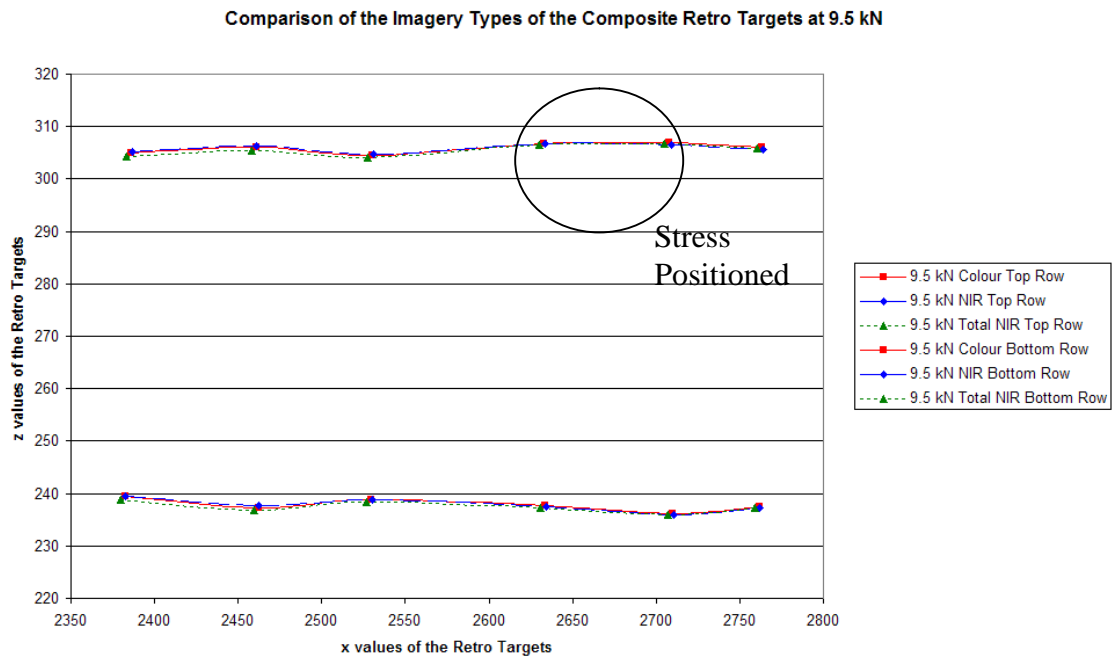


Figure 4.18 Graph of the Imagery Types of Retro-Reflective targets on the Composite beam at 9.5 kN.

Whilst viewing Figures 4.17 and 4.18, it can be seen that the imagery types are within a similar context to each other regardless of which target is being documented at the time. The next set of figures are of the composite beam where there is no stress being applied. The first figure shows Paper-Made targets, while the second shows Retro-Reflective targets.

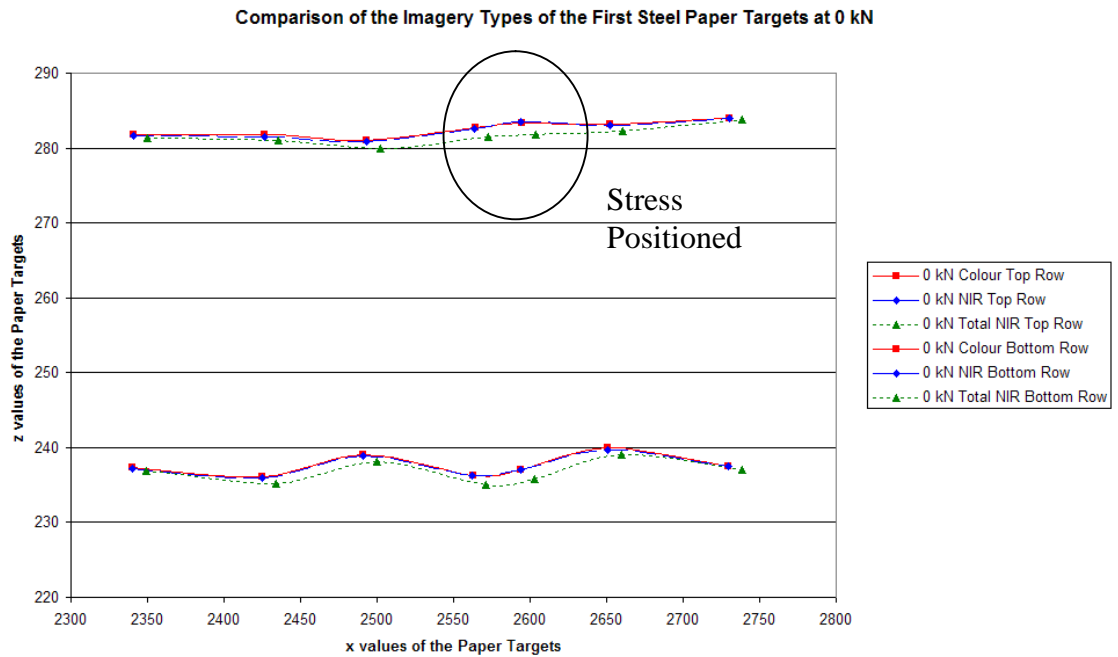


Figure 4.19 Graph of the Imagery Types of Paper-Made targets on the First Steel beam at 0 kN.

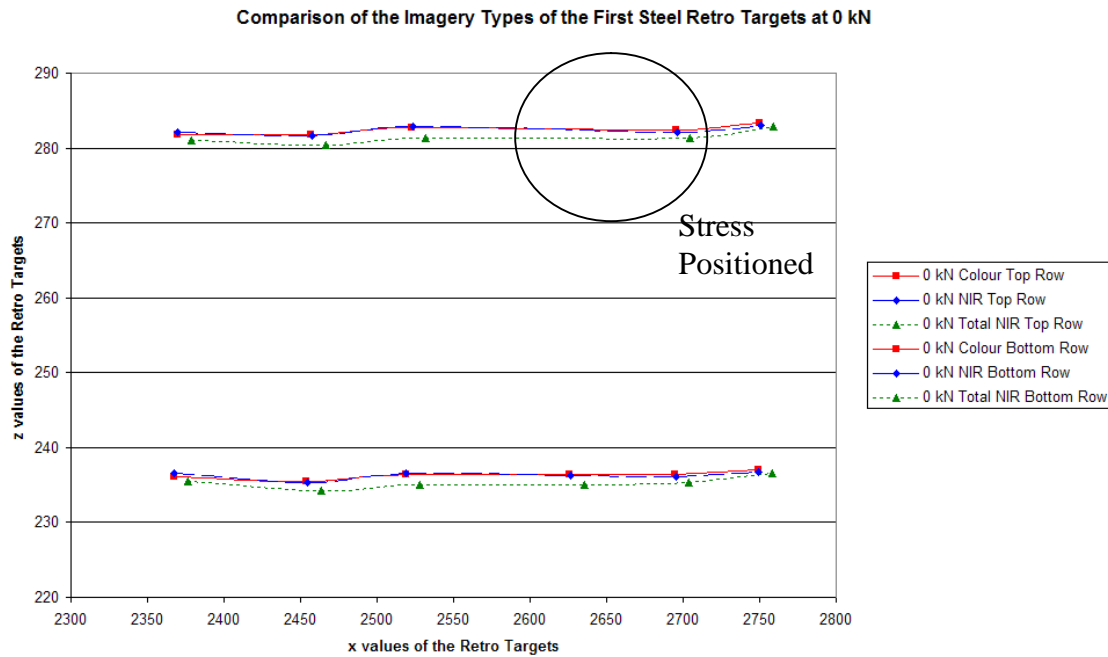


Figure 4.20 Graph of the Imagery Types of Retro-Reflective targets on the First Steel beam at 0 kN.

Whilst viewing Figures 4.19 and 4.20, it can be seen that the Colour and NIR sessions of both targets are within a similar context to each other. However, the Total NIR session for both targets is considerably different, specifically the ‘x values’. This may be due to different factors such as conducting the Total NIR session at a different time. It may also be due to the fact that the beam was not in the precise position when the other two sessions were documented. The next set of figures is related to the first steel beam that had stress applied at 25 kN. The first figure shows the Paper-Made targets and the second shows the Retro-Reflective targets.

Comparison of the Imagery Types of the First Steel Paper Targets at 25 kN

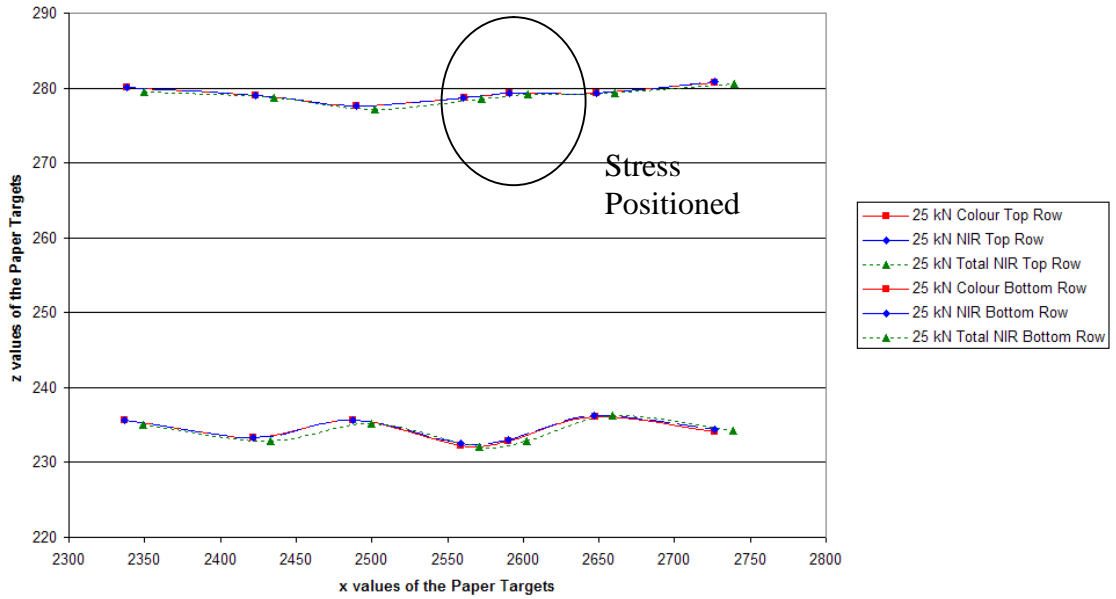


Figure 4.21 Graph of the Imagery Types of Paper-Made targets on the First Steel beam at 25 kN.

Comparison of the Imagery Types of the First Steel Retro Targets at 25 kN

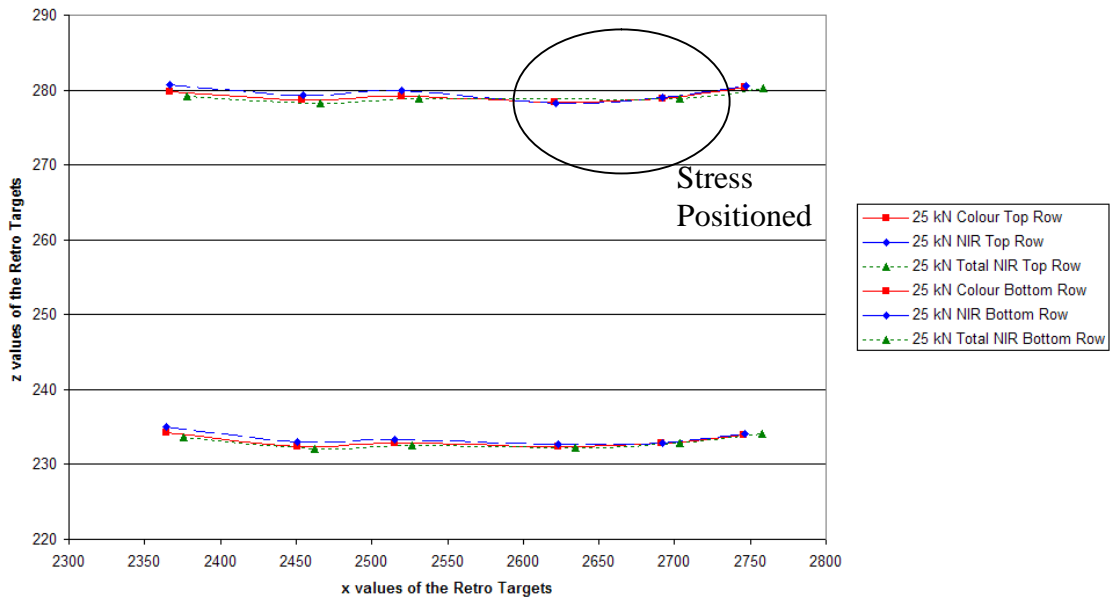


Figure 4.22 Graph of the Imagery Types of Retro-Reflective targets on the First Steel beam at 25 kN.

With viewing Figures 4.21 and 4.22, it is evident that the Colour and NIR sessions of both targets are within similar contexts to each other. However, the Total NIR session is considerably different, specifically the 'x values'. This may be due to conducting the Total NIR session at a different time or where the beam was not in the precise position whilst the other two sessions were being documented. The next set of figures illustrates the first steel beam where stress is being applied at 42.5 kN. The first figure shows Paper-Made targets and the second shows Retro-Reflective targets.

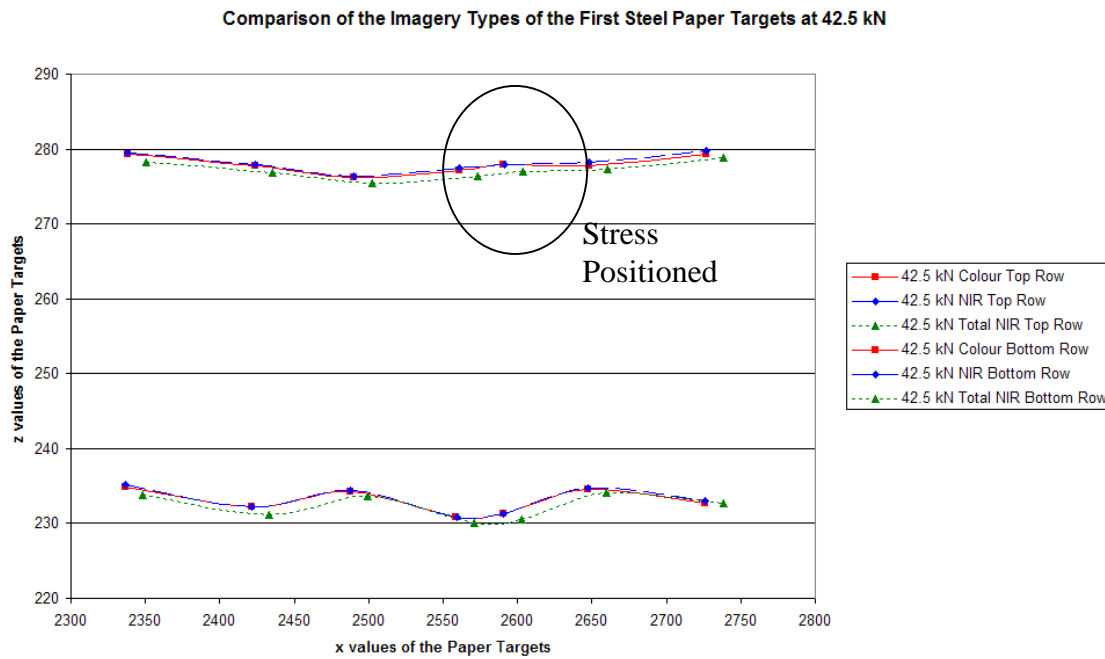


Figure 4.23 Graph of the Imagery Types of Paper-Made targets on the First Steel beam at 42.5 kN.

Comparison of the Imagery Types of the First Steel Retro Targets at 42.5 kN

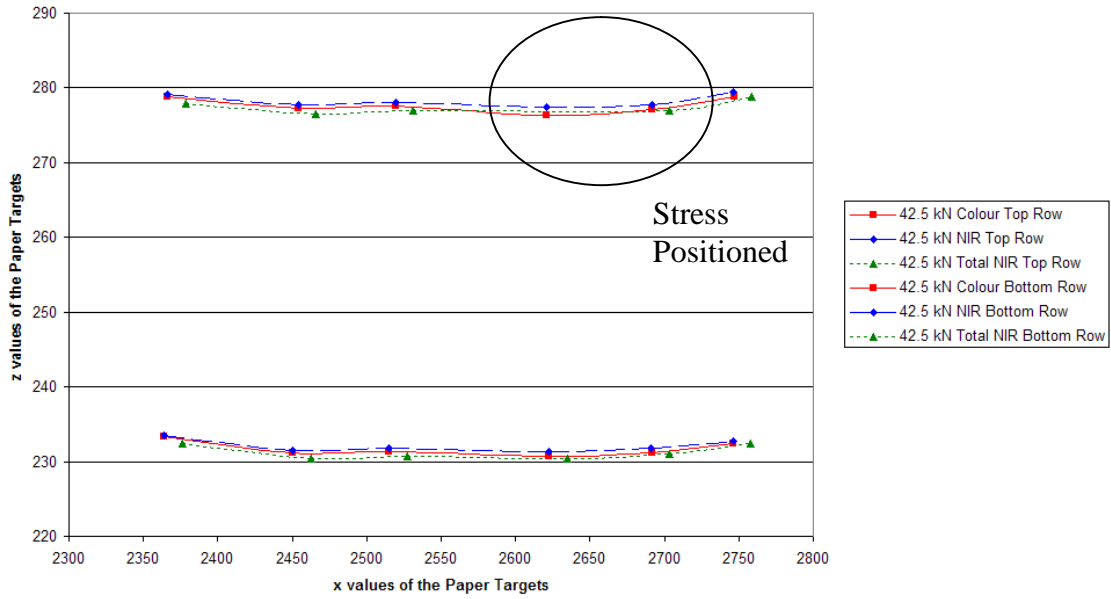


Figure 4.24 Graph of the Imagery Types of Retro-Reflective targets on the First Steel beam at 42.5 kN.

Whilst viewing Figures 4.23 and 4.24, it can be concluded that the Colour and NIR sessions of both targets are within a similar context to each other. However, the Total NIR session is considerably different, specifically the 'x values'. This may be due to conducting the Total NIR session at a different time or where the beam was not in the precise position whilst the other two sessions were being documented. The next set of figures are of the second steel beam where there is no stress being applied. The first figure shows Paper-Made targets and the second shows Retro-Reflective targets.

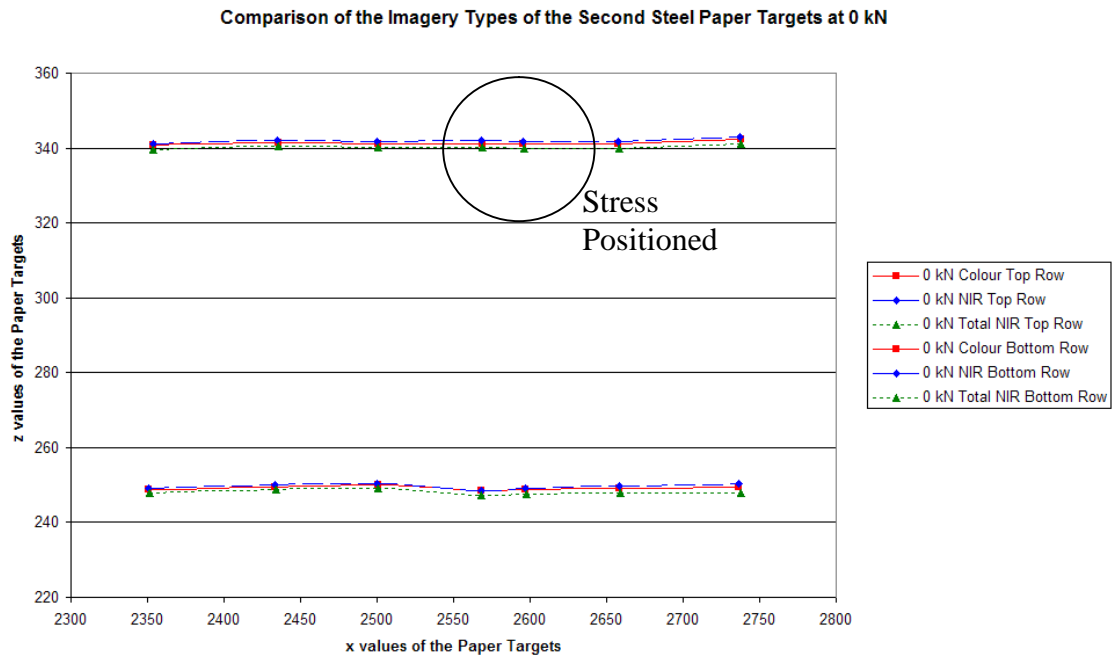


Figure 4.25 Graph of the Imagery Types of Paper-Made targets on the Second Steel beam at 0 kN.

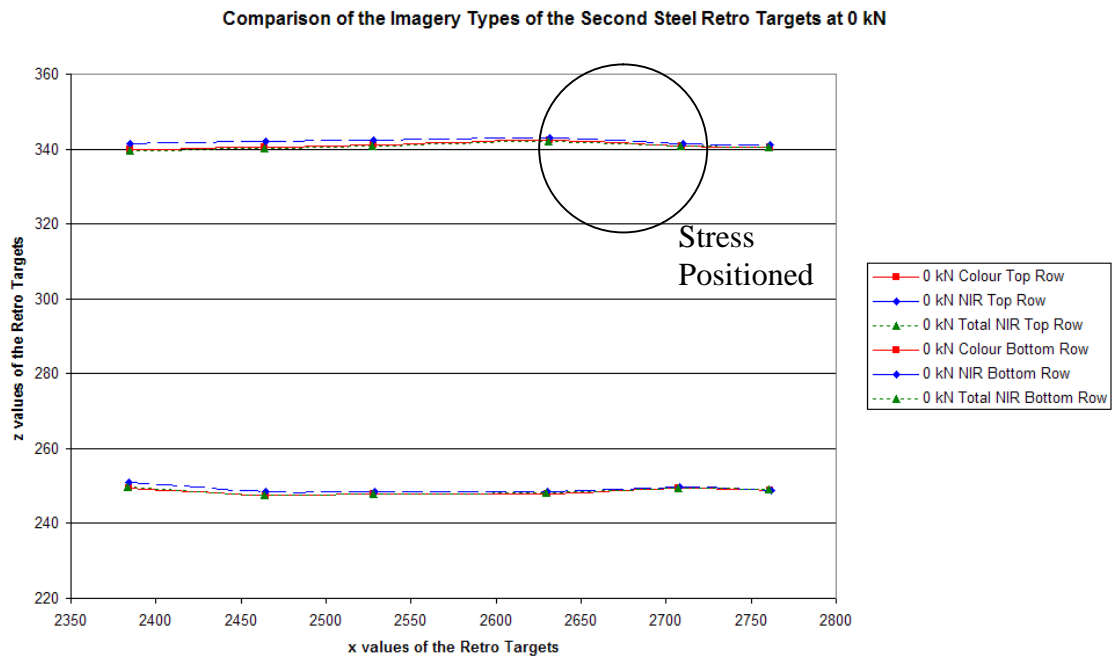


Figure 4.26 Graph of the Imagery Types of Retro-Reflective targets on the Second Steel beam at 0 kN.

Whilst viewing Figures 4.25 and 4.26, it can be seen that the imagery types are within a similar context to each other regardless of which target is being documented at the time. The next set of figures is of the second steel beam where stress is being applied at 25 kN. The first figure shows Paper-Made targets and the second shows Retro-Reflective targets.

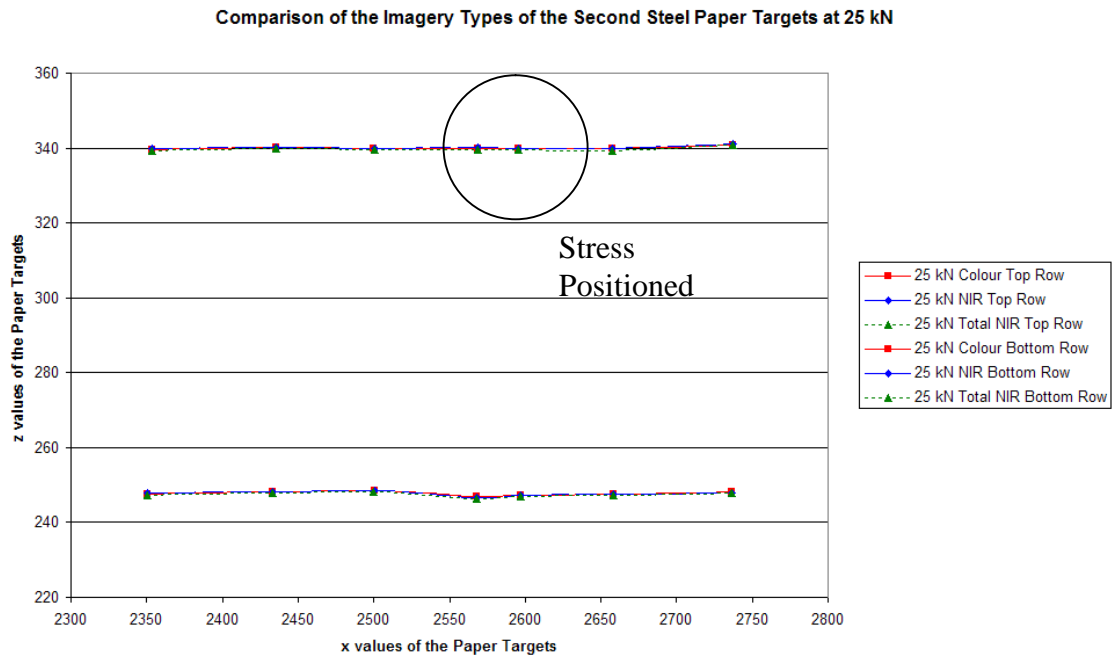


Figure 4.27 Graph of the Imagery Types of Paper-Made targets on the Second Steel beam at 25 kN.

Comparison of the Imagery Types of the Second Steel Retro Targets at 25 kN

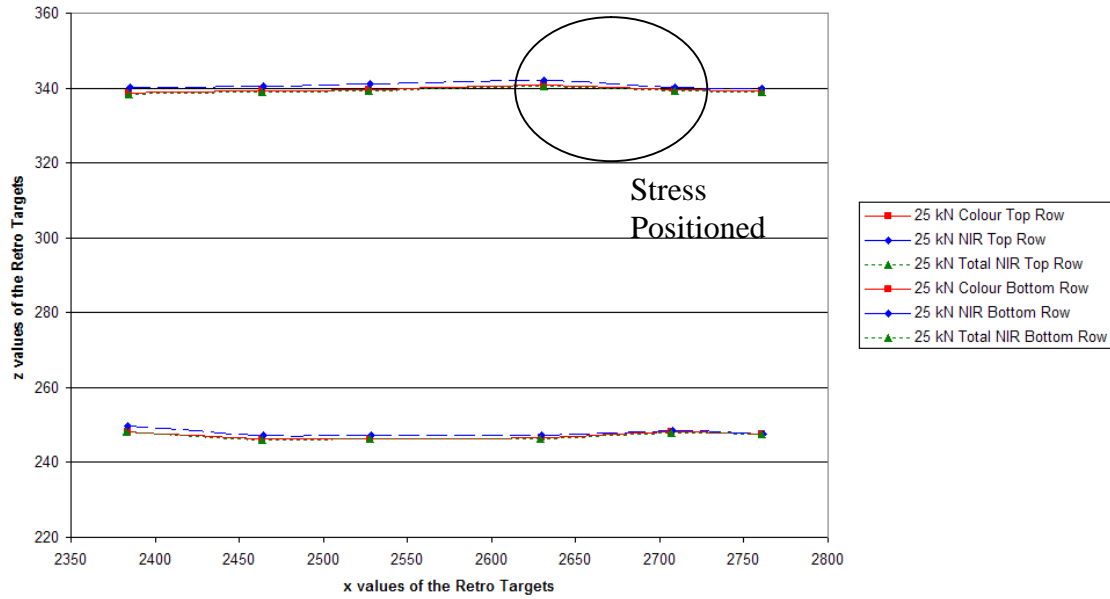


Figure 4.28 Graph of the Imagery Types of Retro-Reflective targets on the Second Steel beam at 25 kN.

Whilst viewing Figures 4.27 and 4.28, it can be seen that the imagery types are within a similar context to each other regardless of which target is being documented at the time. The next set of figures is of the second steel beam where stress is being applied at 45 kN. The first figure shows Paper-Made targets and the second shows Retro-Reflective targets.

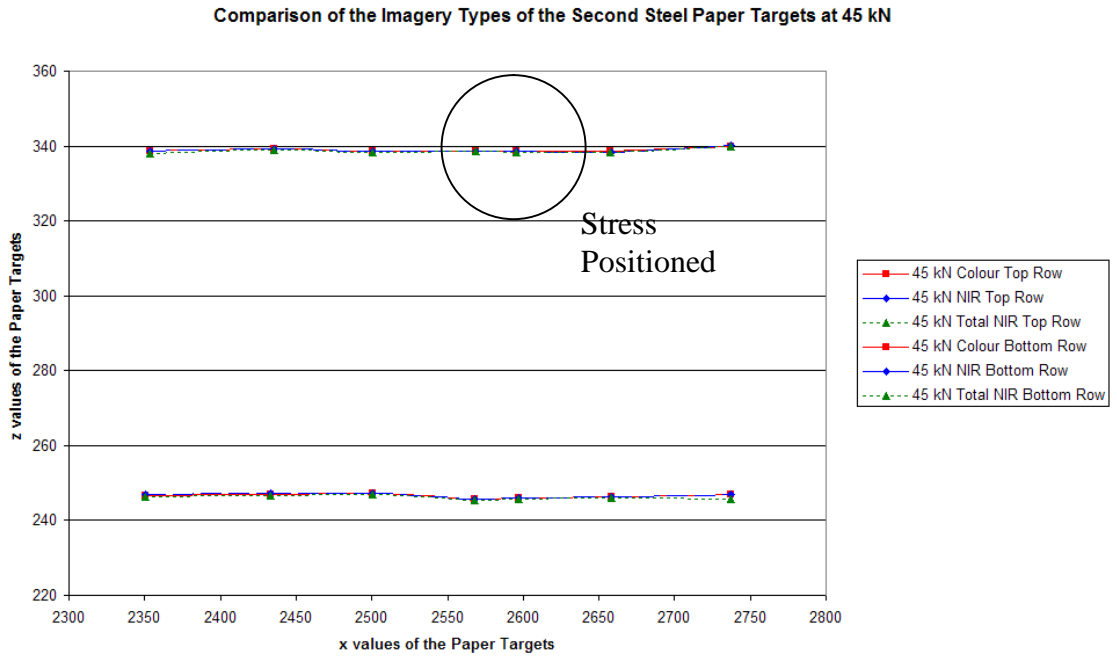


Figure 4.29 Graph of the Imagery Types of Paper-Made targets on the Second Steel beam at 45 kN.

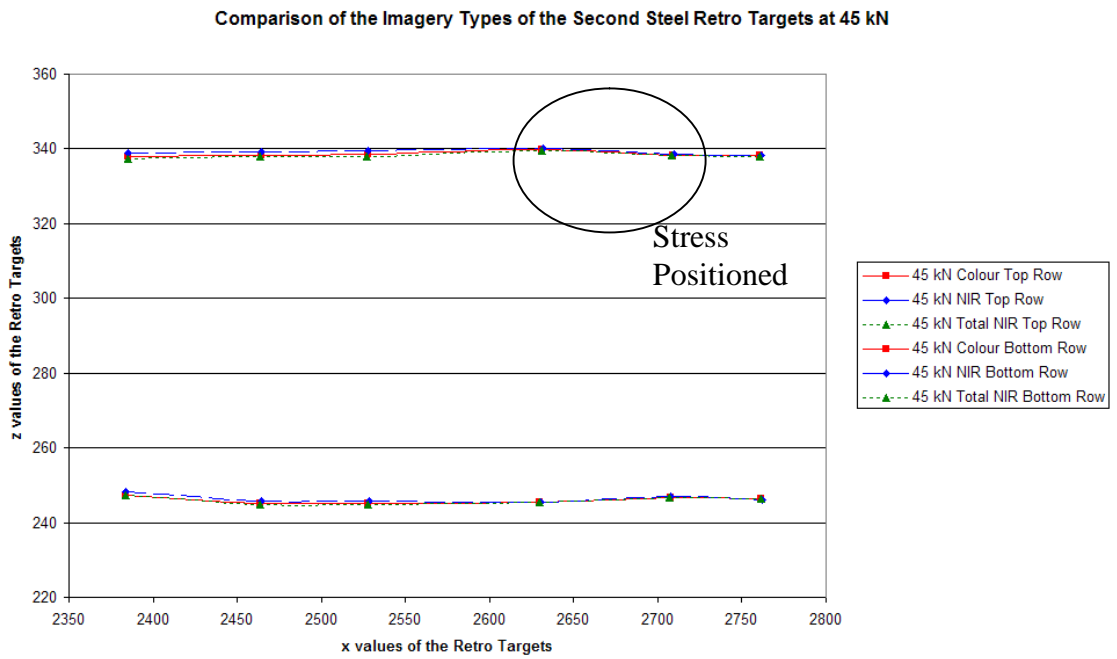


Figure 4.30 Graph of the Imagery Types of Retro-Reflective targets on the Second Steel beam at 25 kN.

Whilst viewing Figures 4.29 and 4.30, it can be seen that the imagery types are within a similar context to each other regardless of which target is being documented at the time. The next set of figures is of the timber beam where there is no stress being applied. The first figure shows Paper-Made targets and the second shows Retro-Reflective targets.

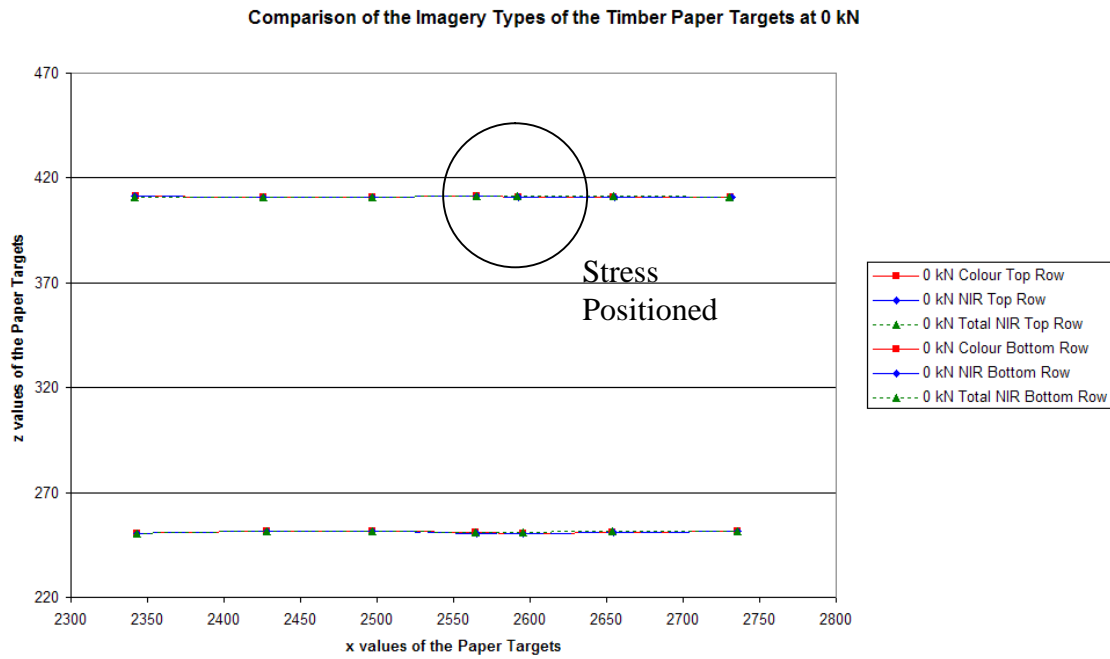


Figure 4.31 Graph of the Imagery Types of Paper-Made targets on the Timber beam at 0 kN.

Comparison of the Imagery Types of the Timber Retro Targets at 0 kN

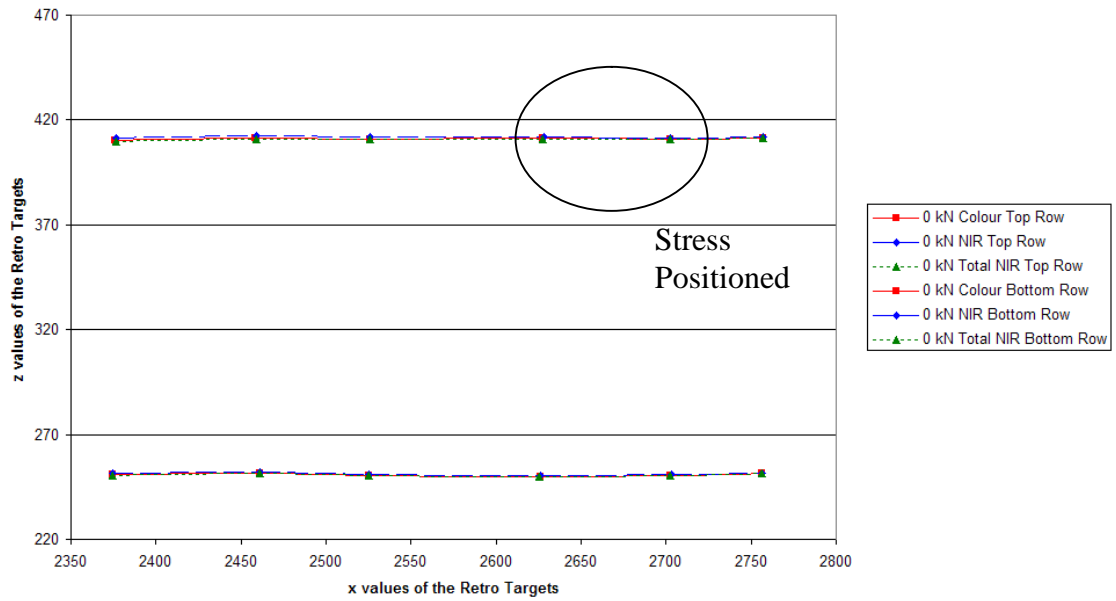


Figure 4.32 Graph of the Imagery Types of Retro-Reflective targets on the Timber beam at 0 kN.

Whilst viewing Figures 4.31 and 4.32, it can be seen that the imagery types are within a similar context to each other regardless of which target is being documented at the time. The next set of figures is of the composite beam where stress is being applied at 25 kN. The first figure shows Paper-Made targets and the second shows Retro-Reflective targets.

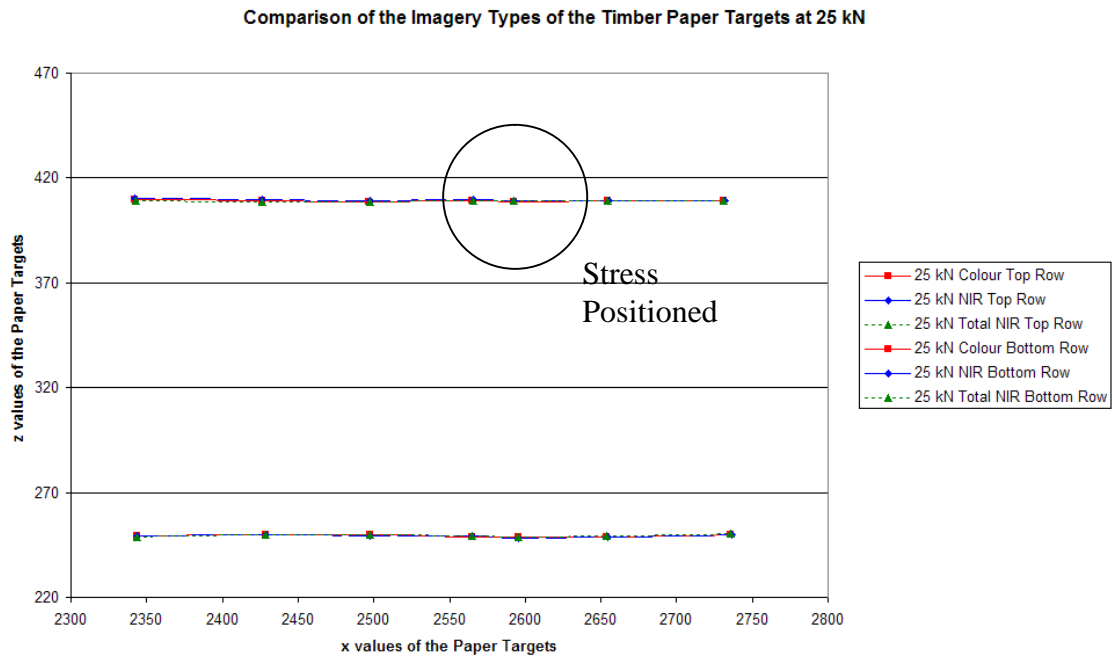


Figure 4.33 Graph of the Imagery Types of Paper-Made targets on the Timber beam at 25 kN.

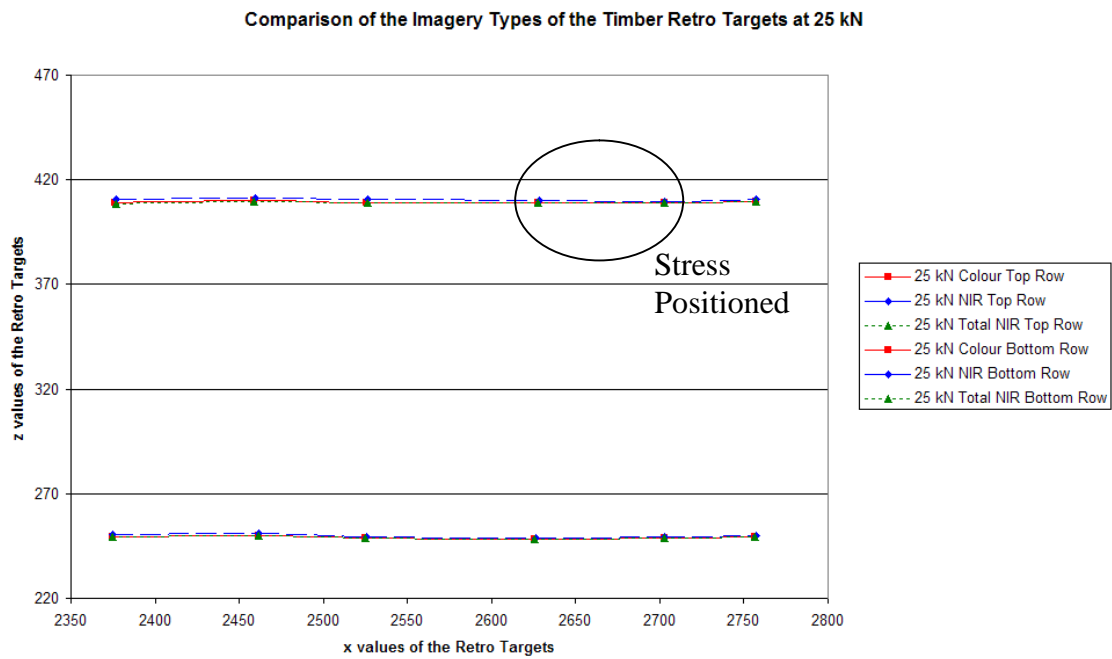


Figure 4.34 Graph of the Imagery Types of Retro-Reflective targets on the Timber beam at 25 kN.

Whilst viewing Figures 4.33 and 4.34, it is evident that the imagery types are within a similar context to each other regardless of which target is being documented at the time. The next set of figures is of the composite beam where stress is being applied at 45 kN. The first figure shows Paper-Made targets and the second shows Retro-Reflective targets.

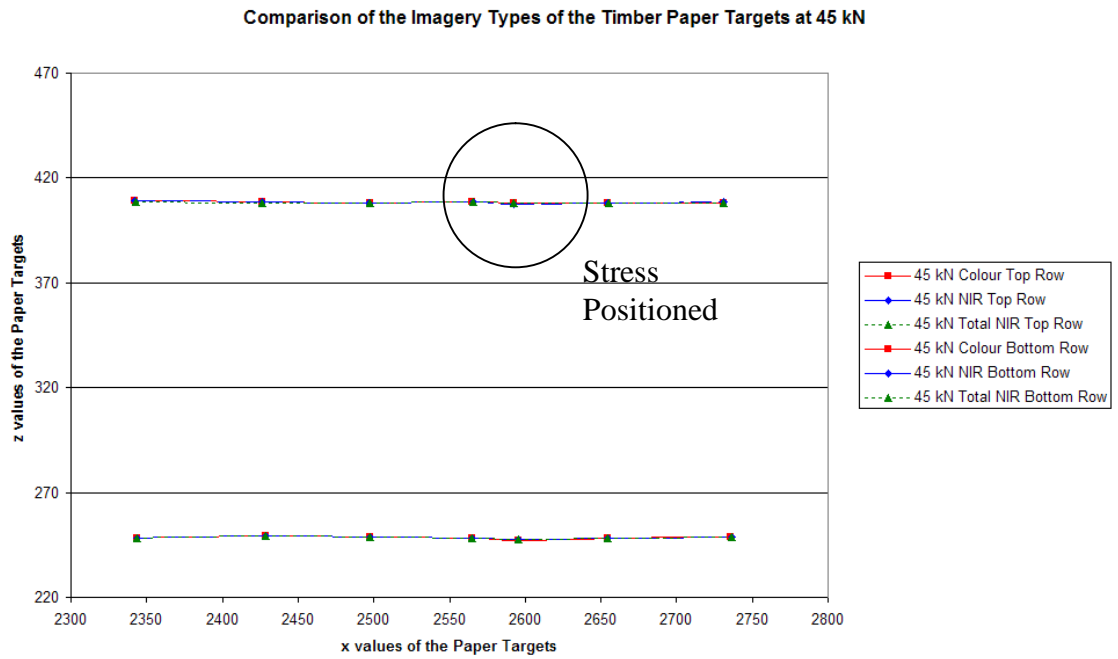


Figure 4.35 Graph of the Imagery Types of Paper-Made targets on the Timber beam at 45 kN.

Comparison of the Imagery Types of the Timber Retro Targets at 45 kN

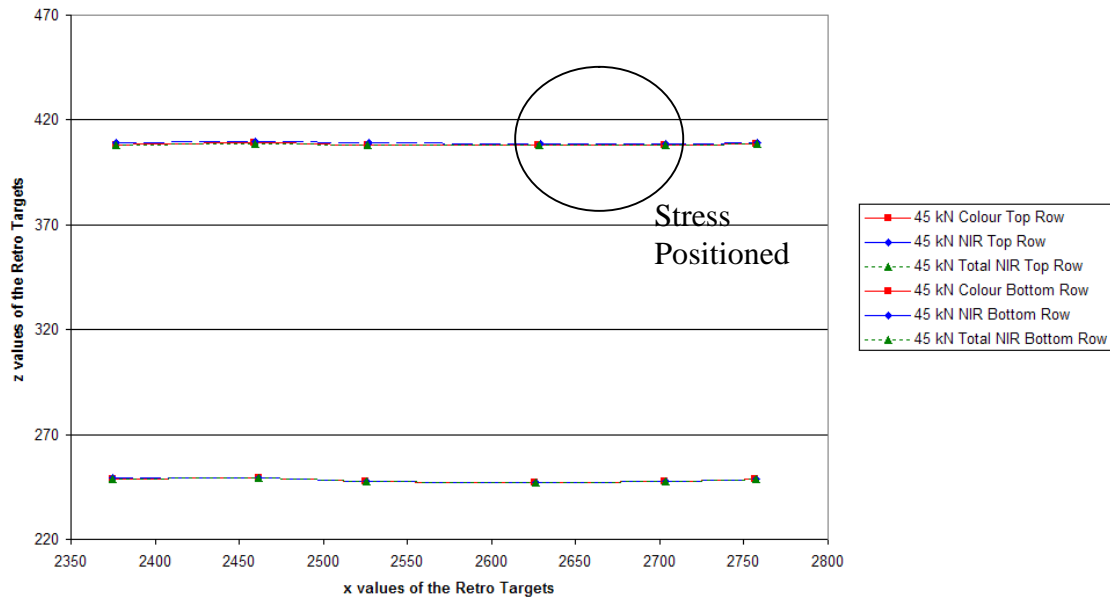


Figure 4.36 Graph of the Imagery Types of Retro-Reflective targets on the Timber beam at 45 kN.

Whilst viewing Figures 4.35 and 4.36, it is evident that the imagery types are within a similar context to each other regardless of which target is being documented at the time. The next figure is of the bridge structure that was conducted in the field-testing.

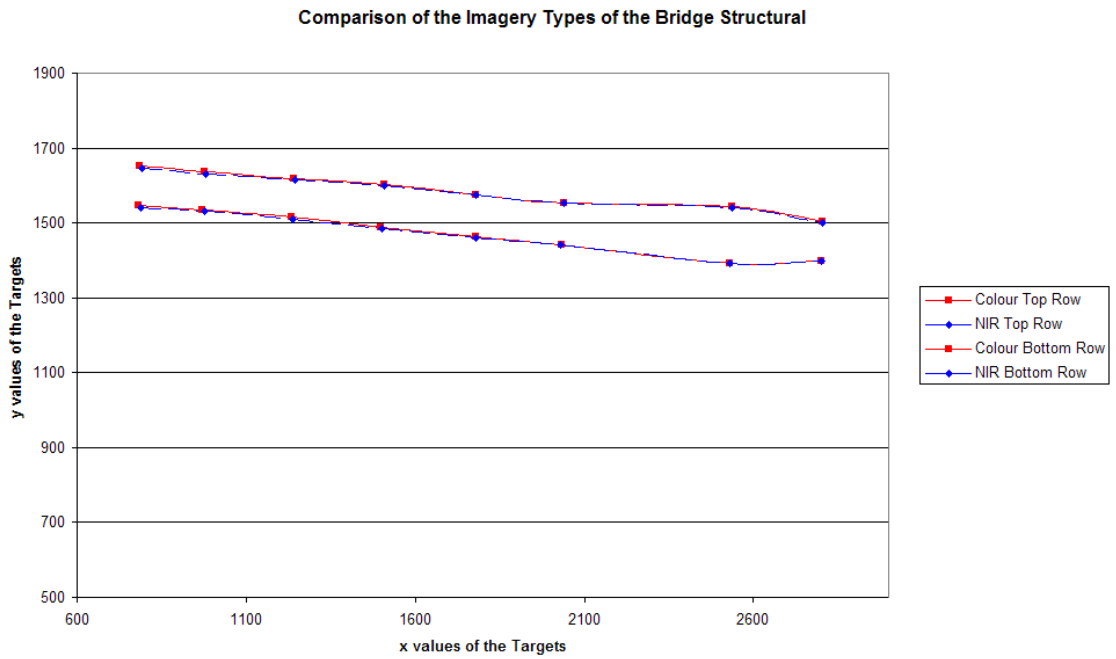


Figure 4.37 Graph of the Imagery Types of the Bridge Structure

Whilst viewing Figure 4.37, it can be concluded that the imagery types are within a similar context to each other. Considering this factor, any field-testing that is conducted is bound to have the same level of similarity between colour and NIR.

4.4 F-Test Distribution

In reference to section 3.10.3 from the previous chapter, the following calculations were conducted in order to determine whether the targets were in similar accuracy of each other in both colour and NIR.

4.4.1 Structural Beams

Below are a series of tables that show F-Tests Values of each beam material at various levels of stress. The table also illustrates which targets were used. The first set of results in Table 4.11, displays the F-Tests values that were calculated in relation to the Concrete beam at various levels of stress and the specific targets that were used.

Stress	Target	F-Test Values	
		Colour – NIR	Colour – Total NIR
0 kN	Paper	0.213 (H ₀ Accepted)	0.058 (H ₀ Accepted)
	Retro	0.005 (H ₀ Accepted)	0.095 (H ₀ Accepted)
7 kN	Paper	0.583 (H ₀ Accepted)	0.001 (H ₀ Accepted)
	Retro	0.000 (H ₀ Accepted)	0.073 (H ₀ Accepted)
13 kN	Paper	0.049 (H ₀ Accepted)	0.023 (H ₀ Accepted)
	Retro	0.000 (H ₀ Accepted)	0.182 (H ₀ Accepted)

Table 4.11 The F-Test values that were calculated between the levels of stress and targets of the Concrete beam. (mm)

In reference to this test, there were a total of 14 Paper-Made targets and 12 Retro-Reflective targets for Colour, NIR and Total NIR. When examining the table for the limits, the degrees of freedom are taken from both targets. The degrees of freedom for Paper-Made targets are now 13 and the Retro-Reflective targets are 11. The 90% and 99% confidence limits for both 'Colour – NIR' and 'Colour – Total NIR' in this table are as follows:

Paper

$$F_{0.10,(14-1),(14-1)} = 2.0802$$

$$F_{0.01,(14-1),(14-1)} = 3.9052$$

Retro

$$F_{0.10,(12-1),(12-1)} = 2.2269$$

$$F_{0.01,(12-1),(12-1)} = 4.4624$$

The F-Test values that were calculated show all Paper-Made targets have probabilities of being 90% less than 2.0802 mm and 99% less than 3.9052 mm. In relation to the Retro-Reflective Targets, these have probabilities of being 90% less than 2.2269 mm and 99% less than 4.4624 mm. In reference to the hypothesis that was stated above, all F-Test values accept this hypothesis as a 'Null Hypothesis', which means that the Colour session and the NIR sessions are in similar context.

The next set of results in Table 4.12, displays the F-Test Values of the wood beam at various levels of stress and the specific targets that were used.

Stress	Target	F-Test Values	
		Colour – NIR	Colour – Total NIR
0 kN	Paper	0.155 (H ₀ Accepted)	0.993 (H ₀ Accepted)
	Retro	0.011 (H ₀ Accepted)	0.006 (H ₀ Accepted)
2.5 kN	Paper	0.888 (H ₀ Accepted)	0.554 (H ₀ Accepted)
	Retro	0.017 (H ₀ Accepted)	0.101 (H ₀ Accepted)
4.5 kN	Paper	0.354 (H ₀ Accepted)	0.994 (H ₀ Accepted)
	Retro	0.001 (H ₀ Accepted)	0.133 (H ₀ Accepted)

Table 4.12 The F-Test values that were calculated between the levels of stress on the Wood beam and the specific targets that were used. (mm)

This test included a total of 14 Paper-Made targets and 12 Retro-Reflective targets for Colour, NIR and Total NIR. Therefore, on examination of the table for the limits, the degrees of freedom that are taken from both targets are now 13 and 11. As a result, the 90% and 99% confidence limits for both ‘Colour – NIR’ and ‘Colour – Total NIR’ in this table are as follows:

Paper

$$F_{0.10,(14-1),(14-1)} = 2.0802$$

$$F_{0.01,(14-1),(14-1)} = 3.9052$$

Retro

$$F_{0.10,(12-1),(12-1)} = 2.2269$$

$$F_{0.01,(12-1),(12-1)} = 4.4624$$

The F-Test values that were calculated show all Paper-Made targets have probabilities of being 90% less than 2.0802 mm and 99% less than 3.9052 mm. In relation to the Retro-Reflective Targets, these have probabilities of being 90% less than 2.2269 mm and 99% less than 4.4624 mm. In reference to the hypothesis that was stated above, all F-Test values accept this hypothesis as a ‘Null Hypothesis’, which means that the Colour session and the NIR sessions are in similar context.

The next set of results in Table 4.13, displays the F-Test Values of the Composite beam at various levels of stress and the specific targets that were used.

Stress	Target	F-Test Values	
		Colour – NIR	Colour – Total NIR
0 kN	Paper	0.968 (H ₀ Accepted)	0.644 (H ₀ Accepted)
	Retro	0.144 (H ₀ Accepted)	0.538 (H ₀ Accepted)
5 kN	Paper	0.165 (H ₀ Accepted)	0.732 (H ₀ Accepted)
	Retro	0.034 (H ₀ Accepted)	0.502 (H ₀ Accepted)
9.5 kN	Paper	0.140 (H ₀ Accepted)	0.112 (H ₀ Accepted)
	Retro	0.016 (H ₀ Accepted)	0.993 (H ₀ Accepted)

Table 4.13 The F-Test values that were calculated between the levels of stress on the Composite beam and the specific targets that were used. (mm)

This test included a total of 14 Paper-Made targets and 12 Retro-Reflective targets for Colour, NIR and Total NIR. Therefore, on examination of the table for the limits, the degrees of freedom that are taken from both targets are now 13 and 11. As a result, the 90% and 99% confidence limits for both ‘Colour – NIR’ and ‘Colour – Total NIR’ in this table are as follows:

Paper

$$F_{0.10,(14-1),(14-1)} = 2.0802$$

$$F_{0.01,(14-1),(14-1)} = 3.9052$$

Retro

$$F_{0.10,(12-1),(12-1)} = 2.2269$$

$$F_{0.01,(12-1),(12-1)} = 4.4624$$

The F-Test values that were calculated show all Paper-Made targets have probabilities of being 90% less than 2.0802 mm and 99% less than 3.9052 mm. In relation to the Retro-Reflective Targets, these have probabilities of being 90% less than 2.2269 mm and 99% less than 4.4624 mm. In reference to the hypothesis that was stated above, all F-Test values accept this hypothesis as a 'Null Hypothesis', which means that the Colour session and the NIR sessions are in similar context.

The next set of results in Table 4.14, displays the F-Test Values of the First Steel beam at various levels of stress and the specific targets that were used.

Stress	Target	F-Test Values	
		Colour – NIR	Colour – Total NIR
0 kN	Paper	0.527 (H ₀ Accepted)	0.556 (H ₀ Accepted)
	Retro	0.000 (H ₀ Accepted)	0.443 (H ₀ Accepted)
25 kN	Paper	0.477 (H ₀ Accepted)	0.018 (H ₀ Accepted)
	Retro	0.081 (H ₀ Accepted)	0.734 (H ₀ Accepted)
42.5 kN	Paper	0.195 (H ₀ Accepted)	0.906 (H ₀ Accepted)
	Retro	0.009 (H ₀ Accepted)	0.000 (H ₀ Accepted)

Table 4.14 The F-Test values that were calculated between the levels of stress on the First Steel beam and the specific targets that were used. (mm)

In reference to this test, there were a total of 14 paper-Made targets used for all levels of stress in the Colour and NIR sessions. In relation to the Retro-Reflective targets, there were a total of 11 targets observed at the initial stress experimentation. Whilst observing the beam at moderate and maximum stress levels, there were a total of 12 observations included in the Colour and NIR session and a total of 11 in the total NIR session. As a result, on examination of the table for limits, the degrees of freedom that are taken from both targets are now 13, 11 and 10. The 90% and 99% confidence limits for both ‘Colour – NIR’ and ‘Colour – Total NIR’ are as follows:

Paper

$$F_{0.10,(14-1),(14-1)} = 2.0802$$

$$F_{0.01,(14-1),(14-1)} = 3.9052$$

Retro

$$F_{0.10,(12-1),(12-1)} = 2.2269$$

$$F_{0.10,(12-1),(11-1)} = 2.3018$$

$$F_{0.10,(11-1),(11-1)} = 2.3226$$

$$F_{0.01,(12-1),(12-1)} = 4.4624$$

$$F_{0.01,(12-1),(11-1)} = 4.7715$$

$$F_{0.01,(11-1),(11-1)} = 4.8491$$

The F-Test values that were calculated show all Paper-Made targets have probabilities of being 90% less than 2.0802 mm and 99% less than 3.9052 mm. In relation to the Retro-Reflective Targets, these have probabilities of being 90% less than 2.2269 mm and 99% less than 4.4624 mm. In reference to the hypothesis that was stated above, all F-Test values accept this hypothesis as a ‘Null Hypothesis’, which means that the Colour session and the NIR sessions are in similar context.

The next set of results in Table 4.15, displays the F-Test Values of the Second Steel beam at various levels of stress and the specific targets that were used.

Stress	Target	F-Test Values	
		Colour – NIR	Colour – Total NIR
0 kN	Paper	0.261 (H ₀ Accepted)	0.000 (H ₀ Accepted)
	Retro	0.000 (H ₀ Accepted)	0.733 (H ₀ Accepted)
25 kN	Paper	0.365 (H ₀ Accepted)	0.595 (H ₀ Accepted)
	Retro	0.002 (H ₀ Accepted)	0.375 (H ₀ Accepted)
45 kN	Paper	0.345 (H ₀ Accepted)	0.000 (H ₀ Accepted)
	Retro	0.001 (H ₀ Accepted)	0.696 (H ₀ Accepted)

Table 4.15 The F-Test values that were calculated between the levels of stress on the Second Steel beam and the specific targets that were used. (mm)

In reference to this test, there were a total of 14 Paper-Made targets and 12 Retro-Reflective targets for Colour, NIR and Total NIR. On examination of the table for the specific limits, the degrees of freedom are taken from both targets and are now 13 and 11. As a result, the 90% and 99% confidence limits for both ‘Colour – NIR’ and ‘Colour – Total NIR’ in this table are as follows:

Paper

$$F_{0.10,(14-1),(14-1)} = 2.0802$$

$$F_{0.01,(14-1),(14-1)} = 3.9052$$

Retro

$$F_{0.10,(12-1),(12-1)} = 2.2269$$

$$F_{0.01,(12-1),(12-1)} = 4.4624$$

The F-Test values that were calculated show all Paper-Made targets have probabilities of being 90% less than 2.0802 mm and 99% less than 3.9052 mm. In relation to the Retro-Reflective Targets, these have probabilities of being 90% less than 2.2269 mm and 99% less than 4.4624 mm. In reference to the hypothesis that was stated above, all F-Test values accept this hypothesis as a ‘Null Hypothesis’, which means that the Colour session and the NIR sessions are in similar context.

The next set of results in Table 4.16, displays the F-Test Values of the Timber beam at various levels of stress and the specific targets that were used.

Stress	Target	F-Test Values	
		Colour – NIR	Colour – Total NIR
0 kN	Paper	0.089 (H ₀ Accepted)	0.000 (H ₀ Accepted)
	Retro	0.002 (H ₀ Accepted)	0.579 (H ₀ Accepted)
25 kN	Paper	0.274 (H ₀ Accepted)	0.001 (H ₀ Accepted)
	Retro	0.002 (H ₀ Accepted)	0.315 (H ₀ Accepted)
45 kN	Paper	0.482 (H ₀ Accepted)	0.165 (H ₀ Accepted)
	Retro	0.001 (H ₀ Accepted)	0.534 (H ₀ Accepted)

Table 4.16 The F-Test values that were calculated between the levels of stress on the Timber beam and the specific targets that were use. (mm)

In reference to this test, there were a total of 14 Paper-Made targets and 12 Retro-Reflective targets for Colour, NIR and Total NIR. On examination of the table for the specific limits, the degrees of freedom are taken from both targets and are now 13 and 11. As a result, the 90% and 99% confidence limits for both ‘Colour – NIR’ and ‘Colour – Total NIR’ in this table are as follows:

Paper

$$F_{0.10,(14-1),(14-1)} = 2.0802$$

$$F_{0.01,(14-1),(14-1)} = 3.9052$$

Retro

$$F_{0.10,(12-1),(12-1)} = 2.2269$$

$$F_{0.01,(12-1),(12-1)} = 4.4624$$

The F-Test values that were calculated show all Paper-Made targets have probabilities of being 90% less than 2.0802 mm and 99% less than 3.9052 mm. In relation to the Retro-Reflective Targets, these have probabilities of being 90% less than 2.2269 mm and 99% less than 4.4624 mm. In reference to the hypothesis that was stated above, all F-Test values accept this hypothesis as a 'Null Hypothesis', which means that the Colour session and the NIR sessions are in similar context.

4.4.2 Bridge Structure

Upon completion of the experimentation on each of the structural beams, another test was conducted on the bridge structure between the Colour session and the NIR session. As a result, an F-Test value was obtained which was 0.502 mm. In reference to the experimentation that was conducted, a total of 16 targets were documented. Consequently, on examination of the table for limits, the degrees of freedom are taken as 15. Hence, the 90% and 99% confidence limits for comparing the Colour and NIR sessions are as follows:

$$F_{0.10,(16-1),(16-1)} = 1.9722$$

$$F_{0.01,(16-1),(16-1)} = 3.5222$$

In relation to the F-Test values of the bridge structure, the targets have probabilities of being 90% less than 1.9722 mm and 99% less than 3.5222 mm. In reference to the Hypothesis that was stated above, this F-Test value is accepted as a 'Null Hypothesis', which means that the Colour session and the NIR session are in similar context.

4.5 Conclusion

On examination of the analysis, it has been established that when comparing the colour imagery to NIR imagery of structure materials at different levels of stress, they are in similar context to the imagery types. It was also observed that the targets that were documented, namely Paper-Made and Retro-Reflective all accepted the 'Null Hypothesis' assumption. However, there were a few inconsistencies noted whilst analysing these results. These inconsistencies are discussed further in the next chapter.

Chapter 5

Discussion

5.1 Introduction

Information relating to the experimentation and results that were calculated from the previous chapter is reviewed in order to determine if this study achieved its aim and objectives. Some of the observations that were noticed in the study are discussed in further detail in this chapter. Examination of the results from the previous chapter reveals evidence of a few inconsistencies. It is understood that these were apparent due to various errors that occurred whilst the experimentation was in progress. These are also discussed in detail in this chapter.

5.2 Experimentation and Analysis of Results

After obtaining these measurements and taking into consideration the stress applied to the structural beams, analysis of the measurements all proved to be within one millimetre accuracy. Therefore it can be assumed that with any level of stress being applied, this technique of photogrammetry is a suitable to be used to determine the health of the structure.

Considering the statistics test results that were calculated, the accuracy of using these techniques was evaluated. This proved to be within the desired accuracy limits. This was due to the fact that the results from all of the targets that were established accepted the 'Null Hypothesis', which stated, colour and NIR imagery conditions are within the same accuracy limits to each other.

When evaluating the suitability of Near Infrared and Colour photogrammetry for various structural beam materials, there were no problems encountered with any of the materials. The results that were calculated proved that each material was within the same level of accuracy, even with stress being applied.

5.3 Problems Encountered

In relation to the second stage experimentation and results, the following problems were encountered:

- There was only one NIR illuminator that was available which made it difficult as the illuminator had to continually be taken off the first camera then placed on the second camera. It was then changed back to the first camera and then to second once more.
- In reference to the targets there were also some minor areas of concern. The targets were placed evenly, however, they should have been placed on a straighter line rather than just placed on an estimated line.
- The concrete beam that was used in the experimentation revealed some safety concerns. It was too big and too heavy for one person to place on the testing machine.
- Whilst the Colour and NIR sessions were performed at the same time, the Total NIR session was documented at a different time. This was evident when examining the graphs of the first Steel Beam which revealed that the Total NIR session is dissimilar to both the Colour and NIR session.

The third stage encountered the following problems in experimentation:

- The floodlight that was underneath the bridge structure proved to be problematic with using the NIR imagery of the camera. In order to turn off this light, the campus security had to request the campus maintenance department turn off the light by removing the bulb for 24 hours.
- In relation to the taking of photographs, the first four photographs were able to have full view of both the targets on the bridge and the control board. However, the last photograph captured the view of the right side of the bridge, but it did not capture the control board.

In reference to the errors that were discovered in both the experimentation and analysis of results, suggested improvements are documented in section 6.3.1. These suggestions are offered so as to ensure similar errors will not occur with further research.

5.4 Conclusion

On completion of the discussion of the experimentation and results, it has been determined that Colour and NIR imagery, are within a similar context to each other when used to monitor a structure. The few errors that were present had minor influence on the computation of results. However, these should be taken into consideration when contemplating further research in order to achieve greater accuracy of results, which is discussed in the next chapter.

Chapter 6

Conclusions

6.1 Introduction

In reference to the experimentation that was conducted and the analysis of the results, it has been discovered that when comparing Colour images to NIR images, they are in close similarity to each other. In relation to the experimentation, key factors that should be considered for future work are discussed in detail. Consequently, there are a few areas that should be examined in greater detail in order to ensure better accuracy. Improvements to these areas would assist in detailing documentation for future research.

6.2 Discoveries of this Study

In reference to section 1.2, the purpose of conducting this study was to determine if using photogrammetry techniques in colour and NIR, could not only detect the stress of structural beams but also compute a 3-D representation of a structure.

It was discovered that when examining both the colour and NIR imagery of each beam and structure, they were all within a similar context to each other. This is apparent with any level of stress being applied or whether the experimentation is being conducted within the laboratory or in the field.

In relation to the experimentation that was conducted, the main aim and hypothesis of this study was to show that the use of photogrammetric techniques with both colour and NIR images is a suitable method for structural beam deformation. This was proven to be conclusive from the study performed.

When comparing the coordinates from the projects that were created, each of the three defined objectives were all accomplished:

- The coordinates that were provided gave accurate 3D measurements from both near-infrared images and colour images to a degree of one millimetre.
- The measurements from both Colour and NIR were all within the accepted accuracy parameters that were established as these measurements all accepted the hypothesis that was previously stated.
- With the various structural beam materials, Colour and NIR imagery was suitable for any structural materials that were experimented on.

Lastly, it should be noted that when documenting these materials with the NIR capabilities of the camera, Retro-Reflective targets are the best choice for 24 hour monitoring within the field. When conducting the experimentation on the beams, the Paper-Made targets were difficult to label accurately since 'Australis' had difficulty in determining these specific targets. However, there were no problems in labelling the Retro-Reflective targets. In conclusion, this experimentation study revealed that Retro-Reflective targets should be used when using NIR imagery over a 24-hour period.

6.3 Further Work

In reference to the research and experimentation that has been conducted in this study, there are areas that could be improved on if performing further research. Developments to further this study could include whether different conditions such as adding more strain onto the beams or taking more images during different weather conditions would affect the outcome and hence reveal different results.

6.3.1 Improvements

In relation to the errors that were discussed in section 3.6, a few errors were evident whilst conducting this study. On reflection and after examination of these errors, it is anticipated that the following corrections could have made the results lie within a more acceptable parameter.

Such examples of improvements relate to the second stage of the experiment where it would have been beneficial to have another NIR illuminator to ensure that the images obtained would be in prestige condition. The targets should be placed on a definite straight line so the representations could be seen more clearly. All beams should be within the safety limits of testing so as not to pose a safety risk when having to lift the beam during the experiment. When conducting the laboratory and field simulations, it should be ensured that these are performed at the same time and not at different sessions. It is very difficult to have the beams in exactly the same positions if these sessions are not occurring at the same time.

Finally, in reference to the third stage, an improvement that should be taken into consideration is related to the control board that was used. The control board should contain more control points. If there were more control points, the results would have shown greater accuracy. If the control board was larger and placed in a more suitable position it would have been in full view of the camera and hence not excluded in any of the images.

6.3.2 Observations on Top

On examination of the research that was conducted, it could be assumed that it would have been a more practical method if the targets were placed not only on the side of the structure, but also on the top of the structure. For example, when monitoring a structure such as a bridge, there are a variety of cameras that are used which take into account the safety of drivers and pedestrians that use the bridge. When setting up this monitoring system, the cameras should have NIR capabilities and the targets should be within full view of the cameras and placed in prominent areas, such as areas where high levels of stress are being applied.

6.3.3 Weather Conditions

Finally, if contemplating further research in this area, it would be beneficial to conduct further experimentation during different weather conditions to see if the comparisons of colour to NIR would reveal similar results. An example of this could include monitoring a structure such as a bridge during rain or foggy conditions. It has been established that weather conditions may cause a series of distortions that affect the results of the photographs. Therefore if further research were planned, it would be beneficial to determine the health of the structure over a 24-hour period in any weather condition.

6.4 Conclusion

On completion of this experimentation and analysis, it is satisfactory to conclude that this study has been beneficial in determining whether Colour and NIR Imagery would be in a similar context to each other when monitoring structural materials.

Further research as previously discussed would also be valuable to this study. As a result, considering these suggestions and possible advancements, it could be assumed that this technique may be useful in determining the health of many uncertain structures.

References

ASM International (2002), 'History of Fractography', in Granta Design Limited (eds), *ASM Handbooks Online: Volume 12, Fractography: Fractography: Principles and Practices*, Viewed 27 March 2011

<<http://products.asminternational.org.ezproxy.usq.edu.au/hdb/index.jsp>>

ASM International (2002), 'Photography of Fractured Parts and Fracture Surfaces', in Granta Design Limited (eds), *ASM Handbooks Online: Volume 12, Fractography: Fractography: Principles and Practices*, Viewed 27 March 2011

<<http://products.asminternational.org.ezproxy.usq.edu.au/hdb/index.jsp>>

ASM International (2002), 'Testing Machines and Strain Sensors', in Granta Design Limited (eds), *ASM Handbooks Online: Volume 12, Fractography: Fractography: Principles and Practices*, Viewed 27 March 2011

<<http://products.asminternational.org.ezproxy.usq.edu.au/hdb/index.jsp>>

Tso, S, Feng, T 2003, 'Robot Assisted Wall Inspection for Improved Maintenance of High-Rise Buildings', *International Symposium on Automation and Robotics*, Pg. 449-455, viewed on the 11 April 2011,

<<http://www.iaarc.org/publications/fulltext/isarc2003-06.pdf>>

Standards Australia 2004, *Bridge Design Part 1: Scope and general principles*, AS 5100-2004, Standards Australia, Sydney, viewed 16 August 2011,

<<http://www.saiglobal.com.ezproxy.usq.edu.au/online/autologin.asp>>

Gao, Z-f, Du, Y-l, Sun, B-c & Jin, X-m 2007, 'Strain monitoring of railway bridges using optic fiber sensors', *Journal of Quality in Maintenance Engineering*, vol. 13, no. 2, pp. 186-97, EBSCOhost, a9h, item: 60340774. viewed 16 August 2011

Nair, A, Cai, CS 2010, 'Acoustic emission monitoring of bridges: Review and case studies', *Engineering Structures*, vol. 32, no. 6, pp. 1704-14, Viewed 01 September 2011, ScienceDirect,

<<http://www.sciencedirect.com/science/article/pii/S0141029610000623>>

Dudescu, C, Somotecan, M & Hardau, M 2009, 'ASPECTS RELATED DIRECT APPLICATION OF STRAIN GAGES ON WOOD', *Annals of DAAAM & Proceedings*, pp. 39-40, EBSCOhost, a9h, item: 47080513. View 01 September

Huang, YH, Liu, L, Sham, FC, Chan, YS & Ng, SP 2010, 'Optical strain gauge vs. traditional strain gauges for concrete elasticity modulus determination', *Optik - International Journal for Light and Electron Optics*, vol. 121, no. 18, pp. 1635-41, Viewed 15 April 2011, ScienceDirect
<<http://www.sciencedirect.com/science/article/B7GVT-4WXRDV6-7/2/279cfca5eb003bd98756f341e7703a3d>>

Jiang, R, Jáuregui, DV & White, KR 2008, 'Close-range photogrammetry applications in bridge measurement: Literature review', *Measurement*, vol. 41, no. 8, pp. 823-34, viewed 21 April 2011, SciVerse, ScienceDirect

Arias, P, Herráez, J, Lorenzo, H & Ordóñez, C 2005, 'Control of structural problems in cultural heritage monuments using close-range photogrammetry and computer methods', *Computers & Structures*, vol. 83, no. 21-22, pp. 1754-66, viewed 21 April 2011, SciVerse, ScienceDirect

Mass, H-G, Hampel, U 2006, 'Photogrammetric Techniques in Civil Engineering Material Testing and Structure Monitoring', *Photogrammetric Engineering & Remote Sensing*, vol. 72, no. 1, pp. 29-45, viewed 22 April 2011

Mills, J, Barber, D 2004, 'Geomatics techniques for structural surveying', *Journal of Surveying Engineering*, vol. 130, no. 2, pp. 56-64

Clarke, TA & Fryer, JG 1998, 'The Development of Camera Calibration Methods and Models', *The Photogrammetric Record*, vol. 16, no. 91, pp. 51-66, viewed 7 May 2011, <http://robots.stanford.edu/cs223b04/JeanYvesCalib/papers/Clarke98_calib_history.pdf>

Chong, AK & Mathieu, R 2006, 'Near infrared photography for craniofacial anthropometric landmark measurement', *The Photogrammetric Record*, vol. 21, no. 113, pp. 16-28, viewed 11 April 2011,

Chandler, JH, Fryer, JG & Jack, A 2005, 'Metric capabilities of low-cost digital cameras for close range surface measurement', *The Photogrammetric Record*, vol. 20, no. 109, pp. 12-26, <<http://hdl.handle.net/2134/2238>>

Rönnholm, P, Nuikka, M, Suominen, A, Salo, P, Hyypä, H, Pöntinen, P, Haggrén, H, Vermeer, M, Puttonen, J, Hirsi, H, Kukko, A, Kaartinen, H, Hyypä, J & Jaakkola, A 2009, 'Comparison of measurement techniques and static theory applied to concrete beam deformation', *The Photogrammetric Record*, vol. 24, no. 128, pp. 351-71, viewed 14 April 2011,

Thomas, H & Cantré, S 2009, 'Applications of low-budget photogrammetry in the geotechnical laboratory', *The Photogrammetric Record*, vol. 24, no. 128, pp. 332-50, viewed 14 April,

Chong, AK 2004, 'Optimising the accuracy of a low-cost photogrammetric motion study system', *The Photogrammetric Record*, vol. 19, no. 108, pp. 296-310, viewed 15 April,

Chong, AK, Ariff, MFM, Majid, Z & Setan, H 2010, 'Night-time surveillance system for forensic 3D mapping', paper presented to Image and Signal Processing (CISP), 2010 3rd International Congress on, 16-18 Oct. 2010. Pg. 502-506, IEEE Xplore, viewed 17 April 2011,

Knudsen, T 2005, 'Technical Note: Pseudo natural colour aerial imagery for urban and suburban mapping', *International Journal of Remote Sensing*, vol. 26, no. 12, pp. 2689 - 98, viewed 19 April 2011,

Luhmann, T, Robson, S, Kyle, S, Harley, I 2006, *Close Range Photogrammetry: Principles, Techniques and Applications*, Whittles.

Shuttleworth, M 2008, Null Hypothesis, viewed 1 October 2011, <<http://www.experiment-resources.com/null-hypothesis.html>>

F-Test Tables, view 1 October 2011, <http://www.stattools.net/FTest_Tab.php>

SVY 2105 Survey computations B: Study book 1 2009, University of Southern Queensland, Toowoomba, pp. 1.10, 2.1, 2.27-2.31

Appendix A

Project Specifications

Student ID: 0050071892
Course: ENG4111
Class: 23309

Name: Daniel J. Pratt
Postal Address: PO Box 7455
Toowoomba MC QLD 4352
Australia

Assessment: ASSIGN 2 PROJECT SPECIFICATION

Due Date: 22-MAR-2011

Submitted To: Faculty of Engineeri

Examiner: Armando Apan



Marker Signature: _____

Mark Given (Office Use Only): _____

Tutor Name:

Tutorial Group Number:

Room:

Day:

Time:

Campus: Toowoomba

STUDENT DECLARATION:

I hold a copy of this assignment which I can produce if the original is lost or damaged.

I hereby certify that no part of this assignment has been copied from any other student's work or from any other source except where due acknowledgement is made in the assignment. No part of this assignment has been written for me by any other person except where such collaboration has been authorised by the Course Team Leader or the examiner concerned.

Signature: DP Pratt

Date: 17/03/2011

- Notes:**
1. An Examiner or a Course Team Leader has, and may exercise, the right not to mark this assignment if the above declaration has not been signed.
 2. If the above declaration is found to be false, further appropriate action will be taken.

Make sure that you have used the **CORRECT** Assignment Cover for your assignment.
Incorrect assignment cover sheets will cause delays.

University of Southern Queensland

FACULTY OF ENGINEERING AND SURVEYING

ENG4111/4112 Research Topic
PROJECT SPECIFICATION

For: Daniel John Pratt (No. 0050071892)

Topic: NEAR INFRARED FOR SMALL STRUCTURAL DEFORMATION STUDY

Supervisor: Prof. Albert Kon-Fook Chong

Sponsorship: Faculty of Engineering and Surveying, University of Southern Queensland

Project Aim: To determine whether using the images of near infrared imaging sensor is comparable in accuracy with the conventional colour images for the detection of deformations within building structure materials.

Programme: (Issue A, 17 March 2011)

1. Perform a laboratory simulation using near infrared imaging optical sensor to determine if the aim of this project can be achieved. Upon the success of this simulation on the 16th of March 2011, the following stages can now proceed.

2. Research all mechanical engineering materials, such as the ASM handbooks, to determine what types of materials (Concrete, steel, plastic and wood) and what methods are necessary for this study. It is essential to provide a general understanding of what materials and methods are used within most of these structures. Mechanical Engineer, Mohan Trada, will be consulted in regards to how the deformities within structure buildings are measured and the achievable accuracy.

3. Research what types of application near infrared is used for, its advantages, its disadvantages and expected results. Research must be taken into account to see what benefit the conventional imaging techniques or laser scanning technology have when detecting the reduced shadows on objects.

4. Research the methods that are normally used to detect deformities within any building structure, along with their advantages and disadvantages to determine which method or methods would be best by comparing statistically the data that will be obtained. Methods referred to are:

- Visual Inspection
- Ruler and Compass
- Close-range Photogrammetry
- Electronic Strain Gauges

5. All equipment that is to be used must be properly calibrated and tested before any work is carried out.

6. Upon completion of the equipment calibrations and testing, the other laboratory simulations will be conducted using the chosen research materials.

7. Analyse the results obtained from these simulations, using the available software, and examine the statistical comparison of the measured results.

8. Use a more conventional method or methods on the same materials in another series of laboratory simulations.

9. Analyse the results and compare the statistical data with the near infrared simulations.

10. Submit an academic dissertation.

If time permits

11. From the laboratory results, determine whether a case study is suitable.

12. Design a shower system where water is poured on both the chosen materials and between the materials and the camera. It can then be determined to see if the same comparison can be made of the data that is produced.

AGREED: D Pratt (Student) [Signature] (Supervisor)

Date: 17/03/2011

Date: 17/03/2011

Examiner/Co-examiner: _____

Appendix B

Risk Assessment

University of Southern Queensland Risk Management Plan

A **hazard** is something with the potential to cause harm.

Risk is the likelihood that a harmful consequence (death, injury or illness) might result when exposed to the hazard.

Risk assessment: The process of evaluating the severity of a risk, for the purposes of prioritising and taking action to control the risk. Assessing a risk involves considering the likelihood of harm arising from a hazard and the severity of the consequences that could result.

Date: 08/06/2011	Faculty/Department: Engineering and Surveying	Assessment completed by: Daniel John Pratt	Contact number: N/A
What is the task? Testing Structural beams on a testing machine in a lower light environment		Location where task is being conducted: Z108	
Why is the task being conducted? For research purposes, more specifically, ENG4111/4112			
What are the nominal conditions?			
Personnel Student, Supervisor & Technician	Equipment Beams, Cameras, Lamps, Support beam, Testing Machine	Environment Air-condition-Room	Other Low Light Environment
Briefly explain the procedure for this task (including reference to other procedures) Studying the strain and stress of structural beams using photogrammetric techniques in normal light environment and lower light environment.			

Lower the fixture onto the beams. (This is to be done for the four beams)	Physical Injury	All persons and obstructions must be out of the way before the fixture is lowered.	1	D	L	Yes	N/A	N/A	N/A	N/A	N/A	Accept
Applying different loads to the beam (This is to be done for the four beams)	Splinters could fly from the concrete, wood and composite materials.	Wearing eye protection during testing and should be a safe distance from the machine. Also, the supervisor and technician must be presented.	2	D	L	Yes	N/A	N/A	N/A	N/A	N/A	Accept
Taking photographs of the beams in normal lighting	N/A	N/A	N/A	N/A	N/A	N/A	N/A	N/A	N/A	N/A	N/A	N/A
Operating the machine and taking photographs of the beams in a low light environment.	There will be lower visibility in operating the machine and equipment. Thus there are a few trip hazards and physical injury risks	There must be a minimum of two torches, one over the machine and one over the cameras. The room must be inspected before turning the lights to a lower setting. The supervisor must be presented.	1	D	L	Yes	N/A	N/A	N/A	N/A	N/A	Accept

USQ RISK RATING ADAPTED FROM AS4360:2004

Note: In estimating the level of risk, initially estimate the risk with existing controls and then review risk controls if risk level arising from the risks is not minimal

TABLE 1 - CONSEQUENCE

Level	Descriptor	Examples of Description
1	Insignificant	No injuries. Minor delays. Little financial loss. \$0 - \$4,999*
2	Minor	First aid required. Small spill/gas release easily contained within work area. Nil environmental impact. Financial loss \$5,000 - \$49,999*
3	Moderate	Medical treatment required. Large spill/gas release contained on campus with help of emergency services. Nil environmental impact. Financial loss \$50,000 - \$99,999*
4	Major	Extensive or multiple injuries. Hospitalisation required. Permanent severe health effects. Spill/gas release spreads outside campus area. Minimal environmental impact. Financial loss \$100,000 - \$250,000*
5	Catastrophic	Death of one or more people. Toxic substance or toxic gas release spreads outside campus area. Release of genetically modified organism (s) (GMO). Major environmental impact. Financial loss greater than \$250,000*

* Financial loss includes direct costs eg workers compensation and property damage and indirect costs, eg impact of loss of research data and accident investigation time.

TABLE 2 - PROBABILITY

Level	Descriptor	Examples of Description
A	Almost certain	The event is expected to occur in most circumstances. Common or repetitive occurrence at USQ. Constant exposure to hazard. Very high probability of damage.
B	Likely	The event will probably occur in most circumstances. Known history of occurrence at USQ. Frequent exposure to hazard. High probability of damage.
C	Possible	The event could occur at some time. History of single occurrence at USQ. Regular or occasional exposure to hazard. Moderate probability of damage.
D	Unlikely	The event is not likely to occur. Known occurrence in industry. Infrequent exposure to hazard. Low probability of damage.
E	Rare	The event may occur only in exceptional circumstances. No reported occurrence globally. Rare exposure to hazard. Very low probability of damage. Requires multiple system failures.

USQ RISK RATING ADAPTED FROM AS4360:2004

TABLE 3 – RISK RATING

Probability	Consequence				
	Insignificant 1	Minor 2	Moderate 3	Major 4	Catastrophic 5
A (Almost certain)	M	H	E	E	E
B (Likely)	M	H	H	E	E
C (Possible)	L	M	H	H	H
D (Unlikely)	L	L	M	M	M
E (Rare)	L	L	L	L	L

TABLE 4 - RECOMMENDED ACTION GUIDE

Abbrev	Action Level	Descriptor
E	Extreme	The proposed task or process activity MUST NOT proceed until the supervisor has reviewed the task or process design and risk controls. They must take steps to firstly eliminate the risk and if this is not possible to introduce measures to control the risk by reducing the level of risk to the lowest level achievable. In the case of an existing hazard that is identified, controls must be put in place immediately.
H	High	Urgent action is required to eliminate or reduce the foreseeable risk arising from the task or process. The supervisor must be made aware of the hazard. However, the supervisor may give special permission for staff to undertake some high risk activities provided that system of work is clearly documented, specific training has been given in the required procedure and an adequate review of the task and risk controls has been undertaken. This includes providing risk controls identified in Legislation, Australian Standards, Codes of Practice etc.* A detailed Standard Operating Procedure is required. * and monitoring of its implementation must occur to check the risk level
M	Moderate	Action to eliminate or reduce the risk is required within a specified period. The supervisor should approve all moderate risk task or process activities. A Standard Operating Procedure or Safe Work Method statement is required
L	Low	Manage by routine procedures.

*Note: These regulatory documents identify specific requirements/controls that must be implemented to reduce the risk of an individual undertaking the task to a level that the regulatory body identifies as being acceptable.

The task should not proceed if the risk rating after the controls are implemented is still either HIGH or EXTREME or if any risk is not As Low As Reasonably Practicable (ALARP).

This Risk Assessment score of Low (L) is only on the condition that all existing and additional controls are in place at the time of the task being conducted.

Assessment completed by:	
Name: Mr. Daniel John Pratt Mr. Mohan Trada Mr James Farrell	Signature: Approved
Position: Student Senior Technical Officer Workplace Health & Safety Coordinator	Contact No: N/A Phone: 46311367 Phone: 46311376
Date: 08/06/2011	
Supervisor	
Name: Dr. Albert Kon-Fook Chong	Signature:
Position: Senior Lecturer	Contact No: Phone: 46312546
Date:	

Guidance Notes for review of Controls and Risk Management Plan.

When monitoring the effectiveness of **control measures**, it may be helpful to ask the following questions:

- **Have the chosen control measures been implemented as planned?**
 - Are the chosen control measures in place?
 - Are the measures being used?
 - Are the measures being used correctly?
- **Are the chosen control measures working?**
 - Have any the changes made to manage exposure to the assessed risks resulted in what was intended?
 - Has exposure to the assessed risks been eliminated or adequately reduced?
 - **Are there any new problems?**
 - Have the implemented control measures introduced any new problems?
 - Have the implemented control measures resulted in the worsening of any existing problems?

To answer these questions:

- consult with workers, supervisors and health and safety representatives;
- measure people's exposure (e.g. taking noise measurements in the case of isolation of a noise source);
- consult and monitor incident reports; and
- review safety committee meeting minutes where possible.

Set a date for the review of the **risk management process**. When reviewing, check if:

- the process that is currently in place is still valid;
- things have changed that could make the operating processes or system outdated;
- technological or other changes have affected the current workplace; and
- a different system should be used altogether

Appendix C

Structural Material Display

C.1 Concrete Material Beam

C.2 Wood Material Beam

C.3 Composite Material Beam

C.4 Steel 01 Material Beam

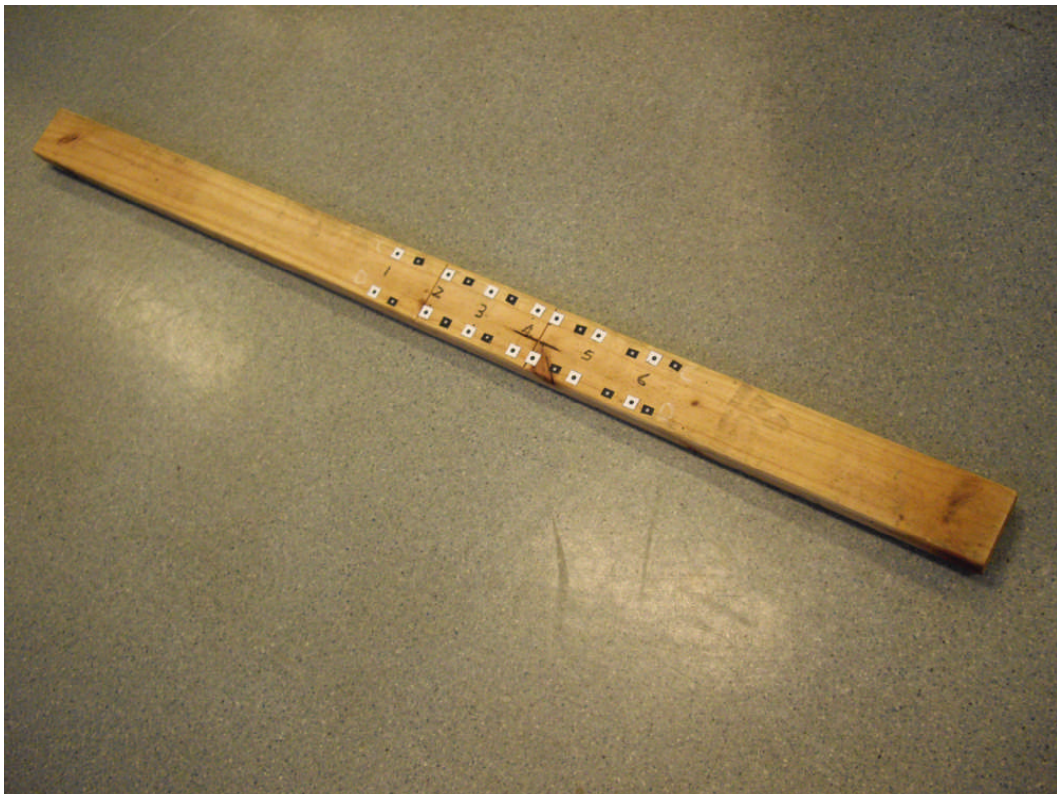
C.5 Steel 02 Material Beam

C.6 Timber Material Beam

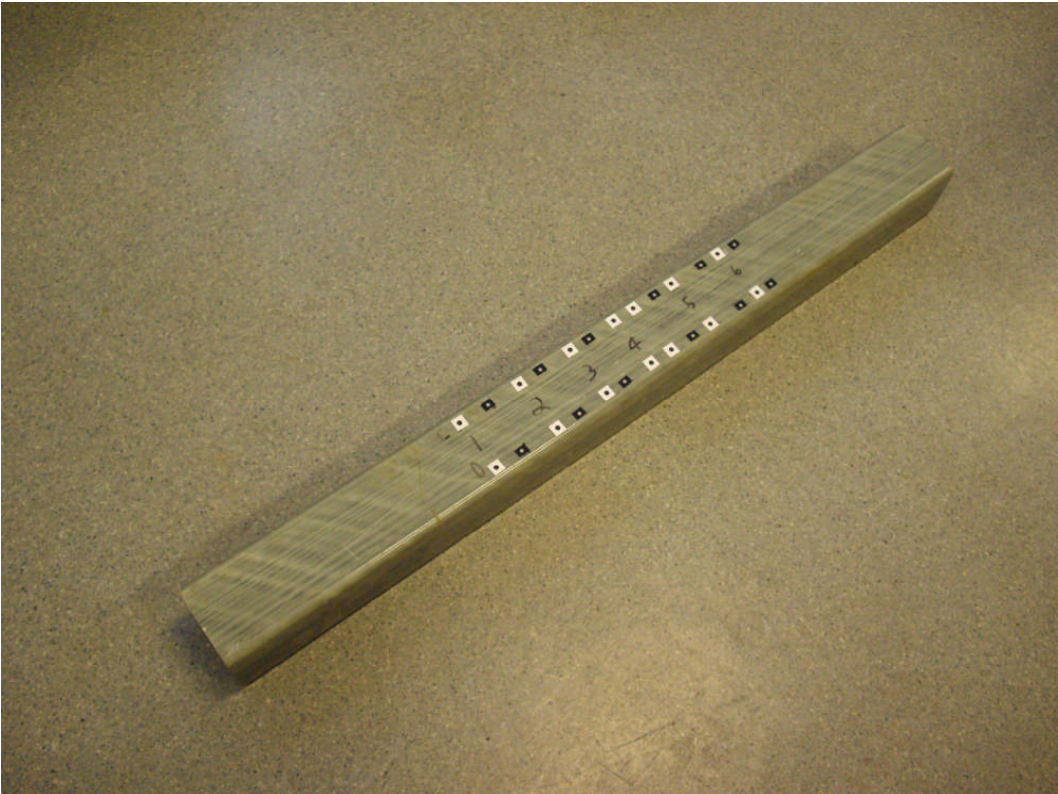
Appendix C.1: Material Concrete Beam



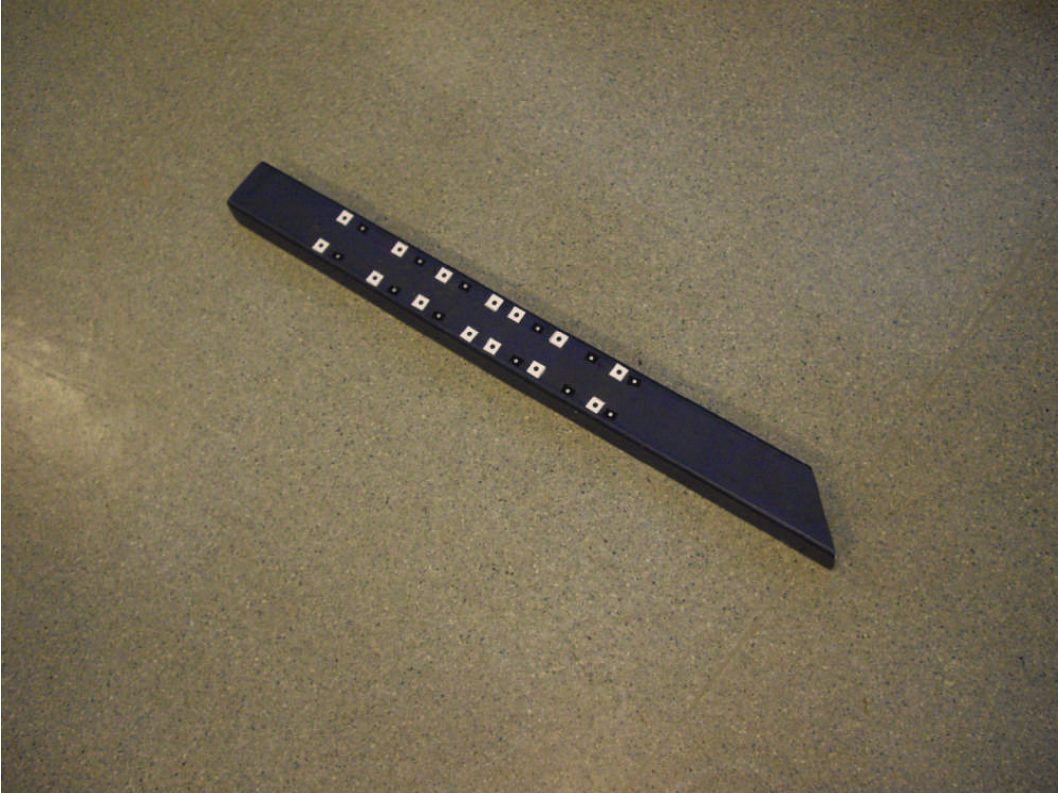
Appendix C.2: Material Wood Beam



Appendix C.3 Composite Material Beam



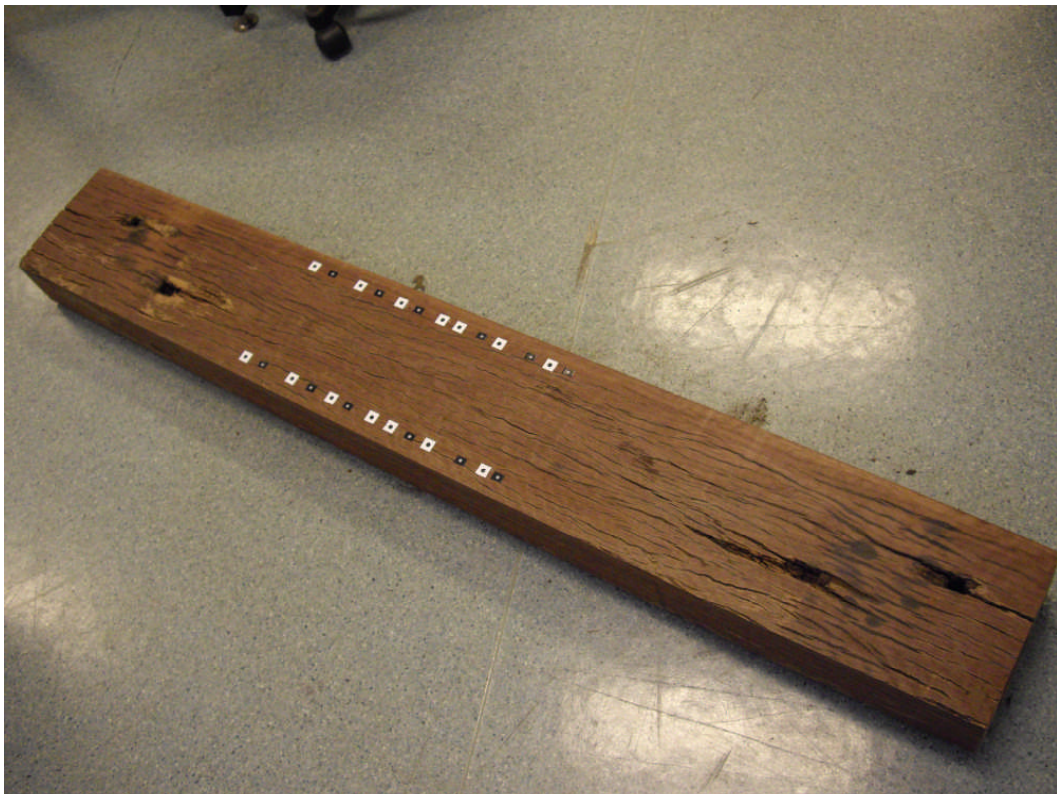
Appendix C.4 Steel 01 Material Beam



Appendix C.5 Steel 02 Material Beam



Appendix C.6 Timber Material Beam



Appendix D

Camera Calibration Parameters Results

D.1 Camera 1 Calibration Parameters (Structural Beams)


D.2 Camera 2 Calibration Parameters (Structural Beams)

D.3 Camera Calibration Parameters (Bridge Structure)

Appendix D.1: Camera 1 Calibration Parameters (Structural Beams)

Camera DataBase [X]

Calibration Time

Camera Id: 

Sensor Size (pixels) Pixel Size (mm)

H:

V:

Type / Serial #: /

Lens Type / Serial #: /

	Current Value	Sigma	Fix
(c)	<input type="text" value="3.041450"/>	1000	<input type="checkbox"/>
(Xp)	<input type="text" value="0.002411"/>	1000	<input type="checkbox"/>
(Yp)	<input type="text" value="0.002904"/>	1000	<input type="checkbox"/>
(K1)	<input type="text" value="-3.0268e-003"/>	1000	<input type="checkbox"/>
(K2)	<input type="text" value="3.3475e-003"/>	1000	<input type="checkbox"/>
(K3)	<input type="text" value="-1.8291e-003"/>	1000	<input type="checkbox"/>
(P1)	<input type="text" value="-1.6641e-027"/>	1e-016	<input checked="" type="checkbox"/>
(P2)	<input type="text" value="-2.2309e-027"/>	1e-016	<input checked="" type="checkbox"/>
(B1)	<input type="text" value="-1.4199e-028"/>	1e-016	<input checked="" type="checkbox"/>
(B2)	<input type="text" value="3.4252e-029"/>	1e-016	<input checked="" type="checkbox"/>


Sigmatas Option

Save changes to this camera

Camera 1. Imagery Type: Colour

Camera DataBase [X]

Calibration Time

Camera Id: 

Sensor Size (pixels) Pixel Size (mm)

H:

V:

Type / Serial #: /

Lens Type / Serial #: /

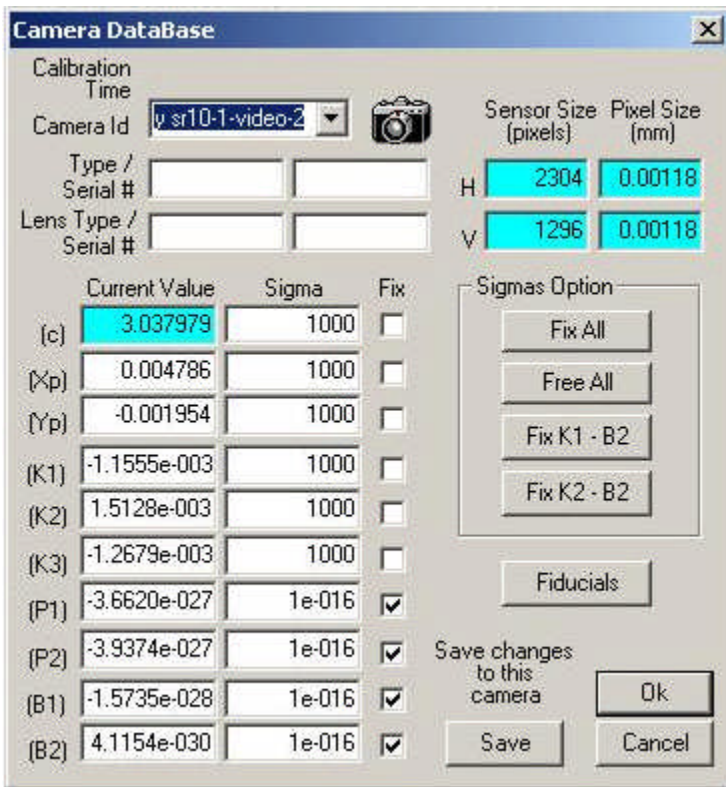
	Current Value	Sigma	Fix
(c)	<input type="text" value="3.040440"/>	1000	<input type="checkbox"/>
(Xp)	<input type="text" value="0.001563"/>	1000	<input type="checkbox"/>
(Yp)	<input type="text" value="-0.007710"/>	1000	<input type="checkbox"/>
(K1)	<input type="text" value="-2.2043e-003"/>	1000	<input type="checkbox"/>
(K2)	<input type="text" value="2.6412e-003"/>	1000	<input type="checkbox"/>
(K3)	<input type="text" value="-1.7789e-004"/>	1000	<input type="checkbox"/>
(P1)	<input type="text" value="-1.0474e-027"/>	1e-016	<input checked="" type="checkbox"/>
(P2)	<input type="text" value="-1.9807e-027"/>	1e-016	<input checked="" type="checkbox"/>
(B1)	<input type="text" value="3.5849e-028"/>	1e-016	<input checked="" type="checkbox"/>
(B2)	<input type="text" value="6.6675e-029"/>	1e-016	<input checked="" type="checkbox"/>

Sigmatas Option

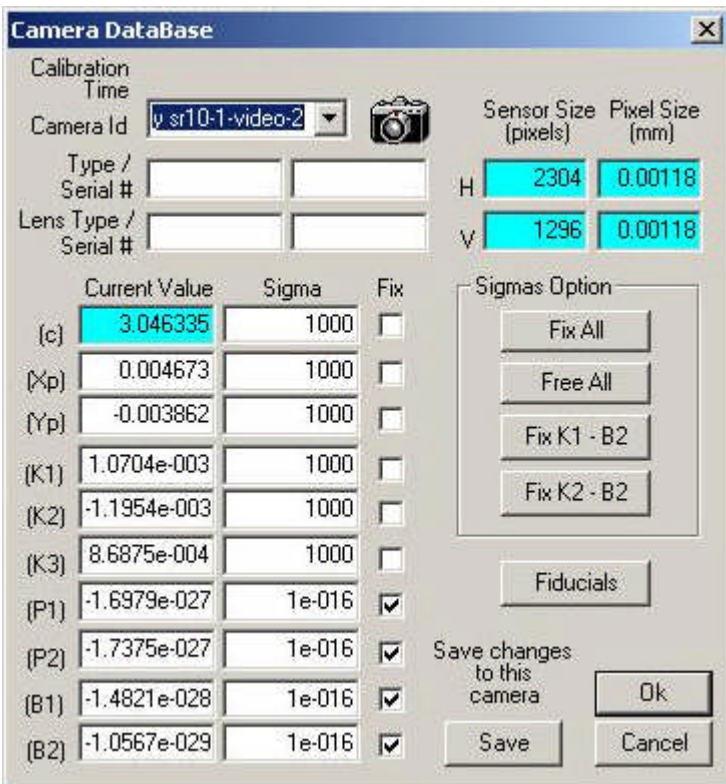
Save changes to this camera

Camera 1. Imagery Type: NIR

Appendix D.2: Camera 2 Calibration Parameters (Structural Beams)



Camera 2. Imagery Type: Colour




Camera 2. Imagery Type: NIR

Appendix D.3: Camera Calibration Parameters (Bridge Structure)

Camera DataBase

Calibration Time

Camera Id: 

Sensor Size (pixels) Pixel Size (mm)

H:

V:

Type / Serial #: /

Lens Type / Serial #: /

	Current Value	Sigma	Fix
(c)	<input type="text" value="3.039886"/>	1000	<input type="checkbox"/>
(Xp)	<input type="text" value="0.002783"/>	1000	<input type="checkbox"/>
(Yp)	<input type="text" value="0.001205"/>	1000	<input type="checkbox"/>
(K1)	<input type="text" value="-1.0130e-003"/>	1000	<input type="checkbox"/>
(K2)	<input type="text" value="1.3238e-003"/>	1000	<input type="checkbox"/>
(K3)	<input type="text" value="-5.4615e-004"/>	1000	<input type="checkbox"/>
(P1)	<input type="text" value="-9.0725e-028"/>	1e-016	<input checked="" type="checkbox"/>
(P2)	<input type="text" value="-1.4228e-027"/>	1e-016	<input checked="" type="checkbox"/>
(B1)	<input type="text" value="-5.5562e-029"/>	1e-016	<input checked="" type="checkbox"/>
(B2)	<input type="text" value="1.4576e-028"/>	1e-016	<input checked="" type="checkbox"/>


Sigmas Option

Save changes to this camera

Camera. Imagery Type: Colour

Camera DataBase

Calibration Time

Camera Id: 

Sensor Size (pixels) Pixel Size (mm)

H:

V:

Type / Serial #: /

Lens Type / Serial #: /

	Current Value	Sigma	Fix
(c)	<input type="text" value="3.049081"/>	1000	<input type="checkbox"/>
(Xp)	<input type="text" value="0.001112"/>	1000	<input type="checkbox"/>
(Yp)	<input type="text" value="-0.006302"/>	1000	<input type="checkbox"/>
(K1)	<input type="text" value="-9.5854e-004"/>	1000	<input type="checkbox"/>
(K2)	<input type="text" value="3.2998e-003"/>	1000	<input type="checkbox"/>
(K3)	<input type="text" value="-1.0737e-003"/>	1000	<input type="checkbox"/>
(P1)	<input type="text" value="-7.4273e-028"/>	1e-016	<input checked="" type="checkbox"/>
(P2)	<input type="text" value="-1.5151e-027"/>	1e-016	<input checked="" type="checkbox"/>
(B1)	<input type="text" value="2.7378e-030"/>	1e-016	<input checked="" type="checkbox"/>
(B2)	<input type="text" value="2.4090e-028"/>	1e-016	<input checked="" type="checkbox"/>

Sigmas Option

Save changes to this camera

Camera. Imagery Type: NIR